Translation initiation by cap-dependent ribosome recruitment: recent insights and open questions

Authors:

First author
Nikolay E. Shirokikh*
0000-0001-8249-358X
EMBL–Australia Collaborating Group, Department of Genome Sciences, The John Curtin School of Medical Research, The Australian National University, Canberra, ACT 2601, Australia
nikolay.shirokikh@anu.edu.au
Conflicts of interest: none declared

Second author
Thomas Preiss*
0000-0001-6273-784X
EMBL–Australia Collaborating Group, Department of Genome Sciences, The John Curtin School of Medical Research, The Australian National University, Canberra, ACT 2601, Australia
Victor Chang Cardiac Research Institute, Darlinghurst, NSW 2010, Australia
thomas.preiss@anu.edu.au
Conflicts of interest: none declared

Abstract

Gene expression universally relies on protein synthesis, where ribosomes recognise and decode the messenger RNA template by cycling through translation initiation, elongation and termination phases. All aspects of translation have been studied for decades using the tools of biochemistry and molecular biology available at the time. We focus here on the mechanism of translation initiation in eukaryotes, which is remarkably more complex than prokaryotic initiation and is the target of multiple types of regulatory intervention. The 'consensus' model, featuring cap-dependent ribosome entry and scanning of mRNA leader sequences, represents the predominantly utilised initiation pathway across eukaryotes, although several variations of the model and alternative initiation mechanisms are also known. Recent advances in structural biology techniques have enabled remarkable molecular level insights into the functional states of eukaryotic ribosomes, including a range of ribosomal complexes with different combinations of translation initiation factors that are thought to represent *bona fide* intermediates of the initiation process. Similarly, high-throughput sequencing-based ribosome profiling or 'footprinting' approaches have allowed much progress in understanding the elongation phase of translation and variants of them are beginning to reveal the remaining mysteries of initiation, as well as aspects of translation termination and ribosomal recycling. The current view on the eukaryotic initiation mechanism is presented here with an emphasis on how recent structural and footprinting results underpin axioms of the consensus model. Along the way, we outline some contested mechanistic issues and major open questions still to be addressed.

Graphical/Visual Abstract and Caption

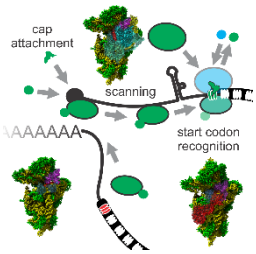

Eukaryotic translation initiation includes small ribosomal subunit cap attachment, mRNA scanning and start codon recognition, followed by large ribosomal subunit joining, and involves a remarkably extended set of initiation factors providing complex control of genes expression.

Introduction

Molecular biology as a discipline was formed in the 1950's around the 'central dogma' and its foundational studies were directed at understanding the processes of transcription of genetic information from DNA into messenger (m)RNA, and translation from mRNA into protein. Understanding the genetic code, and the roles of transfer (t)RNA and the ribosome in decoding it during protein synthesis, were key early advances. It was also realised that ribosomes consist of small and large subunits (SSU and LSU, correspondingly). Most of the decoding-related functions of the ribosome involve regions of the SSU, including the tRNA-binding sites for the incoming aminoacyl-tRNA (A-site), the peptidyl-tRNA (P-site), the outbound deacylated tRNA (E-site) and the mRNA interface[1-3]. Conversely, the LSU contains the peptidyl transferase centre responsible for the

polymerisation of amino acids, as well as surfaces required for handling the nascent polypeptide[4]. There also was an early realisation that the recruitment of the ribosome to the mRNA was an important 'initiation' phase during translation with mechanistic requirements that were distinct from 'elongation', the actual protein synthesis phase, as well as 'termination', where ribosomes stop protein synthesis at nonsense codons and dissociate into free subunits, to enable a new translation round (Fig. 1a).

Many aspects of translation are well conserved throughout evolution. For example, the prokaryotic and eukaryotic elongation and termination phases feature comparable mechanisms and involve broadly similar sets of elongation factors (EFs) and release factors (RFs), respectively[5, 6]. Other aspects are distinctly different, such as the spatial separation of transcription and translation into the nucleus and cytoplasm of eukaryotes, respectively, while prokaryotic mRNAs are translated co-transcriptionally. Further, apart from a conserved stepwise recruitment of ribosomal subunits, prokaryotic and eukaryotic initiation are mechanistically quite divergent. Notably, while three initiation factors (IFs) suffice for the process in prokaryotes, evolution has generated a plethora of additional eukaryotic (e)IFs[7]. Related to this, prokaryotic mRNAs are typically polycistronic and have short untranslated regions (UTRs), while eukaryotic mRNAs usually contain one main open reading frame (ORF) and possess rather longer 5' and 3' UTRs[8].

Extensive research into eukaryotic initiation commenced in the 1970s[9]. The ubiquitous presence of an 'inverted' 3'→5' 7-methylguanosine m^7G(5')ppp(5')N 'cap' structure at the 5' end of eukaryotic mRNAs was discovered[10, 11]. Caps are added to mRNAs co-transcriptionally near transcription start sites and earlier than other pre-mRNA modification events *via* cleaving the γ-phosphate off the mRNA 5'end, followed by GMP transfer from GTP by guanylyltransferase, and its N^7-methylation by (guanine-7-)methyltransferase[11]. In higher eukaryotes, first mRNA nucleotide can then be additionally 2'-methylated in the nucleus, and second – in the cytoplasm[11]. Caps can also be added post-transcriptionally and in the cytoplasm by different eukaryotic viruses[12]. Roles of the cap structure in mRNA stability[13] and translation[14, 15] were realised soon after its discovery; it is now widely accepted that uncapped mRNA in eukaryotic cytoplasm rapidly degrades[16, 17]. However, early mechanistic explanations for attachment of SSUs to mRNA during eukaryotic initiation lacked the elegance of the model established in parallel for prokaryotes, where a specific sequence (AGGAGGU in *Escherichia coli*) is found in mRNA just upstream of start codons. This Shine-Dalgarno sequence was immediately proposed[18, 19] and later structurally demonstrated[20, 21] to recruit the SSU to mRNA through Watson-Crick interactions with the 3' end of the 16S ribosomal (r)RNA. At this early time, it seemed that the only determinant of the start site in eukaryotes was the AUG codon itself, to which ribosomes can bind directly[22]. The overall process of initiation seemed to be less organised than in bacteria[23].

With rare exceptions, such as metazoan replication-dependent histone mRNAs, eukaryotic mRNAs also carry a 3' poly(A) 'tail', which is added co-transcriptionally in a two-step process. Nascent pre-mRNA is first cleaved after recognition of the poly(A) site (located 10-30 nt upstream of the cleavage site), auxiallry signals (CA sequence before and U/GU-rich element ~40 nt after the cleavage site) and U-rich elements with UGUA consensus (upstream the cleavage site)[24]. The recognition and processing is aided by interactions with RNA polymerase II C-terminal domain, and involve cleavage and polyadenylation specificity factor, cleavage stimulation factor, cleavage factors I and II,

symplekin and poly(A) polymerase[24]. Poly(A) is then added from ATP to ~250 nt[25]. mRNAs with longer 3' poly(A) are usually better translated, whereas a shorter 3' poly(A) often results in decreased translation and removal of the mRNA from the translated pool[26-28]. Notably, alternative polyadenylation sites can be preferentially selected under different conditions, and can define additional 3' UTR complexity, include or exclude RNA binding protein (RBP) sites, micro RNA binding sites and even exons and introns[29-31]. 3' poly(A) length can further be dynamically regulated in the cytoplasm, a process highly important for post-transcriptional gene control[32-35].

Importantly, the 5' cap and 3' poly(A) allow the formation of an mRNA 'closed-loop', facilitated by interactions between the cap-binding eIFs and the poly(A)-binding protein (PABP)[36-38]. The closed-loop promotes recruitment of free SSUs from the cytosol and may also participate in the direct recycling of SSUs from termination to initiation within established polyribosomes, or polysomes. Polysome are 'steady-state' assemblies of mRNAs translated by serially elongating ribosomes. The spatial configurations seen for polysomes from different sources are mostly consistent with the closed-loop model, although some of the observed shapes suggest additional or alternative intrapolysomal interactions (Fig. 1b-g).

Figure 1

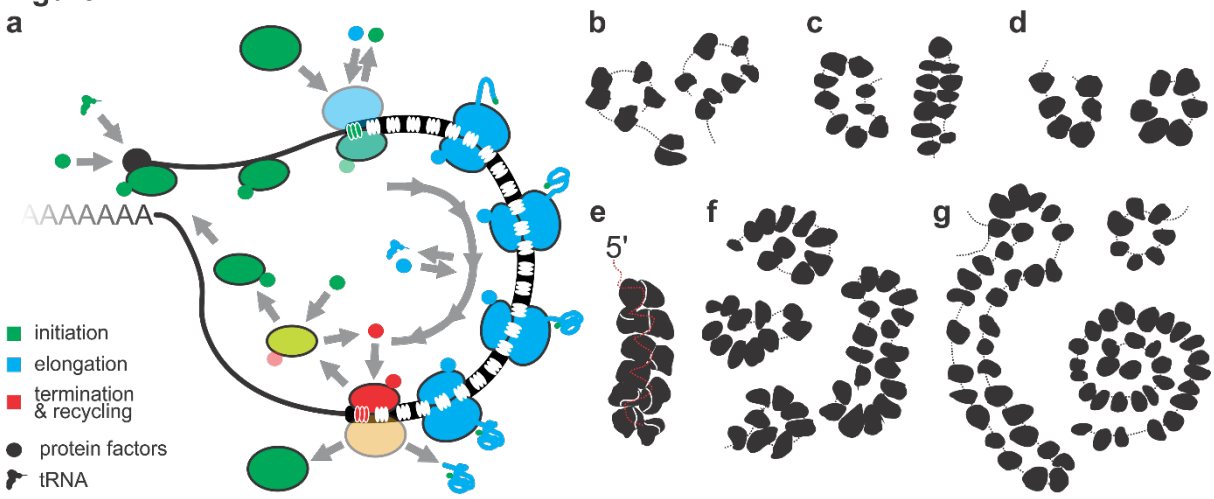

Figure 1. (a) Schematic of the eukaryotic translation cycle showing a single mRNA translated by multiple ribosomes, forming a polysome. Canonical translation initiation (green) begins with the assembly of the small ribosomal subunit (SSU), eukaryotic initiation factors (eIFs) and initiator-methionyl-tRNA (Met-tRNA$_i^{Met}$) at the mRNA 5' end, assisted by 5' cap to 3' poly(A) interactions. The SSU complex then moves in 3' direction until it recognises a start codon, rearranges its configuration and is joined by the large ribosomal subunit (LSU). This commences elongation (blue), whereby ribosomes move through the open reading frame (ORF) and synthesise the polypeptide, aided by elongation factors (eEFs). Termination (red) occurs at nonsense (stop) codons; here eukaryotic release factors (eRFs) assist in release of the completed protein as well as the LSU and SSU, which can be recycled for additional rounds of translation. The gradual displacement of eIFs at start codons is depicted in light moss green (●). Because SSUs at start codons can belong to both, initiation and elongation complexes, they are shown in amazonite (●). The sequential nature of ribosome assembly during initiation (LSU attaches last) and disassembly during termination (LSU leaves first) is shown by sky blue (●) and caramel (●) colours, respectively. Sequential displacement of eRFs with

initially recycling, and then initiation factors upon completion of termination, is depicted by citron (●) SSU and pink (●) coloured eRFs. (b)-(g) Schematics of polysome topologies as detected by electron microscopy. (b) 'Circular' polysomes observed in rabbit reticulocyte lysate on native mRNA with 5' cap and 3' poly(A)[39]. (c) 'Circular' and 'hairpin' polysomes seen in *Tetrahymena pyriformis* cells[40]. (d) 'Circular' polysomes formed in a wheat germ cell-free translation system on capped and polyadenylated (left) and non-capped, non-polyadenylated (right) synthetic mRNAs[41]. (e) 'Linear' polysome formed in a wheat germ cell-free translation system on capped but non-polyadenylated mRNA, featuring interacting SSUs along the central axis of a left-handed (5' to 3') spiral of mRNA[42]. (f) Endoplasmic reticulum (ER)-attached 'circular', 'linear', 'double-row' and 'spiral' polysomes detected in rat hepatocytes[43]. (g) ER-attached 'circular', 'hairpin' and 'spiral' polysomes from rat fibroblasts, showing SSU-inward orientation of ribosomes in the tightly packed curved regions[44].

Decades of biochemistry and molecular biology research have shed much light on the translation process, revealing numerous mechanistic details. However, key contributions have increasingly come from structural biology. Solving the crystal structure of the ribosome was a key advance[45-48] and the structures of multiple auxiliary factors (eIF, eEFs, eRFs) have provided much useful information. The advent of cryo-electron microscopy (cryo-EM) approaches then facilitated the detailed structural characterisation of several ribosome-factor-mRNA complexes thought to represent functional intermediates of translation[49]. In parallel, ribosome profiling, a combination of the purification of arrested ribosomal complexes from living cells with transcriptome-wide sequencing of their RNase-protected 'footprints' on mRNA, provided much complementary insight[50-52]. In this review, we focus on what is known about the mechanism of canonical cap-dependent, scanning-driven translation initiation, drawing primarily on plentiful structural and biochemical data available for mammalian and yeast cells. We outline key discoveries and concepts, and detail how their validity is underpinned by recent cryo-EM, crystallographic, and ribosome footprinting data. We emphasise key areas of agreement and discord between new and old data, as well as aspects of mechanistic uncertainty that urge for further investigation.

OVERVIEW OF CAP-DEPENDENT TRANSLATION INITIATION AND ITS REGULATION

Combining the scanning model with the accumulated knowledge of the identities, interactions and other biochemical activities of the eIFs allowed the construction of what might be a predominant sequence of events during initiation (see Table 1 for the list of main protein factors directly involved in the ribosome-mRNA interactions throughout translation initiation). An overview of this 'canonical' pathway is depicted in Fig. 2. To better represent the topological aspects of the model, we further show the structures of the main eIFs and their locations on the SSU in Fig. 3 (where structural data exist) and Fig. 4 (where eIF locations can only be extrapolated from indirect evidence). It is useful, though somewhat arbitrary, to divide the dynamic process of cap-dependent initiation into several distinct stages. We focus here on mRNA-associated events and divide them, based on the activity of ribosomal complexes as well as their localisation along mRNA, into three stages: 1) attachment to the cap, 2) scanning, and 3) start codon recognition including LSU joining (the latter is sometimes considered as a separate stage).

During attachment to the cap, SSU interactions with mRNA are aided by the eIF4 group of factors. The cytoplasmic cap-binding protein eIF4E (Fig. 4e) interacts with the 5' cap and binds to the scaffold

protein eIF4G (Fig. 4c). The ATP-dependent RNA-helicase eIF4A (Fig. 4a) interacts more transiently with eIF4G:eIF4E to form an eIF4F complex. eIF4F then recruits the SSU *via* eIF4G affinity to eIF1, eIF5 and possibly rRNA (yeast) or *via* eIF4G affinity to eIF3 (higher eukaryotes) (Figs. 3f,g). A pre-formed ternary complex (TC) of the Met-tRNA$_i^{Met}$ (Fig. 3b), GTP and eIF2 (Fig. 3e; not homologous to bacterial IF2) also joins this complex, as do eIF1 (Fig. 3c) and eIF1A (Fig. 3d). eIF1 is analogous to prokaryotic IF3 and functions in destabilising codon-anticodon interactions. eIF1A is a direct homologue of IF1, whose conserved functions are deemed to be that of a 'placeholder' in the SSU A-site, possibly to prevent early elongator tRNA binding, and of a stabiliser of mRNA and Met-tRNA$_i^{Met}$ binding to the SSU.

The SSU and associated factors then commence the scanning stage, by moving 3'-ward on mRNA. This scanning motion can require energy expense through hydrolysis of ATP (or other nucleotide triphosphates) and is thought to be linked to the activity of RNA-helicases, such as eIF4A and DHX29 (Fig. 5c), assisted by the single-stranded RNA binding protein eIF4B (and additionally eIF4H in higher eukaryotes) (Fig. 4c).

The start codon recognition stage begins when SSUs halt their movement over a start codon appearing in the SSU P-site, surrounded by 'strong' nucleotide context. A series of rearrangements is initiated, leading to the dissociation of some of the scanning components, including eIF1 and eIF2:GDP. Met-tRNA$_i^{Met}$, located in the P-site, then binds eIF5B:GTP (Fig. 3h), which is partially homologous to prokaryotic IF2. From here on, eukaryotic initiation strongly resembles its prokaryotic counterpart and concludes in the LSU joining and the release of eIF5B. After each initiation round eIF2:GDP needs to be recycled by its GDP/GTP exchange factor eIF2B[53-55]. This eIF2 recycling is highly regulated and generally considered as an additional stage of initiation taking place away from the ribosome and mRNA.

The cap-and-scanning initiation pathway as summarised above can be seen as universally conserved across eukaryotes, as are the main initiation factor sets[56]. Nevertheless, the prevalence of isoforms for certain eIFs and their regions with strong homology can vary substantially between taxa, especially for the group 4 eIFs. For example, in higher plants additional eIF(iso)4E and eIF(iso)4G can form alternative and well-represented eIF(iso)4F complexes that target specific mRNA subsets and locations[56-59], whereas among the variety of trypanosome eIF4E homologues (~6)[60], eIF4E4 appears as the major active isoform[61]. However, much is still unknown about how this eIF4E variety contributes to possible selectivity of mRNA translation[62, 63]. Importantly, recent structural findings suggest that each of the main initiation stages corresponds to pivotal changes in the SSU conformation and its re-configuring by the binding and release of initiation factors.

Table 1. List of eukaryotic translation initiation factors participating in the consensus initiation pathway, as well as some other proteins with roles in initiation[a].

Initiation factor	Name in yeast	Also known as	MW, kDa (human)[b]	Key function in initiation	References
eIF1	*SUI1* / YNL244C	eIF-1, IF-E1, A121, EIF1A, ISO1	12.7	Destabilisation of codon-anticodon interactions.	[64-69]

eIF1A	*TIF11* / YMR260C	eIF-1A, EIF1AX, EIF1A, EIF1AP1, eIF-4C, EIF4C, IF-E7, IF-M2Bβ	16.5	Control of P_{IN}/P_{OUT} switching during scanning and start codon recognition.	66-71
eIF2 (composite)		eIF-2, IF-MP, IF-1, IF-E2, EIF-3	125.6	Positioning of Met-$tRNA_i^{Met}$ in the SSU P-site during scanning, recognition of the AUG and near-cognate start codons (GUG, AUA, *etc.*) and the consensus nucleotide context.	67-69, 72
eIF2α	*SUI2* / YJR007W	EIF2S1, EIF-2, EIF-2A, EIF2alpha, EIF2, EIF2A	36.1	eIF2 availability by Ser 51 phosphorylation and increased binding to the GDP/GTP exchange factor eIF2B, recognition of the downstream start codon context and stabilisation of P_{IN}.	73, 74
eIF2β	*SUI3* / YPL237W	EIF2S2, EIF2, EIF2B, EIF2beta, PPP1R67	38.4	Binding to Met-$tRNA_i^{Met}$ and eIF5, eIF2 availability by binding to the GDP/GTP exchange factor eIF2B.	75
eIF2γ	*GCD11* / YER025W	EIF2S3, EIF2, EIF2G, EIF2gamma, eIF-2gA, MRXSBRK	51.1	GTP/GDP binding and GTP hydrolysis.	76
eIF2A	YGR054W	eIF-2A, EIF-2A, IF-M1, MST089, MSTP004, MSTP089, CDA02	65.0	GTP-independent Met-$tRNA_i^{Met}$, Leu-$tRNA_e^{Leu}$ binding and start codon recognition, including non-canonical CUG and UUG triplets on specific mRNAs.	77, 78
eIF2D	*TMA64* / YDR117C	Ligatin, HCA56, LGTN	64.7	GTP-independent Met-$tRNA_i^{Met}$ binding and start codon recognition.	79, 80

eIF3 (composite)		IF-3, IF-E3, IF-M5, eIF-3	793.6	Attachment to the cap, assembly of the scanning complex, coordination of cap-dependent mRNA loading, scanning, start codon recognition and LSU joining.	[64, 67-69, 81-83]
eIF3a	*RPG1* / YBR079C	eIF3A, P167, eIF3-p170, eIF3-theta, p180, p185	166.6	MPN/PCI subunit. Interacts with mRNA.	[81-83]
eIF3b	*PRT1* / YOR361C	eIF3B, EIF3-eta, EIF3-P110, EIF3-P116, EIF3S9	92.5	Peripheral subunit. Interacts with mRNA.	[81-83]
eIF3c	*NIP1* / YMR309C	EIF3C, EIF3CL, EIF3S8, eIF3-p110	105.3	MPN/PCI subunit.	[81-83]
eIF3d	N/A	EIF3D, EIF3S7, eIF3-p66, eIF3-zeta	64.0	Peripheral subunit. Direct binding to the cap structures for specific mRNAs. Interacts with mRNA.	[81-83]
eIF3e	N/A	EIF3E, EIF3-P48, EIF3S6, INT6, eIF3-p46	52.2	MPN/PCI subunit.	[81-83]
eIF3f	N/A	EIF3F, EIF3S5, eIF3-p47	37.6	MPN/PCI subunit.	[81-83]
eIF3g	*TIF35* / YDR429C	EIF3G, EIF3-P42, EIF3S4, eIF3-delta, eIF3-p44	35.6	Peripheral subunit. Interacts with mRNA.	[81-83]
eIF3h	N/A	EIF3H, EIF3S3, eIF3-gamma, eIF3-p40	39.9	MPN/PCI subunit.	[81-83]
eIF3i	*TIF34* / YMR146C	EIF3I, EIF3S2, PRO2242, TRIP-1, TRIP1,	36.5	Peripheral subunit.	[81-83]

		eIF3-beta, eIF3-p36			
eIF3j	*HCR1* / YLR192C	EIF3J, EIF3S1, eIF3-alpha, eIF3-p35, p35	29.1	Peripheral subunit.	[81-83]
eIF3k	N/A	EIF3K, EIF3-p28, EIF3S12, HSPC029, M9, MSTP001, PLAC-24, PLAC24, PRO1474, PTD001, ARG134	25.1	MPN/PCI subunit.	[81-83]
eIF3l	N/A	EIF3L, EIF3EIP, EIF3S11, EIF3S6IP, HSPC021, HSPC025, MSTP005	66.7	MPN/PCI subunit. Possible binding to cap structure	[81-83]
eIF3m	N/A	EIF3M, B5, PCID1, TANGO7, hfl-B5, GA17	42.5	MPN/PCI subunit.	[81-83]
eIF4F (composite)			251.2	Formation of mRNA closed-loop, SSU attachment to the mRNA cap, initial mRNA unwinding and loading onto SSU, possibly scanning directionality and motion.	[67-69, 84, 85]
eIF4A	TIF1 / YKR059W TIF2 / YJL138C	DDX2A, EIF-4A, EIF4A, eIF-4A-I, eIF4A-I, eIF-4A, IF-E4, IF-M4, IF_{EMC} EIF4A2, BM-010, DDX2B, EIF4A, EIF4F,	46.2	ATP-dependent RNA-helicase. In eIF4F, it possibly couples ATP hydrolysis with scanning directionality and motion.	[86-88]

		eIF-4A-II, eIF4A-II			
eIF4E	CDC33 / YOL139C	AUTS19, CBP, EIF4E1, EIF4EL1, EIF4F, eIF-4E	28.8	Cytoplasmic cap-binding protein. Interacts with eIF4G. Is regulated by 4E-binding proteins that block its binding to eIF4G.	88-90
eIF4G	TIF4631 / YGR162W TIF4632 / YGL049C	EIF4G1, EIF-4G1, EIF4G, EIF4GI, P220, PARK18 EIF4G3, eIF-4G 3, eIF4G 3, eIF4GII	176.2	Cap-dependent attachment of mRNA to eIF3 (mammals) or SSU (yeast). Possible coupling of ATP hydrolysis by eIF4A with scanning directionality and motion.	88, 91-93
eIF4A	See above	See above	See above	See above	See above
eIF4B	TIF3 / YPR163C	IF-E6, IF-M3, EIF4B, EIF-4B, PRO1843	69.1	Single-stranded RNA binding protein. Possibly contributes to scanning directionality and motion.	94, 95
eIF4H	N/A	EIF4H, WBSCR1, WSCR1, eIF-4H	27.4	Single-stranded RNA binding protein.	96
eIF5	TIF5 / YPR041W	eIF-5, IF-E5, IF-M2A, IF-I1, IF-L2, IF-3, EIF5, EIF-5, EIF-5A	49.2	GTPase-activating protein for eIF2 GTPase. Participates in the control of P_{IN}/P_{OUT} switching during scanning and start codon recognition.	64, 67-69, 97
eIF5A	HYP2 / YEL034W ANB1 / YJR047C	eIF-5A, eIF-4D, IF-M2Bα, EIF5A, EIF-5A, EIF5A1, eIF5AI	20.2	Stimulates peptide elongation during translation of specific codon contexts. Accelerates peptide release during termination.	98, 99
eIF5B	FUN12 / YAL035W	eIF-5B, EIF5B, EIF-5B, IF2	138.8	GTP-dependent Met-$tRNA_i^{Met}$ positioning on the SSU and LSU during subunit	67-70, 100

				joining.	
eIF6	TIF6 / YPR016C	eIF-3A, EIF6, CAB, EIF3A, Integrin beta 4 binding protein, ITGB4BP, eIF-6, p27(BBP), p27BBP	26.6	Ribosomal subunits anti-association and biogenesis; microRNA-mediated silencing.	[101]
PABP	PAB1 / YER165W	Poly(A)-binding protein, PABPC1, PAB1, PABP1, PABPC2, PABPL1	70.7	Binding to poly(A) sequences at the mRNA 3' end, interaction with eIF4G and formation of the mRNA closed-loop in capped mRNAs. Stimulates translation and possibly promotes ribosomal recycling and re-initiation.	[102, 103]
DAP5	N/A	DAP-5, eIF4G2, EIF4G2, AAG1, DAP5, NAT1, P97	102.4	Functional analogue of eIF4G for cap-independent translation initiation on certain mRNAs.	[104]
MCT-1	TMA20 / YER007C-A (possible)	Multiple copies in T-cell lymphoma-1, malignant T cell-amplified sequence 1, MCT1, MCTS1	20.6	GTP-independent Met-tRNA$_i^{Met}$ delivery in complex with DENR on certain mRNAs and during re-initiation after uORF translation.	[105]
DENR	TMA22 / YJR014W (possible)	Density regulated protein	22.3	GTP-independent Met-tRNA$_i^{Met}$ delivery in complex with MCT-1 on certain mRNAs and during re-initiation after uORF translation.	[105]
DHX29	DED1 / YOR204W (analogue	DDX29	155.2	ATP-dependent RNA helicase; required for scanning of 5'UTRs with highly stable hairpin	[106, 107]

) structures.

[a] Only factors that directly interact with-mRNA-ribosomal complexes during cap binding, scanning, start codon recognition and LSU joining stages are listed (see text for additional factors, most notably eIF2B). [b] Molecular weights are given only for major isoforms of the proteins.

Figure 2

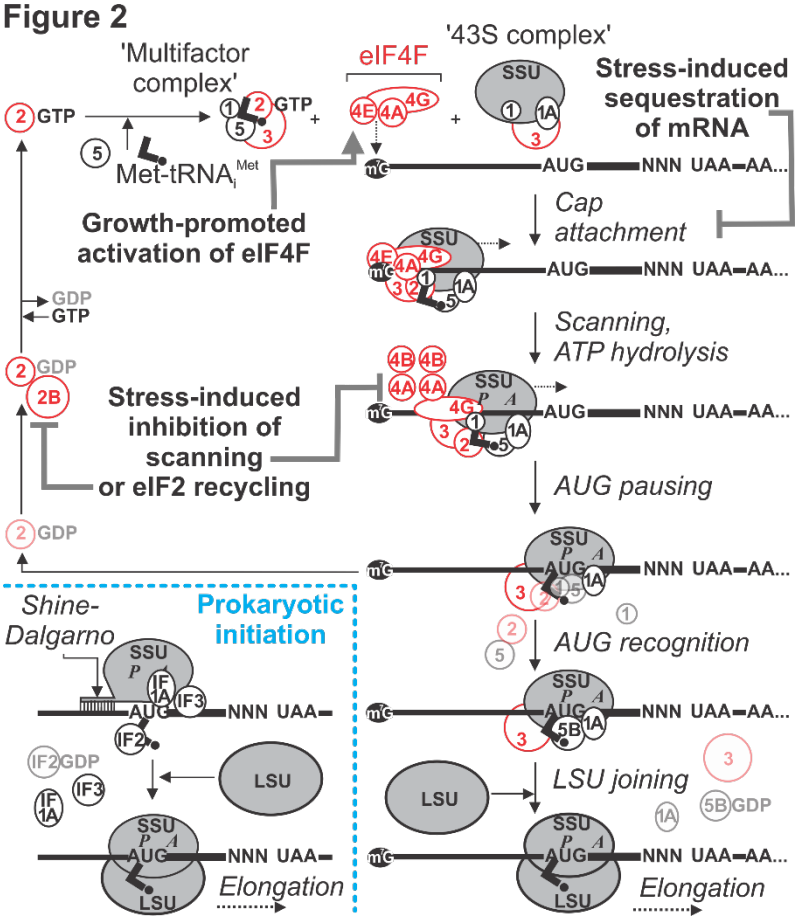

Figure 2. Eukaryotic translation initiation *via* cap-dependent scanning of mRNA. Note that, as initiation is highly dynamic, there is some uncertainty regarding the exact temporal sequence of factor interactions and sub-complex assembly. The schematic presents one possible route of initiation but other routes involving the same factors might well exist, also depending on type of mRNA and experimental system. For example, instead of parallel but separate formation of 'multifactor' and '43S' complexes, the involved factors have also been proposed to assemble with each other in a different order[68, 69, 108]. Late stages of eukaryotic initiation are depicted next to the homologous stages of the much simpler prokaryotic initiation process. Key cellular control inputs are further indicated in bold font. Eukaryotic translation initiation factors (eIFs), whose dysregulation prominently associates with the onset or maintaining of malignant phenotype, are shown in red[109, 110].

Translational regulation during the initiation phase is widely utilised in processes important for multicellular organisms, such as differentiation, cell proliferation and site-specific translation[35, 111, 112]; it further features commonly in pathologies. For example, dysregulation of most of the eukaryote-specific eIFs is implicated in the onset of malignancies and is regarded as one of the

drivers of oncogenesis[113, 114]. Many eIFs are targets for regulation, especially in higher eukaryotes[68, 115]. Examples of such control include phosphorylation of eIF4E-binding proteins (4E-BPs) by mTOR (resulting in the release of 'free' eIF4E and increased eIF4F levels), eIF4E by MNK1/2 (which may be stimulatory to translation), and eIF2α by GCN2, HRK, PKR and PERK (which results in stable binding of eIF2 to eIF2B, decreased levels of TC and skipping of upstream (u)ORFs during re-initiation of scanning)[116-119]. Most of the other eIFs can be phosphorylated as well[68, 120]. Finally, ribosomes can also be phosphorylated (*e.g.* SSUs at RSP6, which may have functional implications in malignant phenotypes)[121, 122], or have an outright different composition, possibly affecting their specific interactions with mRNA[123, 124]. For example, translation of the homeobox protein-coding (Hox) mRNAs was shown to be specifically dependent on the LSU protein RPL38[125].

It should also be noted that many eIFs (especially the eIF4 group) occur as different isoforms and/or paralogues that may function in special modes of initiation and its control. The eIF4E paralogues eIF4E1, -4E2, -4E3, and their isoforms, vary across species and are known to differentially control mRNA localisation to stress granules and processing bodies[126]. eIF4G3 (eIF4GII) (divergent from eIF4G1 (eIF4GI) in the eIF4E-binding N-terminal part) was suggested to have a distinct effect on translation[127, 128]. eIF4GII (but not eIF4GI) cleavage by viral proteases blocks the translation of host proteins[129]. DAP5 (or eIF4GII, p97, NAT1) (Fig. 4c) is ~70% homologous to the middle and C-terminal parts of eIF4GI but lacks the N-terminal eIF4E and PABP binding sites (Fig. 4f); it thus can stimulate cap-independent translation[104, 130, 131]. Although eIFs 4A1 and 4A2 are highly homologous, they are non-interchangeable functionally[132]. The more divergent eIF4A3 protein is not an initiation factor[132]. Prominent examples of eIFs important during developmental processes include DAP5, whose knock-out results in differentiation-resistant mouse embryonic stem cells (while their transcriptional profiles remain the same)[131]; eIF4B, which can control survival and proliferation of the cells[133]; eIF4E, whose liberation from eIF4E-BP interactions[134] coincides with oocyte maturation in mice [135] and whose intracellular location-dependent inhibition defines embryonic patterning in *Drosophila*[136, 137], synaptic plasticity and memory[35], pre-programming of oocytes[111, 138], and regulation of daughter cells growth in yeast[112]; RNA helicases of translation such as DDX3Y, which is essential for spermatogenesis; eIF3 subunit a, which can control translation of important cell cycle regulators and cell entry into the S-phase[139]; eIF3 subunit f, which is critical for maintenance of skeletal muscle size during starvation[140], eif3 subunit h, which directs translation of specific transcripts required for development of brain and eyes in zebrafish[141]; and others[142-145]. Many altered eIFs and their regulators are direct causes of inherited disorders, such as childhood ataxia (eIF2B), diet-induced obesity (eIF2α), diabetis (eIF2α kinase EIF2AK3/PERK), and others[146].

Additionally, eukaryotic mRNAs richly interact with RNA-binding proteins (RBPs), dynamically forming messenger ribonucleoproteins (mRNPs) to control their life cycle, from their production in the nucleus, export into the cytoplasm, localisation and translation, to their eventual decay[147]. RBPs, which can be abundant and universal, such as cap-binding proteins, the major mRNP constituent Y-box binding protein 1 (YB-1)[148], and poly(A)-binding proteins, or mRNA-specific[149]. The diversity and dynamic nature of mRNPs, and the added complexity of translation initiation in eukaryotes allow for a richness of post-transcriptional gene control. Indeed, protein synthesis rates have been shown to differ up to ~1,000-fold between eukaryotic mRNAs[150]. The literature abounds with mechanisms to alter translation initiation in an mRNA-selective way, *e.g.* through *cis*-acting regulatory motifs in the mRNA UTRs[8, 68, 115]. Scanning 'roadblocks' in 5' UTRs are well recognised as the basis of translational

control[8]. This is exemplified by uORF regulatory effects of *GCN4* mRNA in yeast or ATF4 mRNA in mammals, which inhibit main ORF translation when the levels of active eIF2 are high[151, 152], and by the binding of iron-regulatory protein to the ferritin mRNA 5' UTR, which leads to the steric hindrance of the scanning when the cytoplasmic iron concentration is low[153]. Recent insights gained with ribosome profiling approaches confirm widespread effects of 5' UTR uORFs of upstream start codons in the control of canonical initiation[154]. 3' UTRs are also often involved in control of cap-dependent attachment *in cis*, specifically by binding proteins that form a stable closed-loop of mRNA but cannot attach eIF3 or eIF4G[68, 153, 155]. 3' UTR-binding microRNAs may repress translation at different stages of initiation[68, 156, 157]. However, activators of scanning have also been found in 3' UTRs, with 3'-proximally located 'cap-independent translational enhancers' (CITEs) shown to specifically bind components of the cap-dependent initiation and then assist translation similar to the action of the canonical closed-loop of mRNA[158].

While translation of cellular mRNAs is thought to be mostly initiated through cap-dependent scanning, there are multiple documented pathways of initiation that do not fully fit into this model. Internal ribosome attachment to mRNA has been demonstrated for many cases of initiation on viral mRNAs[159-162], as well as for synthetic[163] and naturally occurring circular RNAs[164, 165]. In viral internal ribosome entry sites (IRESes) of types 1-3, specially folded RNA structures within the IRES functionally (and to some extent structurally) mimic eIFs and abrogate at least the dependency on eIF4E (or complete eIF4F) and cap (IRES type 1, full scanning; type 2, limited scanning), or eIF4G and all other group 4 factors (type 3, no scanning). IRESes were also identified for a multitude of cellular mRNAs, although the mechanism(s) of their action remain(s) largely obscure due to the lack of structural information[166-168]. For prominent examples such as the X-linked inhibitor of apoptosis (XIAP) mRNA IRES, independence on eIF2α and direct binding of eIF3 to its structure were reported[169, 170]. Similar to the 3' CITEs, 5' CITEs may function by enhancing the binding of canonical initiation factors and rendering translation less dependent on the 5' cap, while preserving overall 5'-end dependence of initiation. 5' CITEs were suggested as a more conservative explanation of the cellular IRES phenomenon on some mRNAs, such as apoptotic protease activating factor (Apaf)-1 mRNA[158]. The abovementioned Hox mRNA translation functionally demonstrates internal attachment of ribosomes, with cap-dependent initiation seemingly specifically supressed[125]. Recent high-throughput studies facilitated characterisation of initiation by various other 'non-canonical' routes. mTOR-depended regulation of mRNAs with 5'-proximal 'terminal oligopyrimidine' (TOP) sequences (characteristic to many mRNAs encoding eIFs) was identified using ribosome profiling[171]; further investigations detailed existance of non-TOP mRNAs with similar properties[172]. G-quadruplexes in 5' UTRs are often linked to IRES activity[173], and at the same time were demonstrated as prominent determinants of eIF4A-dependency genome-wide[174]. G-quadruplexes are present in 5' UTRs of many oncogenic mRNAs and link elevated eIF4A activity with cancer phenotypes[174]. eIF2A-dependent translation of the phosphatase and tensin homolog (PTEN) mRNA is initiated non-canonically from the CUG codon and leads to the production of PTENα isoform[175]. Synthesis of PTENα from PTEN mRNA requires CUG codon to be placed in a 16 nt palindromic motif CCCGCUC**CUG**GAGCGGG, but the exact details of the mechanism remain unknown[175]. PTEN is a notable tumour suppressor and this pathway exemplifies how alternative initiation is utilised by the cell to differently regulate translation of mRNAs.

Figure 3

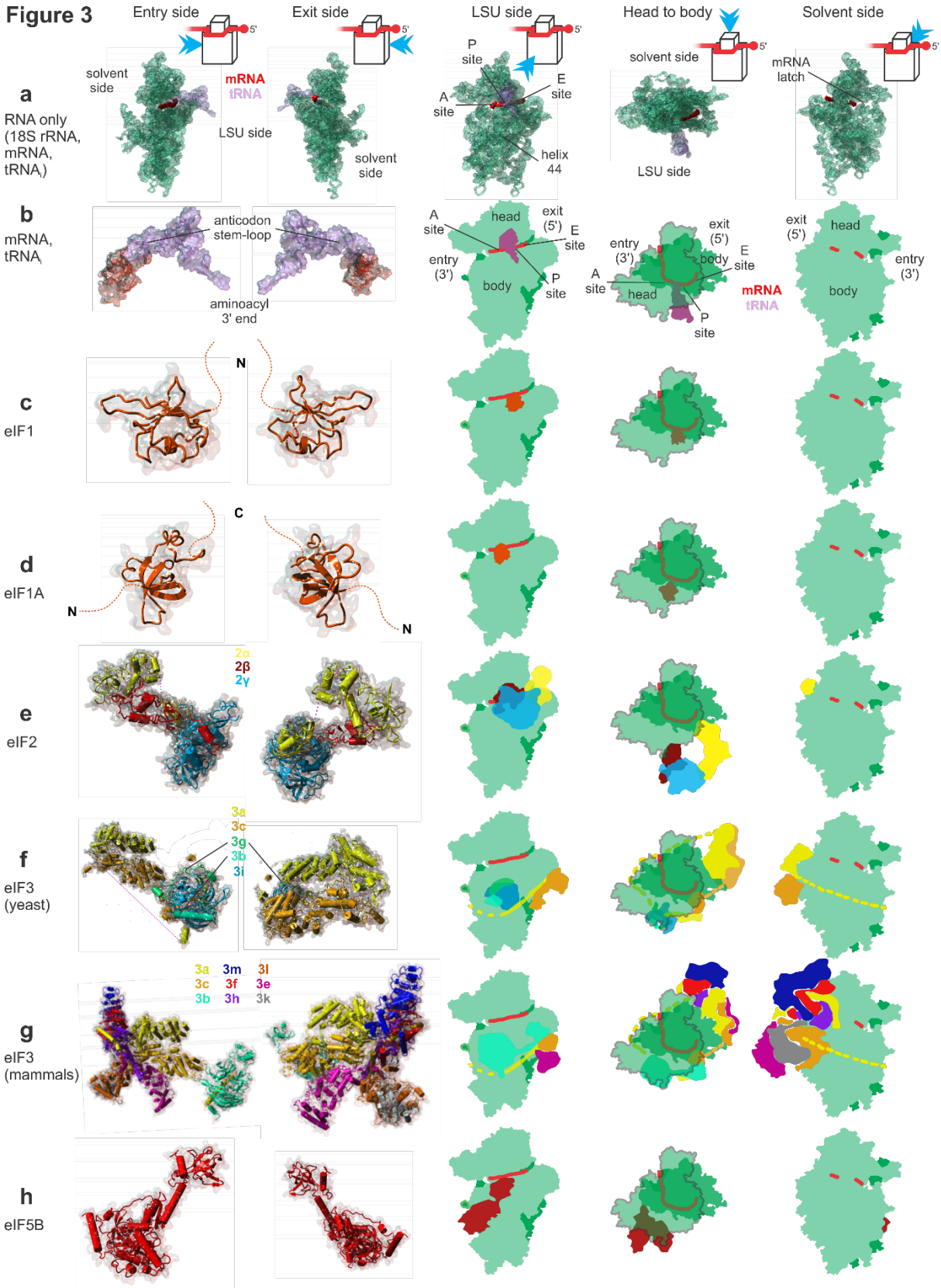
Entry side
Exit side
LSU side
Head to body
Solvent side
a
RNA only (18S rRNA, mRNA, tRNA)
solvent side
mRNA
tRNA
LSU side
P site
E site
A site
helix 44
mRNA latch
b
mRNA, tRNA
anticodon stem-loop
aminoacyl 3' end
head
exit (5')
entry (3')
body
c
eIF1
N
d
eIF1A
C
e
eIF2
2α
2β
2γ
f
eIF3 (yeast)
3a
3c
3g
3b
3i
g
eIF3 (mammals)
3a 3m 3l
3c 3f 3e
3b 3h 3k
h
eIF5B

Figure 3. Structures and ribosomal localisation (directly available from structural data) of the main components of cap-dependent translation initiation. Cartoons on the top indicate point-of-view relative to the SSU oriented head up, intersubunit side front, and mRNA entry side (opposite to the 5' cap) to the left. Surfaces are calculated and outlines are derived from published structural data. Rendering was performed with YASARA[176] Model. (a) Relative arrangement of the SSU rRNA (green), P-site $tRNA_i^{Met}$ (purple) and mRNA (red)[66]. (b) Views of initiator $tRNA_i^{Met}$-mRNA interactions at the P-site of the initiating SSU (left)[66] and schematics of the mRNA and $tRNA_i^{Met}$ location on the initiating SSU with key structural features of the SSUs indicated in outline (right)[177]. In the head-to-body SSU view, the head is rendered semi-transparent to allow observation of the body outline, and the head outline is augmented by a grey bezel line. The darker green areas in all three views (LSU side, head-to-body, solvent side) indicate SSU portions that are located to the rear of the main outline plane to improve depth perception. (c) Secondary structure and surface of the globular ribosome-bound eIF1 core[66] with its N-terminal unstructured extension indicated by the dotted line (left) and outline of its location on the SSU (right)[177]. (d) Same as (c), but for eIF1A[66]. (e) Secondary structure and surface of yeast eIF2 as part of the SSU-bound TC (left) and its outline on the SSU (right)[177]. (f) Same as (e), but for yeast eIF3[177]. (g) Structure of mammalian eIF3 from eIF3:SSU mRNA-free complex also containing DHX29[107] shown with yeast SSU outline and aligned by its eIF3c subunit to the yeast eIF3c in the eIF3:SSU complex)[177] using MUSTANG[178]. eIF3a and eIF3c intersubunit exit side extensions repeated from yeast structure in (f). eIF3b manually docked from the mammalian eIF3 as part of the mRNA-bound SSU complex[179]. (h) Secondary structure and surface of rabbit eIF5B as part of eIF5B:GMP-PNP:Met-$tRNA_i^{Met}$ complex bound to the complete ribosomes in complex with hepatitis C virus (HCV) internal ribosome entry site (IRES) (left)[180] and its outline on the yeast SSU (right)[177]. Alignment of the yeast and rabbit structures was performed by the 18S rRNA trace in YASARA Model.

A paradigm-shifting discovery was the widespread characterisation of *N*^{6}-methyladenosine modified nucleotides (m^6A) in eukaryotic mRNA and their action in the 5' UTR as individual internal ribosome attachment points[181]. m^6A was shown to directly bind eIF3 (skipping cap-dependence and eIF4E action) and promote translation of oncogenic mRNAs[181, 182]. Sometimes, the cap-dependent scanning pathway is antagonised by internal or cap-independent initiation[183-186]. However, these 'alternative' pathways might not be entirely in conflict with the cap-dependent scanning model. In most 'non-canonical' cases, including many of the internal attachment events, elements of (possibly limited) scanning are still in play. Similarly, even though reduced, a (sub)set of 'canonical' scanning factors is utilised in accordance with their established functions[158]. Thus, these other routes of initiation can be viewed as more or less profoundly modified versions of the 'canonical' initiation pathway[187]. There are some truly different established mechanisms, such as initiation at the intergenic regions of dicistroviruses (IRES type 4, an elongation-derived mechanism)[159], eIF2-independent delivery of tRNA[79, 188, 189], initiation from leucine elongator tRNA by the alternative tRNA carrier eIF2A at CUG start codons[190], or initiation on 'leaderless' mRNA by complete ribosomes[191]. Some principal alternatives to Kozak's scanning (such as initiation by mRNA 'looping') have also been proposed[192], however, these are outside the focus of this review.

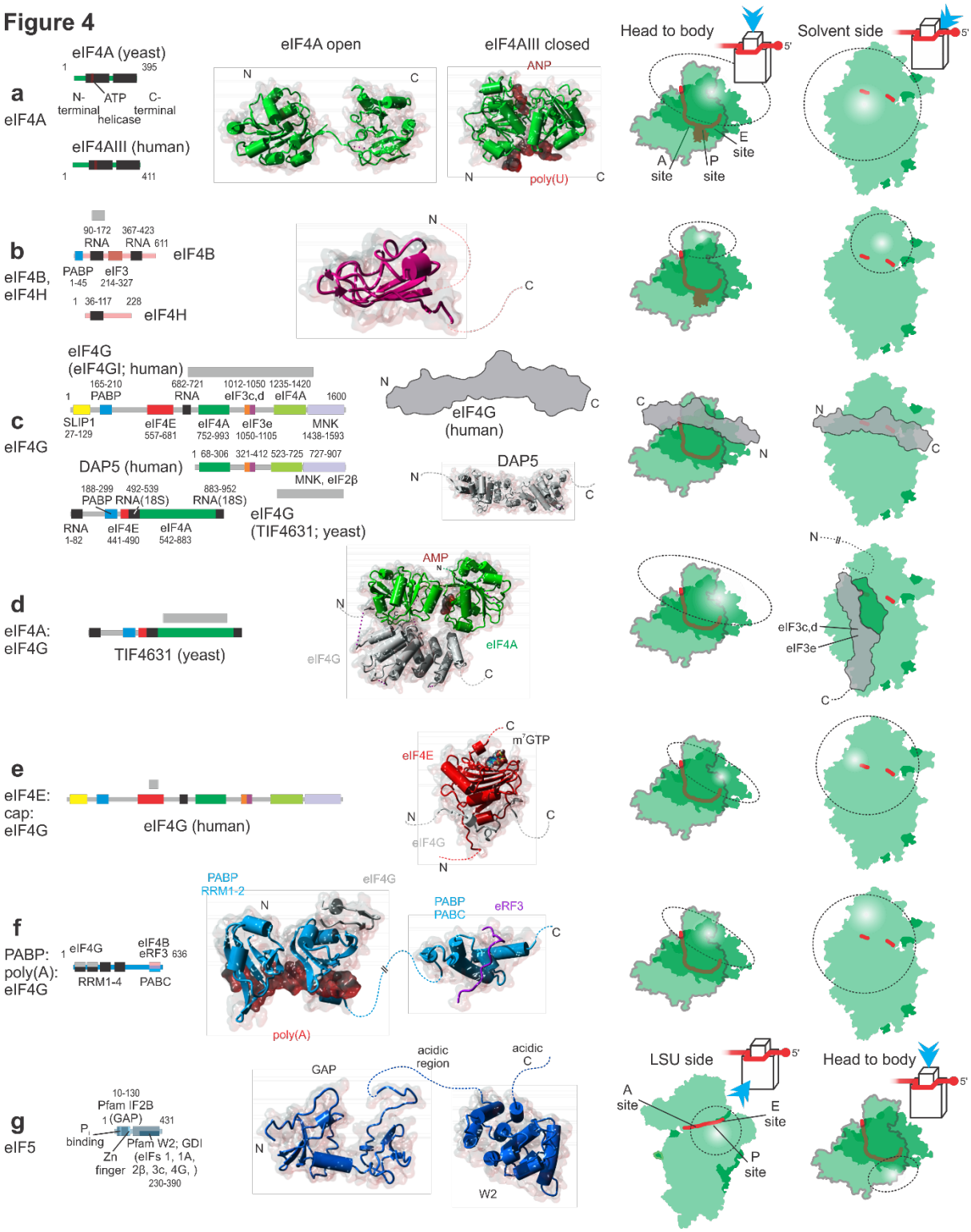

Figure 4. Structures and schematics of possible ribosomal localisation of the main components of cap-dependent translation initiation for which no precise SSU position is known. SSU depiction as in Fig. 3. The likely SSU localisation is shown as a white semi-transparent circle (unless stated otherwise), with a wider region of high-probability of localisation indicated by a dashed black line (right; on the SSU outline). (a) Domain structures of yeast eIF4A and human eIF4AIII (eIF4AI homologue) (left). Crystal structure of yeast eIF4A in the open conformation[193] and human eIF4AIII in

the closed conformation bound to single-stranded poly(U) RNA and AMP-PNP (ANP)[194] (middle). (b) Domain structures of human eIF4B and its partial homologue eIF4H (aligned by the region of homology; left). Solution structure of the human eIF4B amino acids 96-176 (shown by the grey bar in the human eIF4B domain scheme on the left) (middle)[195]. Position of eIF4B on the SSU outline accounting for directed hydroxyl radical mapping data[196]. (c) Domain structures of human eIF4G and DAP5 (eIF4G2, eIF4GII, p97, NAT1, AAG1), and yeast eIF4G (TIF4631) (left). Outline of the small angle X-ray scattering (SAXS) envelope of human eIF4G amino acids 712-1451 (shown by the grey bar in the human eIF4G domain scheme on the left)[197] with the eIF4A-corresponding density cut out manually (middle top). Crystal structure of the N-terminal part of human DAP5[198] (shown by the grey bar in the human DAP5 domain scheme on the left) (middle bottom). eIF4G SAXS envelope (minus eIF4A) shown in-scale with the SSU and positioned as originally proposed[197]. (d) Crystal structure of yeast eIF4G eIF4A-binding domain amino acids 571-853 (shown by the grey bar in the eIF4G domain scheme on the left) bound to yeast eIF4A:AMP complex (middle)[199]. Outline of the human eIF4A:eIF4G SAXS envelope (see (c))[197] shown in scale with the SSU and oriented by eIF4G eIF3 binding sites to the locations of eIF3c,d,e subunits and the position of the functionally analogous HCV IRES (see text) (right)[161]. (e) Domain scheme (left) and crystal structure of human eIF4E bound to human eIF4G amino acids 608-642 (middle)[200]. (f) Domain scheme (left) and combined crystal structures of the human PABP RNA recognition motif (RRM) 1-2 domains bound to $(A)_9$ RNA and amino acids 179-198 of human eIF4G[201], together with PABP C-terminal (PABC) domain bound to amino acids 59-73 of human eRF3B (middle)[202]. (g) Domain scheme (left) and combined solution structure of the N-terminal GTPase-activating protein (GAP) domain[203], together with crystal structure of the C-terminal Pfam W2 domain (middle)[204], of human eIF5. Possible localisation on the ribosome taking into account cryo-EM data (right)[205].

ATTACHMENT TO THE CAP

Canonical translation initiation begins with cap-dependent recruitment of the SSU to the mRNA near the 5' end (Fig. 1a). As the SSU has no intrinsic affinity for the cap, this requires a subset of eIFs to bridge between the SSU and the cap (and the 3' poly(A) as per the closed-loop model). eIFs required for subsequent scanning are also recruited at this early stage. A possible model for these steps is depicted in the upper part of Fig. 2 and described in detail below, however, there are also probable alternative scenarios and open questions, due to the existence of alternative modes of cap recognition and a difficulty of experimentally determining the exact sequence of events.

Assembly of translation components at the mRNA cap

An initial step is attachment of eIF4F to the mRNA cap, which is hypothesised to unfold structure near the 5' end of mRNA, making it capable of entering the mRNA-binding cleft of the initiating SSU in single-stranded form. The 3' poly(A) assists in eIF4F recruitment, through a contact between PABP with eIF4G. SSU recruitment is then brought about by a further interaction of eIF4G with SSU-bound eIF3 (in mammals[206]), which may also be mediated by eIF5 and eIF1 (as there are no eIF3-interacting regions in eIF4G in yeast[207-209]). There is a possibility of direct eIF4G:SSU interaction *via* binding to rRNA in yeast[210]. Yeast eIF4E is an abundant cytoplasmic protein and could thus occupy mRNA caps for most of the time *in vivo* [211]. In mammals, the eIF4E-to-eIF4G ratio can vary depending on conditions and cell type, for example, due to altered abundance of the factors[212] or regulation of

their activity. eIF4E is also known to have higher affinity to the capped mRNA as part of the eIF4F complex[213-215], which can be further positively modulated by eIF4G-PABP interaction[90, 216, 217]. However, eIF4E interactions with eIF4E-binding proteins (eIF4E-BPs) that competitively inhibit eIF4G binding have also been shown to increase upon cap binding[218]. Thus, 'free' eIF4F could displace eIF4E (or eIF4E:eIF4E-BP) from the cap as a first step of initiation, potentially with the assistance of mRNA closed-loop, for many of the steady-state initiation events (Fig. 6a). Alternatively, eIF4F could bind the cap already as part of an SSU complex, as eIF4F can be efficiently isolated from high-salt ribosomal washes but not from ribosome-free cytosolic fractions[219, 220].

Other factors can bind the cap in the cytoplasm to stimulate or inhibit translation. At least during initial rounds of initiation, the predominantly nuclear cap-binding complex (CBC)[221] can be in play; it can also interact with eIF4G and support initiation, although the CBC-eIF4G interaction was found to be dispensable in yeast[222] compared to mammals[223]. Upon thermosensitive eIF4E inactivation in yeast, CBC fails to support high levels of translation[224], leading to low levels of translation of select mRNAs which are sufficient to support non-dividing cells[225]. Metazoans have additional eIF4E-like variants expressed from eIF4E2 (also known as 4EHP) and eIF4E3 genes, which are distinguished by their inhibitory action on translation. 4EHP binds cap but not eIF4G, although its cap affinity is relatively low[226]. While 4EHP can bind the same nuclear transporter as eIF4E (eIF4E1), eIF4E-T, it is not dependent on it for transport and does not revert to cytoplasmic processing bodies or stress granules during cell stress[227]. 4EHP can bind growth factor receptor-bound protein 10-interacting glycine-tyrosine-phenylalanine domain proteins 1 and 2 (GIGYF1/2) to form stabe translation suppression complexes, which prevent excessive translation (and lethality) in mice embryos[228, 229]. Its cap binding activity may be increased by binding to eIF4E-T, and it was also shown to increase micro RNA-directed translation inhibition by the carbon catabolite-repression 4-negative on TATA-less (CCR4-NOT) complex[230]. While conditional knockout of eIF4E3 in mice showed no pronounced effects[231], eIF4E3 was demonstrated to bind cap in a specialised manner which excludes hydrophobic interactions but augments other bonds (electrostatic and van der Waals)[232]. eIF4E3 may be a direct eIF4E (eIF4E1) competitor, alleviating stimulatory effects of eIF4E on certain mRNAs and thus preventing excessive pro-survival and proliferation-inducing activity of eIF4E, effectively being an oncosuppressor[232]. Finally, as recently discovered, eIF3 can also bind directly to the cap, through interactions with its eIF3d subunit[233], and/or also possibly *via* eIF3l subunit[93]. In the case of eIF3d, the resence of a specific stem-loop structure in mRNA induces the 'open' state of the eIF3d, rendering it competent for cap binding[233]. Conversely, removal of eIF3 from this stem-loop during scanning will likely break the eIF3-cap interaction, due to a loss of eIF3d affinity to the cap (see also below).

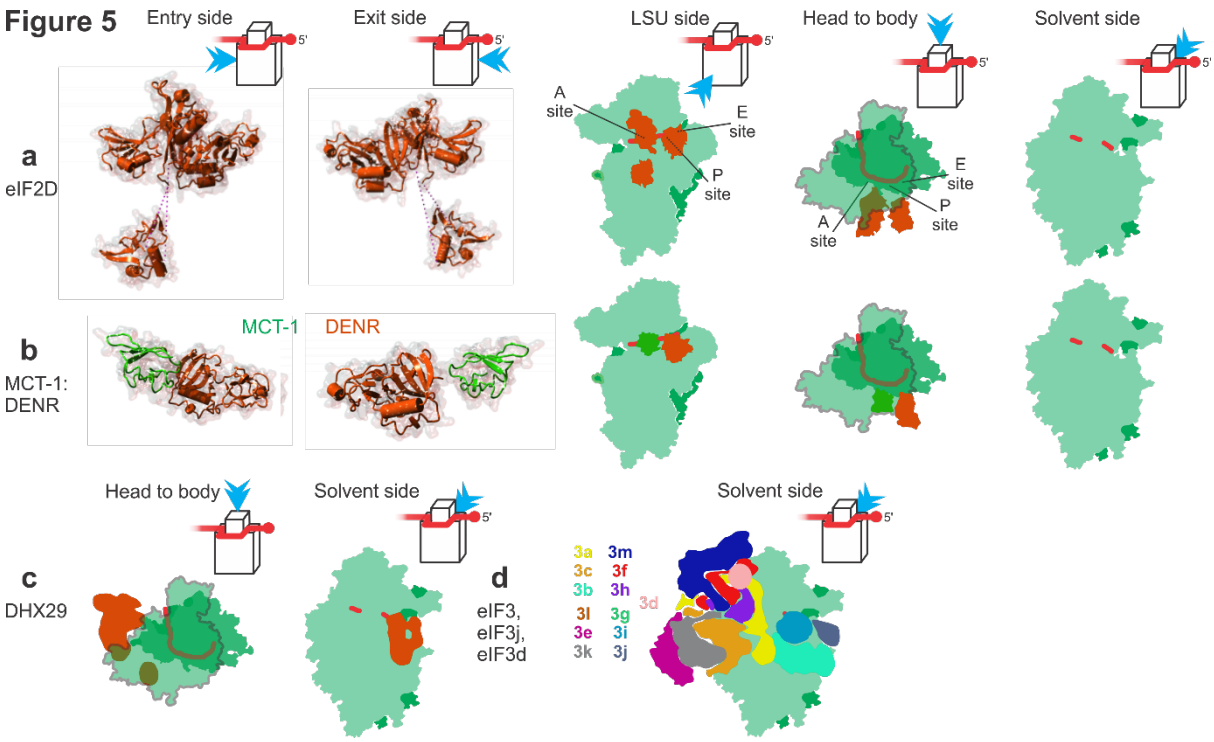

Figure 5. Structures and schematics of ribosomal localisation of some of the additional initiation components including an additional configuration of eIF3, with eIF3j in the entry of the mRNA-binding cleft of the mRNA-free SSUs. Designations and SSU schematics are as in Fig. 3. (a) Cryo-EM structure of human eIF2D bound to the human SSU (left)[105]. Outline of the human eIF2D on yeast SSU (SSU outline as described in Fig. 3); alignment of structures performed by the 18S rRNA trace (right). (b) Crystal structures of human density regulated re-initiation and release factor (DENR; C-terminal half, amino acids 110-198) and multiple copies in T-cell lymphoma-1 (MCT-1) bound to the human SSU (left)[234] and the outline of these factors shown on yeast SSU aligned to the human SSU as in (a) (right). (c) Cartoon of the cryo-EM density localisation of rabbit DHX29 in complex with SSU, eIFs 1, 1A, GMP-PNP:2:Met-tRNA$_i^{Met}$ and 3 modified from the original publication[235] and shown on the yeast SSU outline. (d) Cartoon of eIF3j, eIF3i and eIF3b positions on the solvent SSU side near mRNA entry as observed in the mRNA-free '43S' complexes[83]. A tentative localisation of eIF3d shown as pink circle. Modified from the original publication[83] and shown on the yeast SSU outline and the other eIF3 subunits as in Fig. 3g.

Assembly of a 'multi-factor complex' (also 'multifactor'; MFC; eIF1:(GTP:eIF2:Met-tRNA$_i^{Met}$):eIF3:eIF5) away from the ribsome and mRNA has been described as another early initiation sub-step in yeast[236, 237] and in mammals[238]. The MFC then binds to the SSU to form a '43S' complex or 'native' SSU, which then attaches to eIF4F at the cap (Fig. 6a)[238]. However, it is not evident that such sequence of events represents the predominant initation route. Strong direct interactions of eIF3j at the mRNA entry and eIF1 in the P-site directly with SSU, and eIF1 with N-terminal part of eIF3c near the mRNA exit were proposed to explain the binding of MFC to the SSU[83]. The suggested role of MFC in producing a more 'open' configuration of the SSU capable for mRNA attachment supports this sequence of events[239]. However, some abundant components such as eIF1 and eIF1A can also bind the SSU independently of the MFC[240]. Further, assembly and loading of the MFC (and TC) is not mandatory for commencing the initiation process *per se*. This follows from observations of re-

initiation following translation of uORFs. For example, following uORF1 translation within the 5' UTR of *GCN4* mRNA in yeast, post-termination SSUs remain attached to the mRNA and resume scanning in the absence of TC (and consequently, MFC)[241-243]. From *in vitro* experiments with purified factors, we know that eIF5 (Fig. 4g) presence is not required for cap attachment and scanning and it can be added as late as after start codon recognition without loss of function[244, 245]. Met-tRNA$_i^{Met}$ can be bound to MFC when it loads onto the SSU, or it can join later, individually or as a part of TC[238]. The particular timing and extent of attachment of 'general purpose' initiation factors that bind SSUs less tightly or are not ubiquitous, such as eIF4B, eIF4H, DDX3, DHX29, is also not known. It might well be that in live cells there is no single sequence of factor binding events during cap-dependent SSU attachment that is applicable to all mRNAs and in all situations (similar to early proposals for prokaryotic initiation)[246]; this would have functional implications on the control of different mRNAs. Transcriptome-wide *in vivo* evidence is needed to address these uncertainties.

Loading of SSUs on mRNA

The apparent processivity of scanning and the precision of start codon recognition imply that mRNAs cannot dissociate from scanning complexes with ease, suggesting a locking mechanism permissible to linear sliding of mRNA. One of the first suggested explanations was a 'threading' mechanism of mRNA attachment, where the mRNA 5' end is inserted through a ring-shaped opening in the initiating SSU[247, 248]. However, the discovery of IRESes and m^{6}A-mediated initiation, the cap-binding activity of eIF3d, and the translation of naturally occurring circRNAs, all indicate a more lateral loading of mRNA. It can be argued that eIF4E is located near the SSU platform, close to its E-site and towards the solvent side of the SSU (Fig. 4e; further discussed in the section on scanning below). This view is based on the location of the 5' (outbound) portion of less flexible mRNAs in SSU complexes such as those involving IRESes[180, 249, 250], the crosslinking of upstream mRNA portions with eIF3a, eIF3d and SSU proteins S26, S28[251], and the possible location of the eIF4G binding site for eIF4E in proximity to eIF3e[91, 252, 253], eIF3c and eIF3d[91, 253]. Approximately the same SSU location is designated for eIF3d, which can be considered a functional analogue of eIF4E for *JUN*-like mRNAs[81]. The small size of eIF4E and the interaction with eIF4G through its dorsal surface (Fig. 4e), also make a location of eIF4E close to the P-site decoding centre plausible, leaving little to no gap between the 5' end and the 5' UTR sequence inspected by the decoding centre of the scanning SSU (Fig. 6b).

The overall configuration of the early initiation complex in this case would include mRNA bound with eIF4E (in the form of eIF4F), eIF1A and eIF1 near the mRNA-binding cleft of the SSU, and eIF3 or MFC. Upon SSU binding to the cap and accommodation of mRNA in the mRNA-binding cleft of the SSU, a structural rearrangement of the initial complex ensures that mRNA becomes fully interlocked in the structure. The nature of the rearrangement and the trigger event are incompletely understood; however, detachment from the cap structure (see below) can be a coinciding signal and adoption of eIF1A interactions that bridge SSU head and body, as well as complete accommodation of TC, can form the initial mRNA 'latch'. The proposed cooperative displacement of eIF3j from A-site by eIF1, eIF1A and mRNA[72, 254] and eIF3b binding nearby eIF2 at the intersubunit SSU side[179] can also be the signatures of the rearrangement.

An alternative model more akin to the original 'threading' proposal postulates eIF4E localisation near the mRNA entry site of the SSU (at the solvent side closer to the A-site) was also suggested (Fig.

6c)[93]. An entry-proximal eIF4E position is supported by the ability of the mammalian *in vitro* initiation system to recognise initiation codons very close to the mRNA 5' end (1-2 nt) without apparent back-scanning[93]. In this case, mRNA is supposed to be 'extruded' into the pre-formed channel of the initiating SSU after the initial binding. Despite their differences, both models imply two distinct sub-steps of the process, initial mRNA-cap:eIF4F:initiating SSU interactions that are subsequently rearranged into a scanning-competent interaction with mRNA locked in the SSU independently on the cap structure. The position of the complete eIF4F, or even just the full-sized eIF4G in this complex, remains an important unanswered question; more precise localisation of eIF4G would allow to hypothesise on both, the mechanism of mRNA loading on the SSU and the scanning motion (see below).

Figure 6

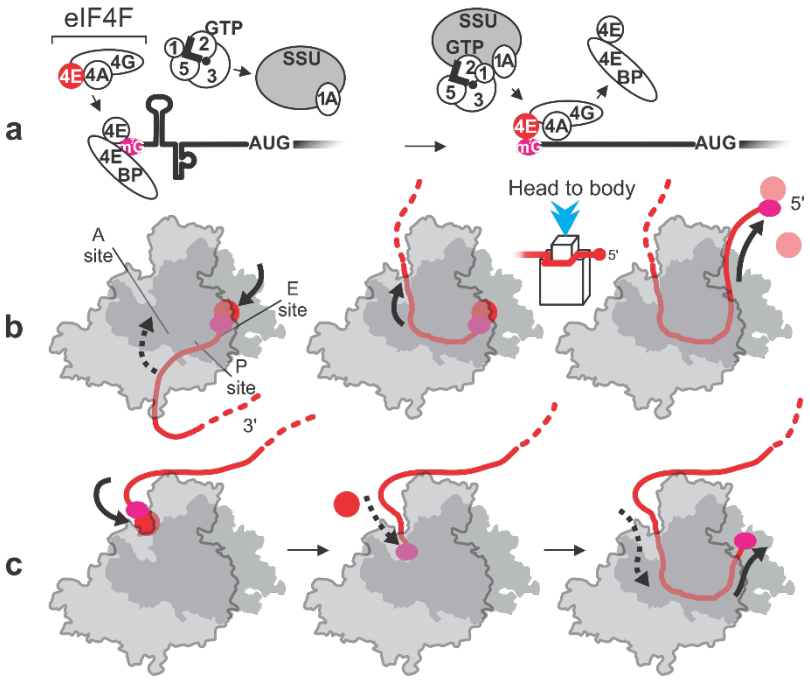

Figure 6. Alternative models for cap-dependent SSU attachment to mRNA. (a) Schematic of interactions between SSU and eIFs at the cap structure. (b) Model of lateral mRNA attachment to the SSU. eIF4E (red) bound to mRNA cap (purple) first attaches near the mRNA exit site, at the solvent side of the SSU near the head-to-body junction. The 3'-ward portion of mRNA is then 'slotted' laterally into the mRNA binding cleft. Once mRNA is stably bound, eIF4E:SSU and likely eIF4E:mRNA interactions are broken as a result of rearrangements upon commencement of scanning, as depicted by possible cap-bound or 'free' eIF4E molecules (red, semi-transparent). Solid arrows indicate completed, and dashed – continuing or anticipated, movemets or processes. (c) Model of mRNA 'extrusion' into the SSU (colour scheme and indications as in (b)). Cap-bound eIF4E first attaches near the SSU mRNA entry. The mRNA then detached from eIF4E and is sequentially relocated (pushed) into the SSU mRNA-binding cleft, first reaching the A-site and continuing to P- and E-sites, and eventually to the mRNA exit site of the SSU. In this case, eIF4E is required to dissociate from the cap structure after mRNA attachment to the SSU. SSU schematics as in Fig. 3.

Release of the cap from translating ribosomes

To allow for mRNA to be translated by multiple ribosomes (as observed by the formation of polysomes), SSU-cap interactions must be broken at some point during translation to enable a new SSU to bind at the 5' end of mRNA. Historically, alternative 'cap-tethered' or 'cap-severed' models were hypothesised for this process. In the cap-tethered model the 5' cap would remain in contact with the initiating SSU at least until the completion of the initiation. This model is compelling as no additional mechanisms are required to explain the SSU detachment from the cap, which would simply be a consequence of the release of the initiation factors upon the assembly of elongating ribosomes. However, systematic increases of the 5' UTR length of reporter mRNAs did not affect protein yield as measured in yeast cells[255]. Provided that availability of active eIF4E and '43S' complexes for attachment to mRNA caps was not a dominant limiting factor in these experiments, this would again imply that multiple SSUs can simultaneously traverse 5' UTRs[255].

Early biochemical *in vitro* evidence using edeine, which renders scanning 'infinite' by attenuating recognition of start codons, had also suggested that multiple SSUs can scan an mRNA simultaneously[256]. These experiments employed a feature of translation complexes, namely that SSUs as well as full ribosomes protect their 'footprint', the mRNA region they are attached to, from nuclease digestion[257-259]. These ribosome footprints can be physically recovered and analysed for footprint size and, potentially, location along mRNAs[259-261,262-264]. For example, this feature was used to discover pausing and stacking of elongating ribosomes, showing that tightly packed disomes, trisomes *etc.* protect proportionally longer mRNA fragments[260]. SSU footprints were observed during translation initiation as well, although their positions could not be retrieved unambiguously with methods of the time[262-264]. The combination of this approach with high-throughput sequencing gave rise to the highly successful 'ribosome profiling' method[50, 259, 265], which was at first limited to recording ribosomes (stalled with antibiotics) during translation elongation. However, the recently developed translation complex profile sequencing (TCP-seq; Fig. 7) method[51, 266] added a formaldehyde crosslinking step to the approach to preserve and detect footprint distribution of any of the translation complexes, including that of initiating SSUs[51, 266]. TCP-seq showed no negative correlation between 5' UTR length and SSU start codon occupancy in live, exponentially growing yeast cells, and no increased 5' end proximal accumulation of SSUs as might be expected from cap-tethered scanning (strong cap:eIF4E:eIF4G:SSU interactions resulting in linger SSU dwell time at 5' ends). Moreover, a subset of SSU footprints representing late intermediates of start codon recognition were extended further upstream to -30 nt on mRNA, consistent with the presence of a second queued-up SSU (Fig. 7a). These observations were made in meta-gene analyses of transcriptome-wide data as well as for a subset of individual mRNAs, and are consistent with the concomittant traversal of 5' UTRs by multiple SSUs. These findings strongly suggest that scanning can take place in a cap-severed mode, although they do not formally exclude the co-existence of cap-tethered mode[51, 266].

Interestingly, recent biochemical observations demonstrated that breaking any link in the mRNA cap:eIF4E:eIF4G:eIF3 interactions or absence of eIF4A effectively turns eIF4E or eIF4E:eIF4G into a competitive inhibitor of initiation[93]. Even more intriguingly, eIF4E was absent from the cap during the later stages of initiation as determined by UV-crosslinking[93], although it is not fully certain whether eIF4E first detached from the cap or from eIF4G with subsequent decrease of the affinity to the cap. Taking into account these data, it may be expected that eIF4E, eIF4A, eIF4G and eIF3 actively participate in the mRNA loading onto the initiating SSU and the subsequent detachment of

the initiating SSU from the cap occurs immediately upon the complete accommodation of mRNA (Fig. 6b,c). This may involve some form of eIF4F disassembly, which is proposed to be triggered by binding to the cap structure[84]. Similarly to the mechanism known for prokaryotes, whereby the first elongation steps destabilise Shine-Dalgarno interactions[267], cap detachment in this case may involve an active (energy-dependent) rearrangement coinciding with the commencement of the 3'-ward SSU motion. Due to the transient nature of the early scanning complexes, determining the exact sequence of events during cap-dependent mRNA attachment will require finely resolved single-molecule kinetic evidence, such as for the eIF4E-cap interactions[90] and initiation on Cricket Paralysis Virus (CrPV) and Hepatitis C Virus (HCV) IRES structures[162, 268, 269].

Figure 7

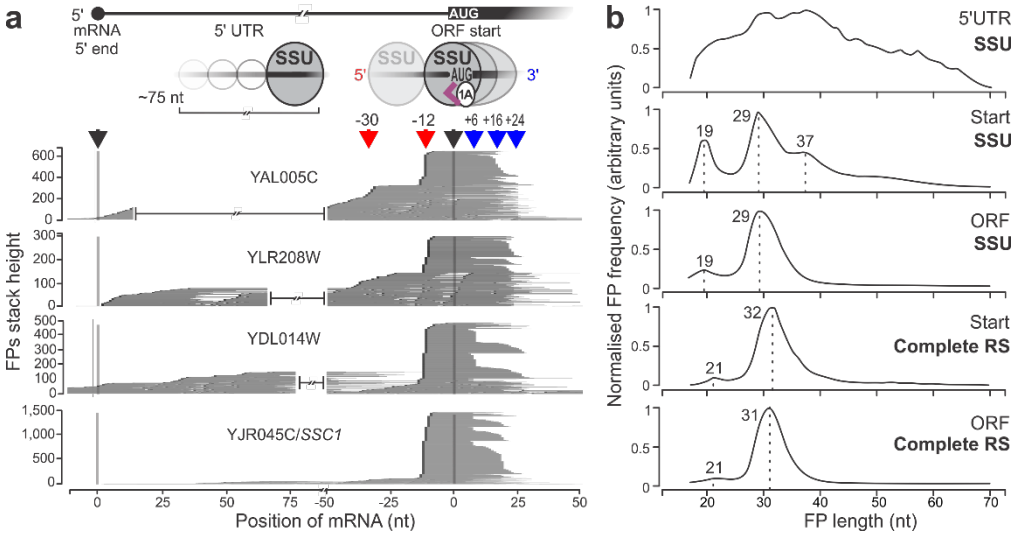

Figure 7. *In vivo* capture of translation initiation intermediates in yeast cells using TCP-seq. (a) Footprints (FPs) of the SSUs fixed within 5' UTRs and at start codons of selected highly efficiently initiated mRNAs. FPs are aligned on mRNAs either by the annotated mRNA 5' end (left part of X-axis before break) or by the start codon in the region corresponding to the +/-50 nt from the first nucleotide of the start codon ('0'; right part of X-axis after break). Metagene modal 5' (red) and three 3' (blue) FP extremities (corresponding to the stages of start codon recognition; see Fig. 9 and the corresponding text) are marked. (b) FP length characteristics for SSU complete ribosome (RS) complexes depending on position along mRNAs. TCP-seq data and some graphic elements were modified from Archer *et al. Nature* 2016[51].

SCANNING

Scanning commences once the SSU has been loaded onto the mRNA 5' end. Key mechanistic aspects of scanning are a movement of SSUs along the mRNA, and continuous inspection of mRNA bases for Watson-Crick interactions with the CAU anticodon of the Met-tRNA$_i^{Met}$ (Fig. 1a and middle part of Fig. 2)[270]. Classic biochemical evidence indicates that the SSU motion is 5'→3' directional, rather than occurring merely by random bidirectional diffusion[255, 271]. However, a direct characterisation of scanning intermediates has proven difficult due to the highly dynamic nature of the process. There are thus several intriguing open questions such as what 'drives' scanning and how is a net 3'-ward movement of the SSU achieved over 5' UTRs.

Factor requirements for scanning

An operational distinction can be made between scanning as it occurs on completely linear (model) 5' UTRs and (natural) mRNA leaders which feature varying degrees of structure. The former can be traversed without energy expense whereas ATP (or NTP) hydrolysis will be required to ensure progress through the latter. Accordingly, translation of mRNA 5' UTRs of poly(U) but not native sequences can occur in *Artemia salina* embryos where eIF3 is not present (and thus eIF4F is unavailable for initiation)[272]. All eIF4-group proteins were not required for initiation on a synthetic mRNA exhibiting an unstructured 5' UTR composed of (CAA) repeats; however, the other features typical for scanning, such as preferential recognition of the 5'-proximal start codons, were preserved[273]. Recognition of start codons is possible with a minimal set of eIFs 1, 1A and 2 on mRNAs comprised of (U,C) sequences in yeast[274] or featuring a poly(A) 5' UTR in a mammalian translation system[275]. SSUs that remained attached to mRNA after termination were able to recognise nearby start codons in both directions (3' but also 5' through so-called 'backward' or 'retrograde' scanning) with the eIFs 1, 1A, 2 and 3 present. However, retrograde scanning was suppressed when eIFs 4F, 4A and 4B were added[276, 277]. This suggests that SSUs can lock on mRNAs, remain attached and slide randomly in the presence of eIFs 1, 1A, 2 (and 3), while eIFs 4F or 4G, 4A, 4B and ATP hydrolysis provide a 3' directionality to their motion. Other RNA helicases have been implicated to further assist scanning on highly structured mRNA leaders[278-281]. Accordingly, while SSUs can navigate moderately structured 5' UTRs aided by eIFs 1, 1A, 2, 3, 4A, 4B, and 4F[273], additional 'support' in the form of DHX29[280, 282], DDX3X[282, 283], or potentially DDX3[284], DHX9[285] and DHX33[286], and others, is required for more structured mRNAs.

More structured 5' UTRs have long been known to inhibit translation[287], including the original *in vivo* observation of inhibition by a ~-30 kcal/mol hairpin[288]. In a purified system with eIFs 4A, 4B and 4F, hairpins with free energy from ~-20 kcal/mol appear to be inhibitory to translation initiation[280], even though the same factors in the absence of initiation complexes were able to destabilise much stronger duplexes[88], even up to ~-150 kcal/mol, by sequentially separating ~11 nt per step with sub-steps down to as little as 2 nt[86]. Therefore, the activity of group 4 eIFs appears to be tightly modulated in the context of SSU scanning, such that their mechanism of action may differ from that of the SSU-free form. For the better-studied example of DHX29, its relative low abundance (~10-fold lower than that of SSUs)[280] suggests an auxiliary role in the scanning, while its localisation in the entry side of the mRNA-binding cleft (adjacent to the A-site) and strong direct interaction with SSUs (and not eIF4G) suggest a different mechanism compared to eIF4A[107, 235, 280, 282]. However, given the high abundance of eIF4A in the cell and its known capacity to destabilise secondary structure through 'mass action' by binding to the single-stranded RNA in its ATP-activated form, rather than by processive helicase activity[86, 289, 290], the prevalence and input of the additional RNA-helicases into translation, as well as their potential allocation to specific mRNAs in live cells, remain to be fully elucidated.

Structure of scanning complexes

Advances in structural modelling of eukaryotic initiation complexes combined with biochemical and genetic evidence acquired in the last decade make it possible to outline several likely structural features of the scanning process (Fig. 8a). Modelling suggests that SSUs adopt a configuration within

scanning complexes that is distinct to factor-free SSUs and complexes involved in later steps of initiation, or SSUs as part of the elongating ribosomes[69, 81, 83, 108, 291].

In all SSU structures pertaining to 'scanning', if the resolution allows its modelling, eIF1 occupies the area immediately below the P-site and makes direct electrostatic contacts with rRNA[83, 205, 292, 293]. This 'insertion' of eIF1 between tRNA and SSU is supportive of its main function in promoting the fidelity of start codon selection by destabilisation of codon-anticodon interactions[66, 205, 292, 293]. The central, well-structured part of eIF1A, another small intersubunit-side bound factor, bridges the SSU head and body directly over the A-site and encloses the mRNA in the mRNA-binding cleft of the SSU, a feature deemed responsible for the processivity of scanning motion. eIF1A localisation at the A-site is also hypothesised to prevent tRNAs from binding to the SSU A-site, a widely conserved role also performed by its bacterial counterpart IF1[66, 293]. The N-terminal portion of eIF1A is distinctively less structured in the 'scanning' complexes[66, 293]. eIFs 1 and 1A are known to bind to the SSU cooperatively, but this is commonly explained *via* their local effects on the nearby SSU rRNA (affecting mostly helix 44), and possibly by interactions with the other factors, rather than their direct binding to each other[293, 294].

eIF2α locates to the E-site in the scanning complexes but is less deeply inserted into the mRNA-binding cleft of the SSU compared to the other initiation complexes. eIF2α does not make contacts with the -3 nt position of mRNA, which is a critical component of the consensus start codon nucleotide context (see below in the 'Recognition of start codons and joining by the large ribosomal subunit' section). eIF2β and eIF2γ do not make much contact with the SSU and mostly extend into the solution at the intersubunit side[205, 235]. Importantly, Met-tRNA$_i^{Met}$, bound to eIF2, adopts a scanning-specific conformation where it is reaching less deeply in the P-site overall, its anticodon is laterally more distant from the P-site mRNA (by ~7 Å), contributing to the wider configuration of the P-site, compared to the other initiation complexes[177, 205]. While the Met-tRNA$_i^{Met}$ maintains its main contacts with the SSU head, head motion (see below) bends the anticodon stem-loop of the Met-tRNA$_i^{Met}$ and laterally distances it from the SSU body[177]. Deeper positioning of Met-tRNA$_i^{Met}$ into the P-site is prevented by eIF1 at this stage.

Consistent with early findings[250, 295, 296], the main 'core' of eIF3 assembled from PCI/MPN domains (eIF3 a, c subunits in yeast; a, c, f, h, e, k, l, m in mammals) resides on the solvent side of the SSU, closer to the exit side of the mRNA-binding cleft and between the head and body of the SSU. A second volume of compact density can be attributed to the eIF3b, eIF3g, eIF3i, eIF3j subunits localised on the solvent and LSU sides of the SSU, but near the entry side of the mRNA-binding cleft[83, 107, 177, 179, 235, 297]. Thus, eIF3 remarkably engulfs SSU from both the solvent and LSU sides, with the extensions of its 'core' a, c subunits, and mRNA-entry b, g, i assembly reaching eIFs 2 and 5 at the mRNA exit side, and 1A at the entry side, correspondingly (see Figs. 3f,g)[177, 179]. eIF3a and eIF3b subunits are thought to provide relatively thin and flexible link between these eIF3 substructures.

While it was not characterised as a highly mobile factor earlier, recent studies show much apparent movement of many eIF3 domains and sub-assemblies across the SSU in synchronisation with different initiation stages. For example, cryo-EM reconstructions of near-native 'scanning' complexes derived from non-fractionated lysate did not reveal eIF3j density in the entry side of the mRNA-binding cleft[179], unlike other reconstructions where no mRNA was present[297]. These data are

consistent with the hypothesis derived from biochemical experiments that eIF3j can function to antagonise binding of mRNA and thus can become lost from the complexes altoghether or detached from the SSU mRNA-binding cleft early on during initiation[72], as confirmed by its absence in the initiation complexes reconstituted at start codons[245]. Further, relocation of eIF3b to the LSU side near mRNA entry and below mRNA-binding cleft, where it may interact with eIF2γ and additionally stabilise position of eIF2 during scanning, has been reported as one of the large-scale rearrangements (Fig. 3g)[179]. Another notable difference to the SSUs unbound with mRNA is the tilting of the whole eIF3 'core' PCI/MPN assembly down from the SSU head[179].

At least some of the mammalian scanning complexes may additionally contain DHX29 interacting with eIF3 subunits b and g directly in the entry site of the mRNA-binding cleft (Fig. 5c)[107]. There may be other constituent parts to the scanning complexes that were either not included into the *in vitro* complex preparations or could not modelled due to insufficient resolution. For example, in some cryo-EM reconstructions, electron density contacting eIF2α, eIF2β, eIF1 and possibly Met-tRNA$_i^{Met}$ can be also attributed to eIF5[205], but a more definitively resolved position of this factor is currently not available.

The overall mRNA path in the scanning complexes may be similar to the other ribosome-mRNA structures, although it lacks the pronounced kink between A- and P-sites characteristic of ribosomes with A- and P-site paired tRNAs, or bacterial translation complexes. It is widely accepted that this smoother passage may facilitate SSU sliding along the mRNA, which is a requirement for scanning[66, 177, 205]. Interestingly, mRNA wraps around at least half of the SSU between head and body, with the inbound and outbound 'trajectories' of mRNA so close together they could overlap at the solvent side[177, 205]. The mRNA is less constrained at the entry side relative to the exit side, where the mRNA-binding cleft is occluded by the densities of eIF1A in the P-site and further 3'-ward by Met-tRNA$_i^{Met}$ and eIF1 at the P-site[177, 205]. The 'head' of the SSU appears to be rotated clockwise by about 3-8°, placing the head P-site slightly towards the body A-site positions compared to the 'empty' SSUs, which is hypothetised to aid in avoiding a steric clash with the Met-tRNA$_i^{Met}$ anticodon[66, 177, 205]. Cryo-EM reconstructions, some of which included a model mRNA, also suggest a pronounced movement of the SSU head further away from the 'body' towards the solvent side of the SSU[177, 240]. Overall, configuration of the SSU described above is most commonly referred to as 'open, scanning-competent' or 'P_{OUT}' (suggesting a more peripheral, outer localisation of Met-tRNA$_i^{Met}$ relative to the SSU P-site). Some cryo-EM reconstructions notably feature the open 'latch' near the entry side of the mRNA-binding cleft of the SSU, which is formed by the helixes 34 of the head and 18 of the body of the SSU (Fig. 8a)[177, 240].

Many features observed in the structures of the putative scanning configuration are consistent with the available crosslinking, protection and mutagenesis data, and hence a more complete picture can be drawn by merging the information from all sources. For example, eIFs 1 and 1A have been previously mapped by the directed hydroxyl radical cleavage method to their respective localisations at the P and A-sites[298, 299]. The role of eIF1 in destabilising codon-anticodon interactions during scanning has been thoroughly investigated[300-304]. The eIF1A N-terminal and C-terminal extensions (unstructured in the 'free' eIF1A form)[304] have been shown to stabilise codon-anticodon interactions and the 'open', scanning-competent configuration of the SSU and TC, respectively[302, 305-307]. Conversely, the eIF1A N-terminal portion is delocalised in the scanning configuration, while the C-

terminal extension is involved in the interactions at the SSU P-site[304]. eIF3c has been implicated in binding to eIF1 and eIF5 in the MFC and possibly in 'scanning' complexes[308-312], with its N-terminal extension reaching towards the P-site[64, 83]. Indeed, eIF3c (likely through its interactions with eIF1 and eIF5) is known to affect the fidelity of the start codon selection[310, 313]. Nuclear magnetic resonance (NMR) chemical shift perturbation suggests that the N-terminal extension of eIF3c partially overlaps with eIF1 interaction surfaces on the SSU and thus may moderate eIF1 function to destabilise codon-anticodon interactions[64]. These findings, combined with mutagenesis and analytical ultracentrifugation data, suggest that the C-terminal portion of eIF5 may bind the N-terminal part of eIF1A in the scanning complexes, resulting in increased affinity of the complex to eIF1 *via* eIF5:eIF1 interactions, and in decreased binding of the C-terminal part of eIF5 to the N-terminal part of eIF2β. This lack of tight eIF2:eIF5 interaction may cause inhibition of GTP hydrolysis in the TC during scanning, which would prevent premature fixation on poorly recognised triplets[64, 302, 312]. Thus, while eIF1A is one of the most conserved initiation factors and is a direct homologue of prokaryotic IF1, it appears to have acquired eukaryote-specific roles in coordinating scanning through its C- and N-terminal extensions. The factor is therefore remarkably persistent during the whole process of initiation, linking eukaryotic scanning with the later stages of initiation that are well-conserved across all life.

In vitro reconstitutions of the 'scanning' complexes and their probing with directed hydroxyl radicals produced at different locations of eIF1A demonstrated substantially more accessible rRNA in the A-site and P-site localised helices[304]. rRNA residues located more distantly to the A and P-sites near the entry side of the mRNA-binding cleft also displayed elevated accessibility, including helices 18 and 34 that form the mRNA 'latch' of the SSU[304]. Importantly, the observed less tight interactions of mRNA with SSUs in the reconstituted *in vitro* models of scanning complexes are recapitulated *in vivo* in a form of shorter nuclease protection observed on the entry side of the scanning SSUs, compared to the later stages of initiation and to the protection of elongating ribosomes with TCP-seq (Fig. 7)[51]. The minimal protection length of ~19 nt[51] appears overall concordant with, but somewhat lower than the 22 nt of the cryo-EM resolved mRNA[205], suggesting that some parts of the SSU-bound, less flexible mRNA are still accessible to the nuclease digestion. While this cannot be used to rule out the 'closed latch' configuration of the scanning SSUs, it strongly evidences higher accessibility of the mRNA in the entry channel of the SSU and lack of stable protection of mRNA in the entry side of the mRNA-binding cleft on average *in vivo*.

Overall, there are multiple indications that the structure of scanning complexes can be highly dynamic. The observed uncertainty of the entry channel configuration in part may be a consequence of the differences in the methods of preparation and in the overall composition of the reconstituted complexes. However, we may also expect large-scale functional molecular motions that depend on the energy expense during scanning, such as proposed for alterations between the 'open' and 'closed' states of the SSU induced by corresponding 'closed' ATP- and RNA-bound and 'open' eIF4A conformations[254]. In this case, different *in vitro* reconstitution models may artificially stabilise a particular conformation of the complexes (as often occurs, for example, in crystallographic studies), resulting in a somewhat different overall geometry. Most importantly, even the combined structural and biochemical data do not unanimously outline the position and possible orientation of eIF4F or eIF4G in any of the initiation complexes, including scanning. Of all eIF4-group factors, only the position of eIF4B was determined in yeast to be at the 'head' on the solvent side of the SSU, closer

to the exit side of the mRNA-binding cleft[196]. These and data on eIF4G interactions with eIF3 subunits c, d, e allow to hypothesise on the position of eIF4G[91, 252]. Because eIF4B can interact with eIF4A within eIF4F, and the main eIF4A and eIF3-binding sites are relatively close together in eIF4G[197], it may be expected that the central part of eIF4G co-localises near the eIF4B-binding site on the SSU. Even more speculative is the orientation of eIF4G on the scanning SSU, given that approximately half of the full-size eIF4G has a highly-elongated geometry and extends for ~200 Å, capable to connect virtually any two points on each SSU side[197]. Based on the closer location of the eIF3c, eIF3d-interacting portions of eIF4G to its N-terminus, compared to the more C-terminal location of eIF3e-binding site[91], the overall linear geometry of the eIF4G middle domain[197], and the mammalian eIF3 orientation on the SSU, the middle portion of eIF4G may be located with N-terminus up closer to the head on the back side of the SSU, with the C-terminal part reaching to contact eIF3e down at the body of the SSU (Fig. 4d, right). However, other possibilities have also been outlined[93], leaving the orientation of this factor on the SSU a major open question. Knowing the positions of the eIF4-group factors will be critical to discern the exact molecular mechanism of the 5'→3' motion during scanning.

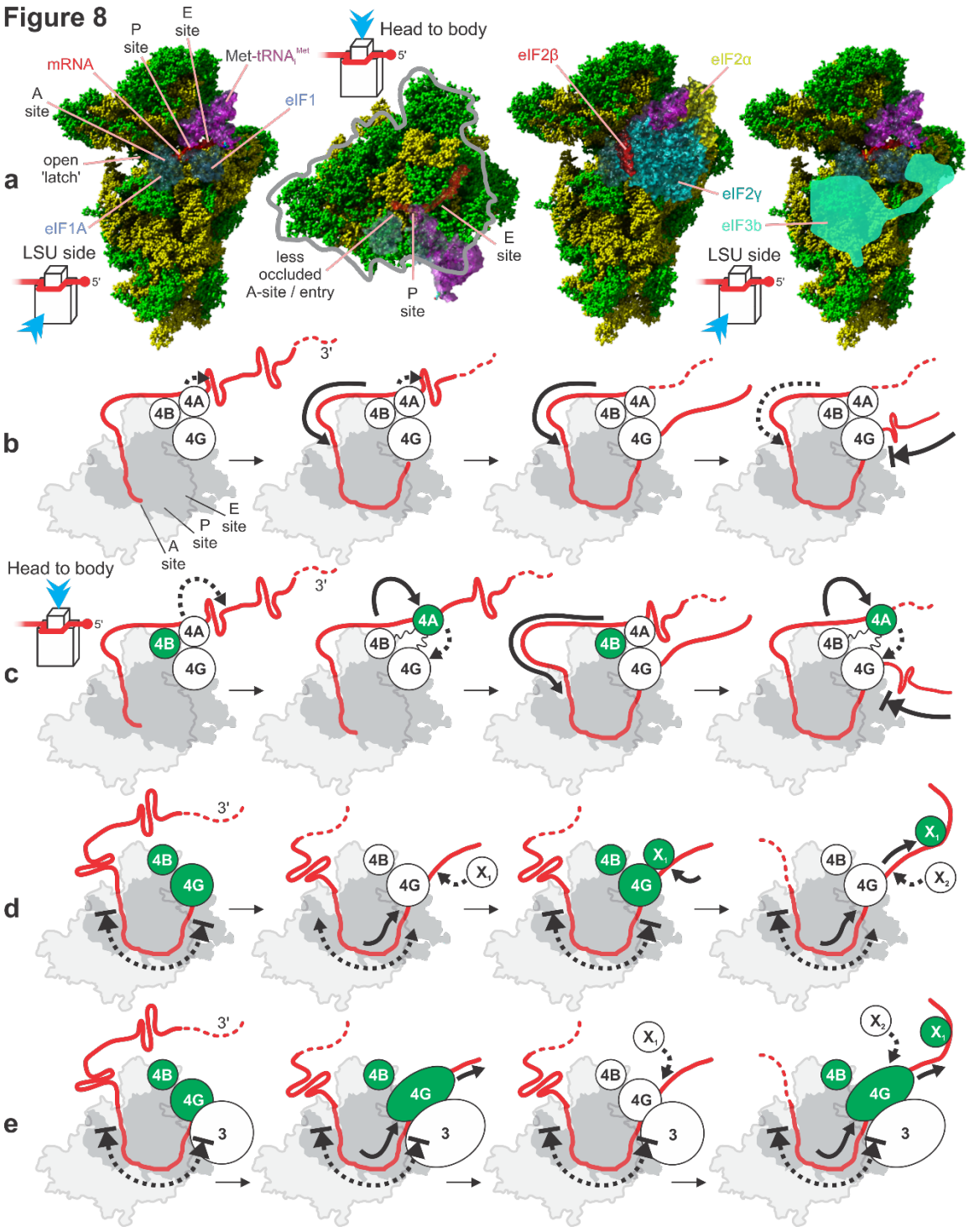

Figure 8. Models of scanning SSU configuration and possible determinants of scanning motion directionality. (a) Combination of the atomic cryo-EM reconstruction structure (PDB entry 3JAQ) and cartoon schematics of the scanning SSU with the scanning-conducive, relatively 'open' mRNA latch and widened and less obstructed mRNA entry marked. Met-tRNA$_i^{Met}$ is in the P_{OUT} conformation, leaning towards E-site and with a loose and more lateral positioning in the P-site. Surfaces of only eIF1, eIF1A (left) and these factors together with eIF2 or eIF3b (right) are shown for simplicity. Atomic ball-and-stick model of rRNA is shown in yellow and ribosomal proteins in green. Grey line on the head-to-body view outlines the SSU head. The mRNA position was taken from the 'closed' SSU

structure (PDB entry 3JAP) aligned with 3JAQ by the rRNA trace in the SSU body region. The superimposed eIF3b cartoon was taken from Fig. 3g. (b)-(e) Cartoons illustrating different concepts and models to explain 5'→3' directional motion during SSU scanning of mRNA. SSU schematics and indications as in Fig. 3. Possible alterations of states of higher (green) and lower (blank) factor affinity to RNA are shown where applicable. (b) eIF4-group factors perform mRNA 'unwinding' in front of the SSU as the structure of the initiation complex directs them to the incoming portion of mRNA (SSU entry) (left plot). The 3'-ward stretch of single-stranded RNA then allows the SSU to spontaneously relocate (diffuse) onto it (middle two plots). Secondary structure can refold upon the mRNA exiting SSU and ensure motion directionality, as no helicase activity is present at the SSU exit site (right plot). (c) eIF4-group factors perform RNA 'unwinding' in front of the SSU by cycles of clamping to the single-stranded RNA. eIF4B has a higher affinity to mRNA (green) while in close contact with eIF4A (left). Upon eIF4A conformational change, eIF4A re-binds to the downstream (incoming) portion of mRNA (green; middle left plot), and then restores its tight binding to the complex, bringing the downstream portion of mRNA along into the SSU and stimulating eIF4B high affinity to mRNA (green; middle right plot). The cycle then repeats (right plot). Note that (b) and (c) are most compatible with an entry-side 'threaded' mRNA loading at the beginning of initiation. (d) eIF4-group factors are sequentially lodged behind the SSU as it takes small 3'-ward advances due to the random (thermal) motion, and act as anti-rollback 'pawl' structures. All factors are tightly bound to the SSU, mRNA and to each other (left plot; green). Due to an induced conformational change, mRNA-bound factor(s) lose affinity to the rest of the complex, but not to mRNA. This allows 3'-ward SSU sliding over mRNA, with accidental and sequential unwinding of some of the downstream structure (middle left plot). When a sufficient exit portion of the single-stranded mRNA is exposed, a new molecule of mRNA-binding factor (X_1) re-binds it, preventing backward SSU sliding (middle right plot). The cycle repeats with the next RNA-binding molecule (X_2; right plot). (e) Similar to (d), but eIF4-group factors (eIF4G) and eIF3 also undergo a large-scale conformational change, possibly induced by the eIF4A enzymatic cycle, and actively pull out a portion of mRNA 3'-ward, after which they re-bind mRNA more proximally to the SSU. Note that (d) and (e) are most compatible with a lateral loading (slotting) of mRNA into the SSU mRNA-binding cleft, where cap-SSU interactions begin near mRNA exit site.

Possible determinants of scanning directionality

To explain the 3'-ward SSU motion on mRNA, two main concepts are currently known, which differ in the likely roles and localisations of the main eIF4-group factors in the scanning SSUs. The first concept has eIF4A 'unwinding' stable RNA helixes in front of the scanning SSU (in cooperation with eIF4G and eIF4B/eIF4H, and possibly another RNA-helicase or single-stranded RNA binding protein) (Fig. 8b)[7, 281, 314, 315]. These 'unwinding' factors would thus localise at or before the leading edge of the SSU, which may be called 'SSU-trailing' or 'pulled SSU' scanning. However, while the unwinding of the secondary structures of mRNA may indeed be required for the 3'-ward motion of the SSU over mRNA (given that only single-stranded RNA can be efficiently scanned), this model does not provide systematic answers for the directional, powered motion, likely conferred by the eIF4-group factors[86, 88, 93, 276, 316, 317]. The re-assembly of RNA structure behind scanning complexes could explain directionality. However, one cannot expect an even distribution of secondary structure or RNA-protein interactions across the entire length of 5' UTRs, and back-scanning is not readily observed on unstructured mRNAs in the presence of eIF4F, eIF4A and ATP[93, 276, 277]. More experiments measuring

the dynamics of scanning will be required to determine if directional scanning is efficient on the unstructured mRNA. Alternatively, still with the scanning 'motor' leading the SSU, directionality could be conferred by the eIF4-group factors continuously re-binding more 3'-proximal single-stranded portions of mRNA (and consequently 'unwinding' or stabilising them in the single-stranded form), while they bind or remain attached to the SSU, with mRNA 'fed' into the mRNA-binding cleft of the SSU (Fig. 8c). This mechanism would thus resemble the well-studied kinesin locomotion along microtubules[318, 319]. In this case, eIF4-group factors would serve not only as the 3'-directed RNA-helicases, but also as the ratchet-and-pawl structure preventing thermal roll-back of the scanning SSU, a function postulated based on the known alterations of eIF4A affinity to mRNA in the ATP and ADP-bound or the cofactor-free states. The observed intrinsic preference of eIF4A in complex with eIF4G to the 3'-portions of single-stranded oligonucleotides may compliment the mechanism of directionality in this case[88], whereas the reciprocal alterations of high and low affinity of the SSU and eIF4A to mRNA[254] may explain a kinesin-like step-wise directional advance. However, the appeal of this model is lessened given that the persistence length of single-stranded polyribonucleotides falls in the range of 3-4 nt[320, 321]. Thus, mRNA would need to be tightly 'channelled' in the scanning complex to support the powered motion and not bulge out of the mRNA-binding cleft of the SSU and between it and the helicase site of action, an assumption that is not readily compatible with the more 'open' entry side configuration of the *in vivo* and *in vitro* SSUs, and more tight interactions with mRNA in the P-site and near the mRNA exit.

The second concept involves the primary action of eIF4A (or its functional substitute) while located behind the SSU relative to mRNA, in what can be called an 'SSU-leading' or 'pushed SSU' scanning. In this case, the directionality of motion would be selected by eIF4A or other associated factors (such as eIF4B or eIF4H) from the random (thermal) short-distance SSU movements along mRNA, by strongly binding to mRNA and preventing backward SSU motion in the ATP-bound state[197, 250, 322]. Re-binding of the new 'motor' factors in the gap of single-stranded RNA upon spontaneous 3'-ward relocation of SSU would thus serve as the 'pawl' and result in the sustained, directional locomotion (Fig. 8d). Thus, the SSU in this case is an integral part of a complex RNA helicase machine, consistent with the proposed function of ribosome as a processive RNA-helicase in prokaryotes[323, 324]. The lodgement of the factors on mRNA behind SSU in this case may additionally provide the necessary 'power stroke' of the locomotion by actively displacing SSU 3'-ward (Fig. 8e). This latter scenario is similar to the translocation of the complete elongating ribosome, or the addition of the newly synthesised residues during DNA replication coupled with the activity of processive DNA helicases, which also use an anti-rollback mechanism to select for directionality of motion[325].

The notable structural resemblance of mammalian eIF3 and also its direct homology with the proteasome lid and Constitutive photomorphogenesis (COP) 9 signalosome are often discussed[81, 326], and raise questions why such a complex structure was duplicated during evolution. What is perhaps less appreciated, is the remarkable mechanistic similarities of the processes in which eIF3 and proteasome lid are involved. In the proteasome, the eIF3-like proteasome, COP9, Initiation factor 3 (PCI)/Mpr1/Pad1 N-terminal (MPN) core regulates recognition of the ubiquitinylated portion of the protein, its subsequent irreversible binding ('commitment') to the proteasome, and removal of the ubiquitinoylation once the first unfolded portion of the protein enters the proteasome core[327]. The PCI/MPN lid, in complex with α-helical ring-shaped AAA-ATPases, is thought to provide energy for the protein unfolding by stronger binding of the unfolded chains in the ATP-bound state, and then to

participate in the sequential translocation of the unfolded peptide into proteasome[327]. The whole sequence of events is reminiscent of mRNA cap recognition, detachment from the cap, and the subsequent ATP-dependent pulling of mRNA. The most actively mobile proteasome subunit is Rpn11 located in the centre of the PCI domain assembly[327], and is homologous to the eIF3f[81]. The absence of eIF3f in yeast may be functionally compensated for by the eIF3a PCI domain portion that occupies a similar location and is proposed to substitute for the possible SSU-interacting functions[297]. Thus, it is tempting to speculate on a more active involvement of eIF4G and eIF3 PCI/MPN core in the large-scale motions that may be induced in these factors by eIF4A cycling through its 'closed' and 'open' states, while it is bound to eIF4G (Fig. 8e). Overall, the pushed-SSU model and the proteasome lid homology may be more supportive for the eIF4G localisation on the solvent side of the SSU and nearby mRNA exit (with the abovementioned caveat that its elongated shape allows it to reach between any points on one side of the SSU). eIF4G interactions with eIFs 4A, 4B and 4H, and relatively high abundance of these factors, further suggest a possibility of their multiple transient binding to mRNA behind the scanning SSU. In this case, possible dissociation and re-association cycles of eIF4F components driven by eIF4A-mediated ATP hydrolysis, as suggested in multiple studies based on the biochemical properties of these factors[84, 328-330], may explain controlled recruitment and release of the new 'pawl' factors behind the SSUs. However, the ratchet-and-pawl concept is not completely incompatible with the entry-side localisation of eIF4G-attracted eIF4A on mRNA either. Moreover, eIF4-group factors may in fact act on both, incoming and outbound portions of the scanned mRNA, where the structure of the incoming mRNA is destabilised by the additional helicases such as DHX29 or DDX3[284], and also eIF4A, which later is transferred to the outbound portion of mRNA.

Interestingly, *in vivo* TCP-seq data shows substantial heterogeneity of footprint sizes for scanning SSUs (ranging from ~17 to ~70 nt). The additional regions of protected mRNA are on the 5' side of the SSU (Fig. 7)[51]. This 'trailing tail' behind the scanning SSUs may be a result of the proximity to some large additional structures in the scanning complexes, such as eIF3 and eIF4G. The overall span of eIF4G potentially can cover single-stranded polyribonucleotide of a comparable length, but the extensions of 5' UTR to ~30 nt were reported to be sufficient to stabilise eIF3 binding[245]. However, even if the outbound mRNA is making tight contacts with these structures, it is difficult to explain relatively homogeneous distribution of the protected fragment lengths over the entire range (Fig. 7b), and the fast disappearance of this protection once SSUs arrive at start codons[51]. More likely, the additional 5'-ward protection is resulting from transient, multiple, but small mRNA-binding units, such as eIF4A or eIF4B, as outlined above. Defining the exact nature of the extended mRNA protection generated by the scanning SSUs thus appears critical to the understanding of the mechanism of scanning motion. Overall, the debate over what provides scanning directionality can be seen as part of a deeper fundamental issue. As it was already emphasised in the literature, there is no absolute certainty on the mechanism of action for even the well-studied, 'processive' replicative helicases. Both, the active duplex separation and the advantageous binding to single-stranded patches stripped by thermal motion, are probable[323, 331-333]. Solving the mechanism of scanning motion presents a unique opportunity to address this question for a larger macromolecular structure where the localisation of the helicase can be discerned.

Questions raised above can be expected to be even more intriguing to solve for translation initiation in higher Eukaryotes. Indeed, it is well-known that yeast 5' UTRs are short and somewhat less

structured compared to, for example, mammalian 5' UTRs[334]. Furthermore, the eIFs constituting the scanning machinery are more divergent in yeast compared to their mammalian counterparts. In *S. cerevisiae* (for which TCP-seq data were obtained), eIF3 has a substantially reduced number of the core subunits, and its interaction with the SSU can be somewhat different. *S. cerevisiae* eIF4G lacks eIF3, MNK, eif2β and the second eIF4A binding sites, and instead interacts with the SSUs directly. *S. cerevisiae* do not code eIF4H, and their eIF4B does not readily dimerise, unlike in mammals or higher plants[335]. There is a considerably smaller overall variation of eIF isoforms and alternatives in yeast, but especially so for the group 4 eIFs and translation-associated RNA helicases. Thus, initiation in higher Eukaryotes promises elevated complexity, but also a 'more comlete' scanning machinery, which would be extremely interesting to investigate, and which may more explicitly exhibit features of the scanning 'motor'. We can expect to encounter even more scanning roadblock events due to the more structured, long and complex 5' UTRs and more diverse set of active RBPs, a possiblility to directly detect pronounced internal ribosome entry (especially in the longer 5' UTRs), and better understand dynamics of the process due to the presence of more SSUs in the longer 5' UTRs[266]. At the same time, while there seem to be no technical limitations to perform TCP-seq in cells other than yeast, attribution of the SSU footprints to mRNA isoforms, especially those with variations in the 5' UTRs, may present a problem[266]. Developing algorythms for isoform deconvolution could become useful to solve these problems[336-338].

Non-canonical scanning and alternative models

Some examples of non-canonical scanning have been documented and alternative mechanisms for inspection of 5' UTRs by the SSU have also been suggested[339]. The experimentally tested cases involve discontinuous SSU migration along the 5' UTR, or 'shunting', a mechanism that was originally proposed to explain apparent skipping of a large portion of Cauliflower Mosaic Virus (CMV) 35S RNA by the scanning SSUs[340]. Shunting was suggested to be involved in many other cases of initiation on viral RNAs ('tripartite' 5' UTR of late adenoviral RNA[341]; RNA of plant pararetroviruses[342, 343]; Sendai virus Y proteins mRNA[344]; avian reovirus S1 mRNA[345]), but also on certain cellular sequences (Heat shock 70 protein mRNA[346]; cellular Inhibitor of Apoptosis 2 (cIAP2) mRNA[345]; and possibly others[347-350]).

The exact molecular mechanism of shunting remains unidentified; however, it was proposed that special hairpin structures and surrounding sequences not only impede continued linear motion by scanning SSUs but also cause them to relocate to regions downstream[341, 342, 351]. Additionally, uORFs often found in the shunted 5' UTRs were demonstrated to facilitate shunting compared to continuous scanning, suggesting that re-initiation may be a requirement of the apparent nonlinear SSU movement[352, 353]. In this case, scanning would be resumed from SSUs that remain attached to the mRNA, similar to the well-studied examples of re-initiation upon termination on cellular[242, 243, 354-356] or viral[357-366] uORFs, but in front of a stable structure (hairpin). Thus, shunting may require re-binding of the scanning SSUs downstream across a stable structure while they remain attached to the initial location on the mRNA[342, 353, 367]. *In vitro* reconstructions provide direct evidence that in certain conditions canonical factors responsible for scanning can assist in the bypassing of stable stem-loops. Passing of stable structures through the entry side, but not the exit side, of the SSU mRNA-binding cleft was proposed to occur in the presence of eIFs 1, 1A, 2, 4A, 4B, 4G[282], suggesting

that efficient skipping of 5' UTR portions during shunting may require additional special interactions with mRNA and/or an incomplete (for example, post-termination) scanning SSU configuration.

Activities of DENR:MCT-1 and the homologous eIF2D (ligatin) (Fig. 5a,b) were demonstrated during re-initiation[276, 316, 368]. They can explain cases of eIF2-independent initiation[79, 189, 191], which were reported to be responsible for the specific translation of uORF-containing mRNAs promoting proliferation and oncogenic regulation, as well as genomic instability[369-373]. Interestingly, while the mRNA 'latch' remained closed in the recent structural reconstructions with these factors, the mRNA-binding cleft of the SSUs appeared to be less occluded, mostly due to the absence of eIF1A and eIF2α[105, 234]. eIFs 1 and 1A were also shown to antagonise activity of eIF2D (ligatin) in the reconstituted translation system[189, 276, 316]. Thus, DENR:MCT-1 and eIF2D (ligatin) may be more conductive to the lateral attachment of mRNA, prompting their further investigation in shunting-like events.

Some data suggested that shunting may be promoted by complementarity interactions between mRNA and rRNA[346, 374], which is another long-standing alternative paradigm of eukaryotic initiation[374-379] that, however, has had limited experimental support. Recent structural studies directly reveal that limited base-pairing between SSU RNA (helix 16 of 18S rRNA near the entry to the mRNA-binding cleft) and non-paired bases of the 'three-way junction' structure of histone h4 mRNA (located downstream from the start codon), can occur[380]. Histone h4 mRNA-18S rRNA interactions were proposed to provide direct tethering of the SSUs to the start site and its elevated preference to other sites[380], thus contributing to the observed cap-dependent, but scanning-deprived, initiation on the h4 mRNA[381, 382]. The likely competition of the complementarity interactions with the DHX29 helicase binding site on the SSU[107, 280] may explain why certain RNA structures can be more efficiently bypassed during scanning *in vivo*[380]. Recent biochemical evidence prompts re-surfacing of the role of rRNA-mRNA base-pairing in scanning-based initiation also at the mRNA exit side. Complementarity interactions between the termination upstream ribosome binding site (TURBS) and helix 26 of SSU rRNA (near the mRNA exit side) were shown to be required for the re-initiation on *Caliciviride* mRNAs [383, 384]. Notably, TURBS-mediated reinitiation was possible without eIF3 and was compatible with either canonical eIFs 1, 1A, 2 or eIF2D (ligatin)[316].

Examples of shunting and possible lateral re-binding of SSUs have inspired an alternative to the scanning model. In the 'mRNA looping' hypothesis, which can be viewed as an extreme case of non-linear motion or shunting, SSU hopping from the 5' cap to random locations in the 5' UTR was suggested as a mechanism of systematic start codon search[192, 385]. While *in vivo* snapshots of scanning SSU distributions obtained with TCP-seq do not provide a proof of elevated attachment to cap structures at the steady-state, or prevalence of non-homogeneous distribution of scanning SSUs (Fig. 7a), cases of SSU pile-ups were observed in multiple 5' UTRs that were not previously attributed to initiation through uORFs[51]. It thus will be critical to distinguish between potential internal ribosome entry, shunting or pausing due to complementarity interactions with scanning SSUs in the future, and to elucidate the extent of these events of initiation across transcriptomes in different *in vivo* cellular environments.

RECOGNITION OF START CODONS AND JOINING BY THE LARGE RIBOSOMAL SUBUNIT

The third stage of cap-dependent initiation involves recognition of the start codon of mRNA while the SSU is still engaged in 5'→3' directional motion, arrest of this motion and the subsequent joining of the LSU. LSU joining results in the assembly of the elongation-capable ribosome, with its P-site occupied by Met-tRNA$_i^{Met}$ that serves as nascent 'peptide' (in this case – just the methionine residue) donor in the subsequent first transpeptidation reaction. Thus, the whole first half of the start codon recognition process in eukaryotes is unique and substantially differs from the prokaryotic initiation, where SSUs do not have to transition from the powered 5'→3' motion into a stall.

The consensus initiation model proposes pausing of the scanning SSUs over the start codons located in the strong nucleotide context, as the first step of start codon recognition. Pausing allows cognate codon-anticodon interactions to affect eIF2 and the small eIFs 1 and 1A, which trigger the transition of the SSU from its scanning-competent mode to its subunit-joining mode, and thus control the fidelity of the start codon recognition across mRNAs. The transition process begins with the hydrolysis of eIF2-bound GTP, dissociation of eIF1 from the complexes and P_i release from eIF2:GDP (Fig. 2). This is followed by a major conformational rearrangement of the SSU resulting in a more tight ('locked') binding to mRNA, preventing further SSU sliding. The eIF2:GDP then leaves the complex, allowing eIF5B:GTP to bind to Met-tRNA$_i^{Met}$ and SSU, and begin the evolutionarily conserved subunit joining process. Owing to the fact that many of the start codon recognition complexes can be artificially stabilised and purified or assembled *in vitro*, there is now an extensive structural insight into the major start codon recognition stages (Fig. 9). This is complemented by biochemical and kinetic data for the well-defined 'checkpoints', as well as many ribosome profiling datasets where initiation site frequencies were determined. Further, *in vivo* SSU footprinting by TCP-seq demonstrates at least three different large-scale conformations over start codons, re-capitulating some of the *in vitro* conclusions (Fig. 9a)[51].The most mechanistically intriguing part of the process remains the initial pausing and the transition of the moving SSUs to a complex that is almost irreversibly fixed at start codons. Otherwise, the start codon recognition appears as one of the better-understood initiation stages mechanistically, with recent structural works starting to fill in some very fine details of its sub-steps.

Rearrangement of the scanning complexes

Compared to 'scanning' SSUs, the structures of early-stage start codon recognition complex prominently feature rearrangements of the position of Met-tRNA$_i^{Met}$ in the P-site. Already in the beginning of start codon recognition, the entire TC appears to relocate closer to the mRNA in the SSU, resulting in a more stable binding and more tight interactions between SSU, Met-tRNA$_i^{Met}$ and mRNA. In several cryo-EM reconstructions of complexes stabilised with non-hydrolysable GTP analogues, SSUs transition from the P_{OUT} state characteristic to mRNA binding and/or scanning to the antagonised 'P_{IN}' state. In the P_{IN} state, Met-tRNA$_i^{Met}$ is positioned ~7 Å deeper in the P-site, with the 3' acceptor stem relocated upward and towards the A-site. This relocation is stabilised by Met-tRNA$_i^{Met}$ interactions with eIF2γ, as well as by displacement of tRNA from E-site area by eIF2α (Fig. 9; compare b1 and c1 with b2 and c2)[177, 205]. This Met-tRNA$_i^{Met}$ conformation begins to resemble some prokaryotic initiation complexes, as was noted for the archaeal SSUs[179, 205, 386]. In the P_{IN} state, the three conserved G:C base pairs of the Met-tRNA$_i^{Met}$ anticodon stem make specific contacts with rRNA bases, which is suggested to be one of the factors responsible for the selective Met-tRNA$_i^{Met}$ binding[66, 205].

The mRNA path during start codon recognition appears similar to the 'scanning' complexes; the bases of nucleotides adjacent to the start codon are unstacked from their neighbours and can make contacts with the P-site rRNA[66, 205]. The mRNA 'latch' formed by the rRNA helices 18 and 34 in the entry side of the mRNA-binding cleft is closed in all structures modelling early start codon recognition. The overall mRNA-binding cleft configuration appears tighter, and the P-site arrangement is more compact in the P_{IN} state[177, 179]. The head of the SSU is rotated clockwise by a further ~5°, which is proposed to facilitate a more stable TC binding[66, 177, 205]. The SSU head was reported to be tilted (swivelled) towards the SSU body at the intersubunit side for ~4°, further narrowing the mRNA-binding cleft in the late start codon recognition complexes[179].

When eIF1 is present in the complexes, it is slightly displaced away from Met-$tRNA_i^{Met}$ and may induce electrostatic repulsion between its conserved negative residues and tRNA, but still maintain contacts with the P-site base pairs[177, 205]. Notably, eIF1A makes stacking interactions with the +4 mRNA nucleotide (adjacent to the AUG from 3'-side in the A-site), which is an important start codon context determinant. The eIF1A N-terminal part, which is unstructured in the scanning complexes, becomes stabilised and approaches the codon-anticodon pair from the A-site, suggestive of its role in P_{IN} stabilisation[205]. eIF1A C-terminal extension, in contrast, becomes de-localised and possibly uncoupled from eIF1 and Met-$tRNA_i^{Met}$[205]. Interestingly, in the start codon-SSU complexes purified from mammalian cell lysate and also stabilised with non-hydrolysable GTP analogue, densities could not be attributed to eIF1 and eIF1A[179]. Thus, *in vitro* reconstruction with an excess of eIF1 and eIF1A may be relevant to an earlier and relatively less stable intermediate immediately prior to the dissociation of these factors. eIF2 primarily interacts with the SSU head[177, 179] in the start codon recognition complexes. eIF2α as part of the TC locates deep in the E-site and can make direct contacts with mRNA residues -3 and -2[177, 179, 205]. Notably, unlike in the scanning complexes, eIF2β repositions towards, and makes direct contacts with, the SSU head, additionally interlocking mRNA in the SSU mRNA-binding cleft. At the same time, eIF2β loses its eIF1 and eIF1A interactions at this stage, suggestive of its role in stabilisation of the scanning configuration where it interats with these factors[177].

A lateral displacement of the core PCI/MPN eIF3 subunits was reported to coincide with the P_{IN} state, suggesting large-scale molecular motions of eIF3 during start codon recognition[177, 179]. Although there is some discrepancy in the attribution of the electron density, it was suggested that eIF3i and eIF3g are present at the entry side below the mRNA-binding cleft on the intersubunit surface of the SSU, and may contact eIF2γ upon start codon recognition. Thus, eIF3i and eIF3g may actively participate in the stalling of scanning SSUs at start codons[177]. Alternatively, eIF3b also relocates to the intersubunit SSU side below A-site from the solvent-side entry and makes contacts with eIF2γ up until the early start codon recognition stage (Fig. 9 b1,2, c1,2). This eIF3b relocation is hypothesised to additionally stabilise eIF2β interactions with eIFs 1 and 1A and be conducive to scanning[179]. Upon establishing the complete codon-anticodon interactions and the likely release of eIF1, eIF3b binding may become destabilised and approximately the same position could be re-taken by the eIF3i and eIF3g subunits (Fig. 9 b4, c4)[179]. Therefore, replacement of eIFb with eIF3i and eIF3g may be one of the major structural events during start codon recognition and can signify establishment of stable codon-anticodon interactions.

Notably, in the mRNA-free SSUs neither eIF3b, nor eIF3i and eIF3g, were observed in this location and instead were localised near the mRNA entry at the solvent side, and eIF3j was reported to bind near the intersubunit entry side in the mRNA-free complexes (Fig. 5d)[83, 107, 297]. Thus, eIF3 may remain attached to the SSUs through eIF3i and eIF3g at least until the subunit joining step, with the possible role of these eIF3 subunits in the interim Met-tRNA$_i^{Met}$ stabilisation and eIF5B binding control[179]. There is limited structural evidence that eIF5 may be present in the early P_{IN} complexes closer to the A-site and maintaining contacts with eIF1 and eIF2γ (Fig. 4g)[205].

The observed structural rearrangements immediately upon start codon recognition correspond well to the biochemical evidence. Dissociation of eIF1 was shown as one of the key steps during start codon recognition[307]. The role eIF1A C- and N-terminal of eIF1A extensions, and their sequential re-localisation, was extensively studied by mutagenesis and localisation approaches[305, 306, 387, 388]. Involvement of eIF2α in the stabilisation of the -3 nucleotide of mRNA (adjacent to the start codon from E-site) was shown[73, 389], as well as eIF2β contacts with eIF1 and Met-tRNA$_i^{Met}$[390, 391].The binding of eIF3 to the SSU through its 'peripheral' subunits was previously demonstrated[253, 392-394], as well as its involvement in the fidelity of start codon recognition[313, 393, 395]. The eIF5 N-terminal part was shown to bind eIF2 and structurally mimic eIF1, antagonising its binding. Its C-terminal part was observed to exclusively interact with eIF1 or the N-terminal part of eIF2β, and participate in the control of eIF2 release[394, 396-398]. The C-terminal part of eIF5 was also shown to interact with eIF3c[313]. More recent evidence includes the involvement of eIF3c interactions with limited eIF1 surfaces and the C-terminal part of eIF5 during scanning, which cease upon start codon recognition and result in an extended eIF3c attachment to eIF1 incompatible with eIF1 SSU binding[64].

The exit part of the mRNA-binding cleft together with eIF2α were demonstrated as contributors of the P_{IN} stabilisation at AUG codons[73], and a lesser accessibility of the entry side of the mRNA-binding cleft and P-site were shown[304]. Thus, an overall sequence of events can be reconstructed, where the scanning SSUs first temporarily stall (pause) over the start codons, assisted by strong codon-anticodon interactions and additionally by binding of, at least, -3 and +4 mRNA nucleotides to rRNA and eIF2α or eIF1, respectively (Fig. 9 a1-d1). These interactions re-structure the open scanning SSU configuration to the early closed P_{IN} state. The eIF1A N-terminal part becoming structured in the A-site and near the codon-anticodon interactions in the P-site appears as the main driver of this rearrangement, yielding a more stable complex (Fig. 9 a1-d1). The eIF1A N-terminal part also loses its affinity to the C-terminal part of eIF5, which induces eIF5 binding to the N-terminal part of eIF2β. The eIF5 C-terminal:eIF2β N-terminal interaction displaces eIF1 from its binding site on eIF5. The eIF1A C-terminal part becomes displaced from the P-site and may interact with the N-terminal part of eIF5 (Fig. 9 a2-d2). This results in the eIF1 displacement which may be further promoted by eIF3c binding to the eIF1 surfaces that are required for its interaction with SSU. eIF displacement concludes the early start codon recognition stage. The subsequent eIF1 dissociation from the complex triggers P_i release from eIF2:GDP:P_i, and the TC, together with eIF5, lose affinity to the SSUs (Fig. 9 a3-d3). Dissociation of eIF2 enables displacement of eIF3b from the intersubunit surface, and eIF3i and eIF3g may re-bind in the vicinity of Met-tRNA$_i^{Met}$, preventing premature LSU attachment or re-binding of eIF2:GTP, in the 'late' P_{IN} SSU. eIF3i and eIF3g possibly additionally stabilise the 'post-eIF5' configuration of the SSU, (Fig. 9 a4-d5).

One of the remaining mysteries of start codon recognition is the exact timing and trigger of induction of eIF2-bound GTP hydrolysis, and the mechanism of the P_i release. In the absence of the corresponding structures, it is not fully clear whether eIF5 acts as a classical GTPase by providing an 'arginine finger' or whether it stimulates eIF2's own GTPase activity[7, 68, 307]. More importantly, it was suggested that GTP hydrolysis may occur already *en route* in the scanning SSUs, with the start codon recognition triggering eIF1 and consequently, P_i and eIF2:GDP release[390]. Thermodynamically, the GTP hydrolysis step is a more irreversible process and thus it could be preferred as the driver for the large-scale rearrangements, as in many known G-proteins. However, the strict requirement of the initial rapid response at start sites could have modified this evolutionary conserved mechanism towards a somewhat more reversible, but faster acting pathway. Hypothetically, the GTP hydrolysis rate of ~5 s^{-1} observed in the scanning complexes could contribute to the known skipping of 5'-proximal start codons, owing to the comparably fast ~10 nt/s scanning motion[255, 271, 273, 390, 399]. In this regard, it is also noteworthy that up until the eIF5B:GTP (and possibly LSU) attachment, start codon recognition is not irreversible in a strict sense. For example, it was demonstrated that eIF1 can destabilise weaker P-site mRNA:Met-$tRNA_i^{Met}$ interaction after GTP hydrolysis and the departure of eIF2[301]. Similarly, it was shown that SSUs in the P_{IN} state can be spontaneously (diffusionally) displaced from the start codons and resume scanning towards the more downstream triplets[400]. These results suggest that at least up until eIF5B attachment, SSUs do not fully lose the ability to scan mRNA, and that prolonged pausing at start sites, if not concluded with eIF2 dissociation, may deteriorate the fidelity of start codon recognition, rather than improve it.

Intriguingly, i*n vivo* SSU fooptrinting with TCP-seq demonstrates three predominant SSU configurations at start codons where the major protection change occurs over the inbound (3', entry) portion of the mRNA (Fig. 7)[51]. Using the extended 5' protection characteristic for scanning SSUs (see above in the Scanning section) and accumulation of the queued SSUs in front of the start codons, it was possible to assign these complexes to early, middle and late stages of start codon recognition. Importantly, in full concordance with the other evidence these complexes showed increasing length of protection of the entry mRNA portion over time. Thus, it is possible that several key start codon intermediates with relatively long half-lives (and thus important for the overall initiation rates) can be monitored and quantitatively assayed for each mRNA *in vivo*. The sub-second dynamics of the eIF1 displacement make these steps likely transparent for TCP-seq[274], and the presence of the 5'-extended protection, allow to suggest that the first *in vivo* intermediate is a paused scanning SSU still in the P_{OUT} configuration (protecting overall just ~19 nt of mRNA; Fig. 9 a1). The relatively slow eIF1 dissociation and P_i release (~2 s)[274] suggest that the second stage represents complexes in the early P_{IN} state up until the dissociation of eIF2. The early *in vivo* 'P_{IN}' complexes have mRNA protection extended further by 10 nt in 3' direction (Fig. 9 a2, a3). The third type of *in vivo* start codon complexes has most extended 3' protection, longer by 8 nt than the middle type and protecting ~37 nt overall (Fig. 9 a4, a5). This 3'-ward increase in protection may represent rearrangements of the peripheral eIF3 subunits and the overall more 'prokaryotic' position of Met-$tRNA_i^{Met}$ as in leans towards A-site in the late P_{IN} complexes. Alternatively, the longest SSU footprints over the start codons could be explained by eIF5B binding (see below), or be a mixture of these complexes, given that *in vitro* measured dynamics of eIF5B association and dissociation are relatively slow[401]. Importantly, from these data the start codon recognition stage also appears as clearly rate-limiting for ~65% of the quantified transcripts, as can be measured by the ratio of the start codon

SSU pileups *vs.* scanning SSU pileups in the 5' UTR. Because different fast scanned mRNAs demonstrated varying prevalence of the short, intermediate and long footprints at the start codons and no SSU pileups were detected 5' proximally in their ORFs, dynamics of different start codon recognition sub-steps may vary substantially across the transcripts. Thus, start codon recognition may play a somewhat unexpected role where it additionally shapes the speed of translation initiation transcript-wise. The exact determinants of this speed shaping, and the actual eIF composition of the *in vivo* start codon intermediates remain to be elucidated.

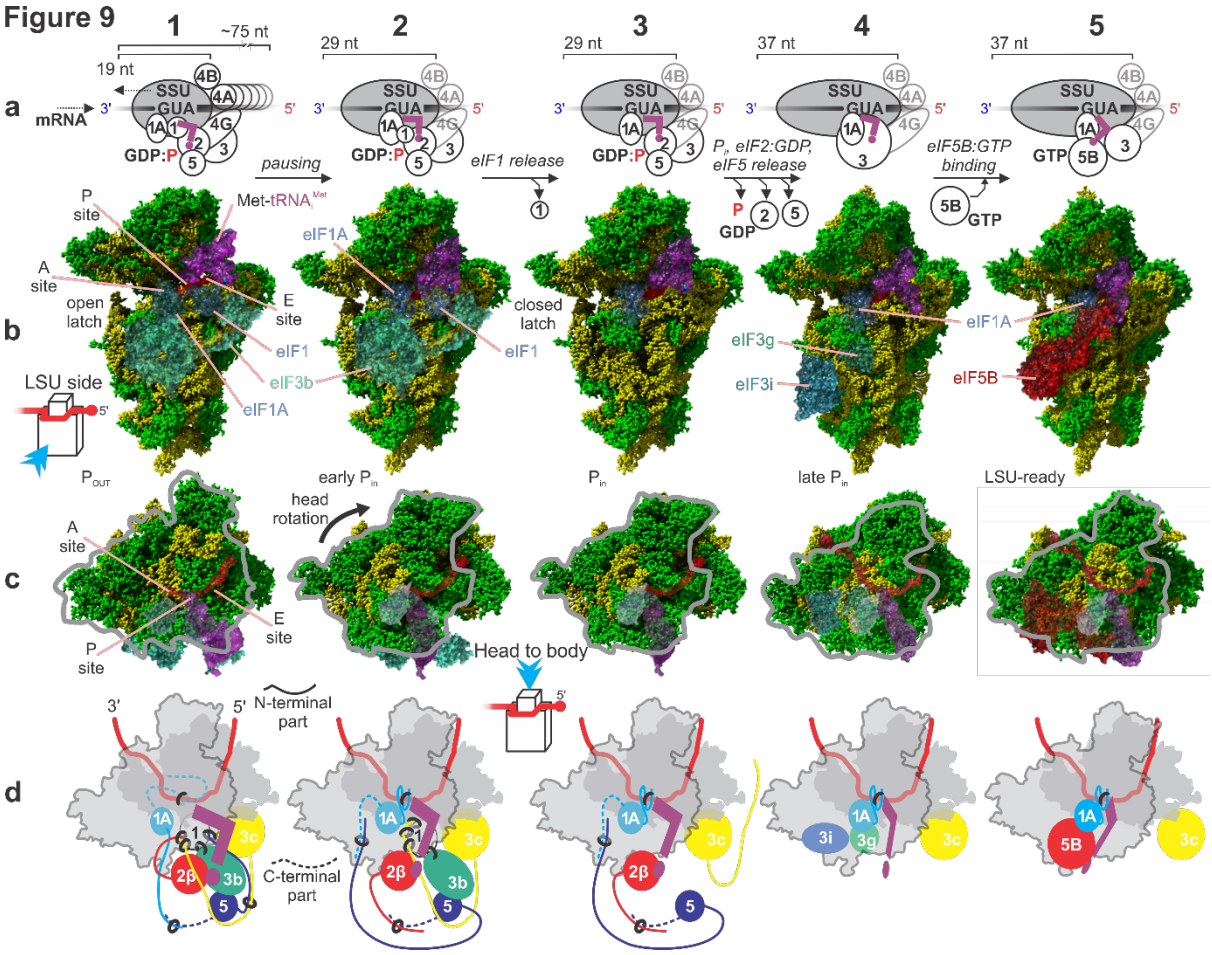

Figure 9. Possible configurations of the initiating SSUs induced as they progress through the start codon recognition stages (1-5). (a) Cartoon schematics depicting the possible composition of the eIFs in the start codon SSUs and the corresponding *in vivo* TCP-seq footprint lengths[51, 266] (see text). (a1) Represents initial pausing over the start codons while SSU remains in its scanning configuration featuring the open latch, head swivelled to the solvent side, and the $tRNA_i^{Met}$ displaced laterally from the P-site in the scanning-compatible P_{OUT} conformation; (a2) depicts early stage of start codon recognition where the mRNA latch is tightened and mRNA entry more constricted, with $tRNA_i^{Met}$ moving further into the P-site and partially acquiring P_{IN} state, which induces delocalisation of eIF1 and loss of most of its interactions within the complex; (a3) shows the stabilised P_{IN} with the $tRNA_i^{Met}$ strongly bound in the P-site, resulting in the full arrest of the SSU sliding on mRNA as eIF1 leaves the initiation complex; (a4) depicts the initiation complex after phosphate release gated by the eIF1 detachment, also resulting in the release of eIF2:GDP and eIF5 from the SSU; (a5) shows the last stage of the start codon recognition process where the $tRNA_i^{Met}$ is re-bound by eIF5B:GTP, resulting

in the re-adjustment of its position, making it compatible with the productive LSU attachment. (b) Combinational structures of the SSU reorganisation viewed from the LSU side and corresponding to the start codon recognition stages as shown in (a), with the focus on the intersubunit surface rearrangements. Densities of only mRNA, $tRNA_i^{Met}$, eIFs 1, 1a, 3b, 3i, 3g and 5B are shown for simplicity. SSU depicted as described in Fig. 8a. (b1) Structure of the yeast initiating SSU in the open state (PDB entry 3JAQ)[177] with eIF3b (PDB entry 5K1H)[179] modelled as described in Fig. 8a. mRNA model aligned from the closed state (PDB entry 3JAP) by the 18S rRNA trace in the body region of the SSU. (b2) Same as (b1), but for the SSU in the closed state (PDB entry 3JAP)[177]. (b3) Same as (b2), but with the densities of eIF1 and eIF3b omitted. (b4) Structure of the rabbit late P_{IN} SSUs (PDB entry 5K0Y)[179] with the eIF1A density modelled from the yeast closed state (PDB entry 3JAP) by aligning the 18S rRNA trace in the body region of the SSU. (b5) Structure of the rabbit SSU complexed with eIF5B:GMP-PNP in the PRE-translocation-like state (PDB entry 4UJD)[180] during the late start codon recognition stage (derived from the complete ribosome structure by removing LSU-related densities). mRNA and eIF1A models aligned from the yeast closed state SSUs (PDB entry 3JAP) by the 18S rRNA trace in the body region. (c) Same as (b), but in the head-to-body view with the head density shown as semi-transparent and circumvented by the grey line. (d) Cartoon schematics of the key interaction between the LSU-side factors progressing through the start codon recognition stages corresponding to the models in (a)-(c). Head-to-body view as in (c) schematised as in Fig. 3. (d1) Multiple interactions between LSU-side eIFs guided by the C- and N-terminal parts of eIF1A and eIF5 converge on eIF1 binding and stabilise the scanning configuration. (d2) eIF1A C-terminal part is displaced from the P-site upon early P_{IN} state, leading to the structuring of its N-terminal part in the A and P-sites and stabilisation of the codon-anticodon interactions. Interaction of the liberated eIF1A C-terminal part with the N-terminal part of eIF5 and the liberated eIF5 C-terminal part with the eIF2β destabilise eIF1 binding. (d3-d5) The eIF1A and eIF45-guided cascade of rearrangements leads to the loss of affinity to eIF1 and adoption of the stable scanning-arrested P_{IN} configuration and gated release of P_i, followed by the eIF2:GDP and eIF5 dissociation.

Assembly of elongation-capable ribosomes

Initiation concludes with the eIF5B-assisted joining of the LSU (Fig. 10a). Model structures of ribosomes at the start codon where Met-$tRNA_i^{Met}$ is bound to eIF5B stabilised with non-hydrolysable GTP analogues were obtained for yeast (assembled with 'non-structured' (U,C)-containing synthetic mRNA, SSUs, LSUs, Met-$tRNA_i^{Met}$, eIFs 1, 1A, 2:GTP, 5 and 5B:GMP-PCP)[402] and mammalian (mRNA containing HCV IRES, SSUs, LSUs, Met-$tRNA_i^{Met}$, eIFs 3 and 5B:GMP-PNP)[180] initiation systems and demonstrate highly similar overall arrangements, also reminiscent of bacterial initiation complexes[*e.g.*403]. Notably, a structure of eIF5B bound to the SSUs alone have not yet been obtained (although bacterial complexes with analogous configuration exist), but may represent another intermediate of initiation. Another point of view is that there is no such distinct intermediate in eukaryotes, and all three components (SSUs with mRNA, Met-$tRNA_i^{Met}$ and the residing eIFs, LSUs and eIF5B:GTP) can only form unstable bilateral complexes with relatively short half-lives, which only become productive upon the binding of the third partner. On the SSU side of the ribosome-eIF5B complexes (Fig. 10b-d), eIF5B adopts conformation markedly distinct from its 'free' form with its tRNA-binding domains more extended and reaching anticodon stem-loop from the main ribosome binding side located peripherally on the intersubunit surface down from the mRNA-binding cleft entry towards the middle of the SSU body (Fig. 10b-c). eIF5B makes multiple contacts with the SSU,

as well as with the LSU, as could be expected from its subunit 'bridging' function[180, 402]. The overall conformation of the SSU itself remains not altered substantially compared to the previous steps, but the position of Met-tRNA$_i^{Met}$ and SSU relative to the LSU are considerably different[180, 402]. In the yeast complexes, the SSU is rotated slightly (~3.5°) counter-clockwise relative to the LSU along the axis perpendicular to the intersubunit plane. Met-tRNA$_i^{Met}$ is stabilised in a position different from the regular P-site bound tRNA, and appears in a 'hybrid' ('P/I') state overall leaning towards the A-site with the CCA 3' end bent towards the mRNA-entry side by eIF5B, and the tRNA body located generally closer to the SSU than in the prokaryotic complexes (Figs. 9, 10)[180, 402]. Interestingly, the reconstruction in the mammalian system resulted in subpopulations of complexes demonstrating SSU 'rolling' (rotation along the axis aligned with the head-to-body direction and the intersubunit plane) relative to the LSU, which is unique to eukaryotes[180]. Relating these complexes to the pre- and post-translocation elongating ribosomes allowed to infer the likely mechanism of the eukaryotic subunit joining. The initial binding occurs with Met-tRNA$_i^{Met}$ not fully accommodated in the LSU P-site (with Met-tRNA$_i^{Met}$ CCA3' located in the LSU A-site), but allowing its slotting into the LSU cavity without affecting the complex geometry, followed with the entire SSU assembly rolling 'back' (~6° clockwise around the head-to-body vector) on the LSU, which results in the full accommodation of the Met-tRNA$_i^{Met}$ in the ribosomal P-site in a conformation compatible with the subsequent elongation phase. The 'reverse rolling' likely immediately precludes or follows eIF5B-bound GTP hydrolysis and was also suggested as the main driver of the eIF5B affinity loss and its release from the ribosome [180]. Thus, while eukaryotic ribosomes seem to utilise a unique mechanism of the subunit joining, eIF5B function in adjusting Met-tRNA$_i^{Met}$ conformation remains well-conserved across all life.

Figure 10

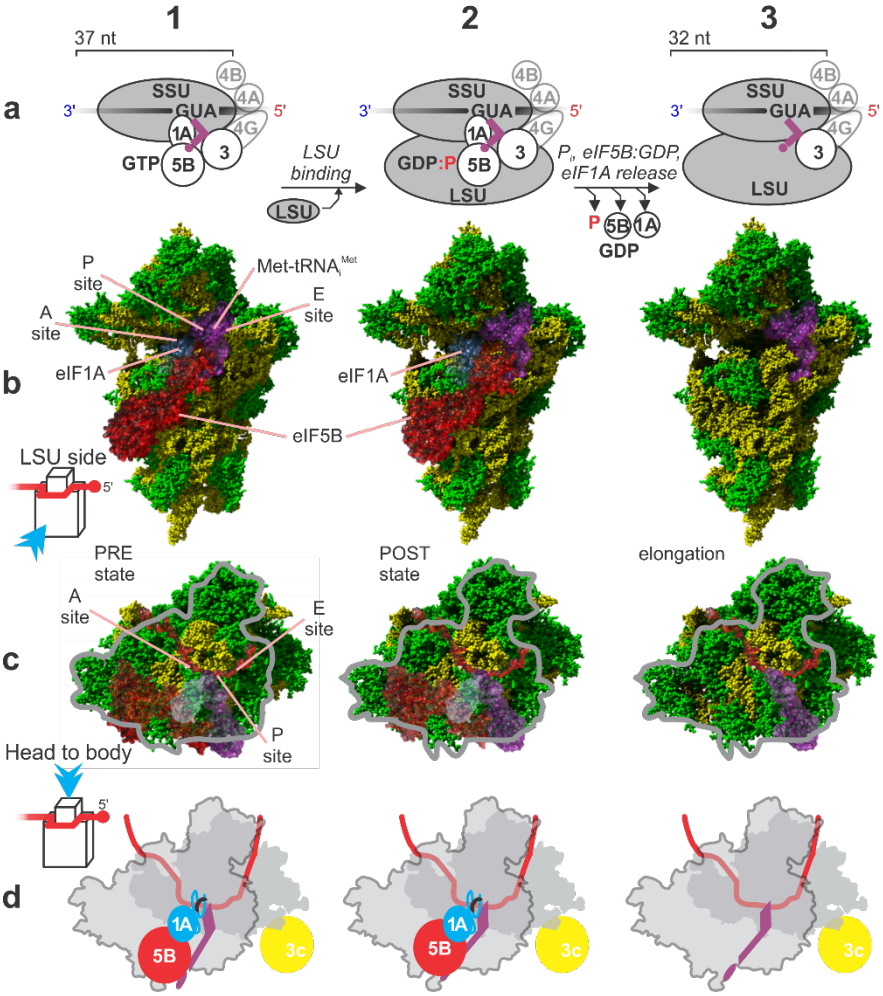

Figure 10. Possible configurations of the initiating SSU as it progresses through the postulated stages of LSU joining. Figure layout as described for Fig. 9. (a1) Represents PRE-translocation-like state of the SSU:(GTP:eIF5B: Met-tRNA$_i^{Met}$) complex when eIF5B:GTP first attaches to the late-P$_{IN}$ SSUs and reorients the tRNA$_i^{Met}$. This complex may now productively bind LSU. (a2) Depicts POST-translocation-like state of the SSU:(GTP:eIF5B: Met-tRNA$_i^{Met}$) complex, adopted upon attachment to the LSU and ~6° SSU back-rolling on it along its head-to-body vector, fully slotting the tRNA$_i^{Met}$ into the LSU P-site. This stage may coincide with the hydrolysis of the eIF5B-bound GTP. (a3) Represents the first elongation intermediate, with the complete ribosome protecting ~32 nt over the start codons as determined by the *in vivo* TCP-seq footprinting[51, 266]. (b1) Structure of the rabbit SSU complexed with eIF5B:GMP-PNP in the PRE-translocation-like state (as in Fig. 9b5). (b2) Structure of the rabbit SSU complexed with eIF5B:GMP-PNP in the POST-translocation-like state (PDB entry 4UJC)[180]. mRNA and eIF1A modelled as described for Fig. 9b5. (b3) Hypothetical rabbit SSU structure corresponding to the first elongation intermediate, derived from (b2) by removing the eIF5B- and eIF1A-corresponding densities. (c) Corresponds to (b), but from the head-to-body point of view. (d) Cartoon schematics corresponding to (c) depictes as described in Fig. 3.

Whereas the mechanics of subunit joining seem to be well-understood, certainty is lacking for the time points of the release of eIFs that remain associated with the ribosome at these stages. After the initial start codon recognition stages (Fig. 9), the SSUs are presumably left with eIF3 (contacting the

intersubunit area below A-site with its eIF3i and eIF3g subunits and PCI/MPN core), and possibly the eIF4-group factors and eIF1A. This transition state is one of the remaining structurally uncharacterised intermediates, and it is unclear how Met-tRNA$_i^{Met}$ position is stabilised in these complexes. The fact that such a complex cannot be efficiently obtained *in vitro* by mixing the respective factors and an unstructured mRNA suggests that either mRNA remains tightly interlocked and thus cannot get out (and in) of the SSU, or that these complexes are highly unstable. *In vitro* purification of the post-eIF5 complexes supports the first alternative[245]. As it was suggested, eIF3 can provide a ribosome anti-association activity at this stage[179]. Density has not been attributed to eIF1A in these complexes, and thus it may be concluded that it is unstably bound or dissociated at the stages of the eIF5B attachment. Similar to this, and to the situation with the sequence of eIFs attachment during cap recognition, there is no certainty whether eIF5B first attaches to the SSU in the closed state followed by the LSU attachment, or whether the LSU first binds to eIF5B prior to subunit joining, although mechanistically this is a less principal question to the regulation of the initiation outcome and rates. *In vitro* experiments suggest that the presence of LSU is not mandatory for the eIF5B attachment, LSUs do not efficiently attach without eIF5B[188, 244]. In this regard, it is peculiar that eIF5B is a non-essential gene in yeast[404]. Thus, either subunit joining has more relaxed eIF requirements in lower eukaryotes, or other mechanisms or factors may be involved. It is also incompletely understood when eIF3 and eIF4-group factors leave the ribosomes. Indeed, whereas eIF3 'peripheral' subunits may completely detach from the intersubunit SSU side, detachment of its 'core', although it may become more laterally oriented, is not certain. In this low-affinity state eIF3 may remain attached to the elongating ribosomes for some time, which was originally suggested as one of the mechanisms explaining re-initiation after short ORFs[363, 405, 406]. In the case of mammalian ribosomes, this enables a possibility of eIF4-group factors remaining on the ribosomes as well, and in case of yeast translation raises a question of what mechanism controls eIF4G release. As it was discussed above, the most 3'-extended *in vitro* SSU footprints obtained with TCP-seq can also be a result of eIF5B binding[51]. Thus, in the future, TCP-seq targeted at the SSUs and complete ribosomes containing eIF5B, eIF3 and group 4 eIFs could be used to provide a more definitive answer to the sequence of events and discern when eIF5B becomes associated with the initiation complexes, and when eIFs 1A, 3 and 4-group leave the ribosomes *in vivo*.

Determinants of start codon recognition

The prevalent start codon in eukaryotes is the methionine-encoding AUG, which is recognised by a special Met-tRNA$_i^{Met}$ during initiation[301, 407, 408]. Nevertheless, AUG is used as the start for only ~50% of coding regions in mammals[409], as compared to ~82% in bacteria[410]. While these proportions may be somewhat affected by the non-equilibrium effects of the ribosome profiling technique, it makes evident that eukaryotic start sites selection is far more complex than initially thought. The use of alternative start codons can be classified either by the so-called 'near-cognate' interactions within otherwise identical, canonical initiation through scanning, or by alternative initiation pathways employing special components and a different tRNA, such as it was exemplified by eIF2A and Leu-tRNA$_e^{Leu\ [190]}$, where perfect base-pairing is achieved at the non-AUG (CUG) codon. The near-cognate start codons may often involve imperfect base-pairing where 1st nucleotide of the codon non-canonically interacts with the 3rd U residue of the Met-tRNA$_i^{Met}$, such as in the case of UUG, GUG and CUG triplets[409]. The same triplets appear as the most preferred near-cognate codons in bacteria[410]. In eukaryotes, however, other near-cognate start codons with substitutions in the 2nd and 3rd

nucleotides are encountered relatively frequently and cumulatively contribute to the relatively less frequent use of AUG[409, 411]. In this regard, a remarkable difference is that prokaryote-dominant GUG and UUG near-cognate codons are much less utilised in eukaryotic initiation, with the evidence of selective GUG and AAG suppression by eIF1, and AUA suppression by both eIF1 and eIF1A. In contrast, CUG is not supressed, and with occurrence rate of ~20%, can be considered as a true eukaryotic start site alternative[71, 409, 411]. Given that eukaryotic SSUs scan long sequences of nucleotides, such selective suppression of the stronger-binding triplets appears as an evolutionary mechanism responsible for the overall highly precise eukaryotic start site selection[67, 71, 411].

Critically, the transition from the scanning-competent mode into the arrested mode at the start codon must be a relatively fast process, to be compatible with scanning speeds of ~10 nt/s[271, 412]. The fidelity of codon recognition thus becomes paramount, and the more complex eukaryotic machinery displays features developed specifically to facilitate 'on the fly' recognition of the cognate *vs.* false start sites[67, 71, 301, 398]. The readiness and the composition of the scanning complex itself during initiation on various mRNAs is one of the key determinants of start codon recognition capability, which can be programmed by the levels of various active eIFs accessible to the initiating SSUs at the moment. For instance, increased eIF1 levels or decreased TC levels can promote more 'scan-through' events and weak start sites will be skipped more frequently[65, 151, 413]. The controlled (increased or decreased) 'leaky scanning' through start sites, combined with uORFs, upstream start codons, and alternative start sites, provides a vast regulatory potential[65]. However, for this system to work and from a gene-wise perspective, the key start site determinants are those encoded by the sequence (and structure) of the mRNA. Classically, the 'consensus' nucleotide 'context' or 'Kozak consensus' sequence is considered as the second important start site determinant (after the start codon itself, as discussed above in the introduction to the 'Recognition of Start Codons and Joining by The Large Ribosomal Subunit' section). For mammals, the consensus sequence is usually referred to as ($G_{-9}C_{-8}C_{-7}G_{-6}C_{-5}C_{-4}$)$Pu_{-3}C_{-2}C_{-1}$**A**$_{+1}$**U**$_{+2}$**G**$_{+3}G_{+4}$[414], and is substantially different across the taxa. For example, the yeast consensus is considered as ($A/U_6A_5A/C_4$)A_3A_2A/C_1**A**$_{+1}$**U**$_{+2}$**G**$_{+3}$ ($U_{+4}C_{+5}Py_{+6}$)[415], and the consensus in higher plants is A_{-3}(A/C)$_{-2}A_{-1}$**A**$_{+1}$**U**$_{+2}$**G**$_{+3}G_{+4}C_{+5}$[416]. These sequences were derived from a compilation of relatively abundant, well-translated mRNAs. Current genome-wide data suggest less stringent context criteria and more diverse combinatorial possibilities, the rules of which remain to be outlined in detail[50, 65, 409, 417, 418].

While the mechanistic aspects of the SSU reconfiguration at start codons are well understood, perhaps one of the largest remaining mysteries in the start codon recognition is the exact mechanism by which the start codon-adjacent nucleotide context is influencing different stages of the process. Conceptually, several possibilities can be outlined. First, by altering the affinity of the initiating SSU to mRNA, start codon context can affect the speed of scanning. For example, slower scanning due to the downstream structure has been originally suggested to explain more efficient start codon recognition[419]. Interactions of the N-terminal part of eIF1A, together with the helix 44 of SSU rRNA with the nucleotide next to the P-site (position +4), were proposed to contribute to mRNA pausing during scanning[66]. Both +4 and -1 nucleotides are unstacked from the adjacent mRNA nucleotides and are interacting with rRNA (-1) and eIF1A (+4) and these as well as nucleotide -3 interactions with different initiation components (*e.g.* eIF1A, A/P/E-site rRNA, eIF2α, *etc.*)[66, 205] were further proposed as the factors contributing to the SSU pausing. Particularly, evidence exists towards eIF2α interactions with nucleotides in positions -2, -3, which are thought critical for

successful start codon context recognition during scanning[73, 389]. Second, start codon context, by forming specific (but not necessarily strong) interactions with the components of the initiating SSU, can signal for the rearrangement of the complex, triggering faster transition to the next stage. For example, such specific signals may speed up the release of eIF1 and eIF2, and thus force the scanning SSU into the late closed state faster. Less evidence has been accumulated for this possibility; however, this may be due to the transient nature of the involved intermediates, rather than their absence. A combination of the pausing and triggering mechanisms may be a third alternative.

It should be mentioned that while generally widespread, start codon context may not be present on some mRNAs. The simplest example of this are extremely short or completely lacking 5' UTRs[191, 420]. SSUs may still be binding to mRNA through regular eIF4E:cap interactions, however no scanning commences during initiation and thus there is no requirement for nucleotide context to interact with the scanning SSUs. Another specialised case of such a functional replacement of the start codon context is the Translation Initiator of Short 5' UTR (TISU) element C/$G_{-4}A_{-3}A_{-2}G/C_{-1}$**A**$_{+1}$**U**$_{+2}$**G**$_{+3}G_{+4}C_{+5}G_{+6}G_{+7}C_{+8}$, a start site configuration often found in well-translated mRNAs with extremely short 5' UTRs (as little as 4 nt 5' UTR length with median ~12 nt)[339, 421]. Detailed structural explanations for TISU function are still to be discovered, but this is a physiologically relevant start site shown to be frequent in mitochondria- and metabolism-related genes, translation of whose mRNAs is not repressed under energy-defifient conditions, in contrast to the majority of canonically scanned mRNAs[422]. TISU element is not scanned as can be inferred from its unique stimulation by eIF1, which normally would increase bypass of the start codons[423]. Instead, it is hypothesised that the TISU element can stimulate eIF4F release from the initiation complex once the mRNA was bound to the SSU, eliminating scanning and possible eIF4F interference with start codon located short of mRNA 5' end[422].

In vivo TCP-seq SSU footprinting over the start codons provides an intriguing, and somewhat unexpected insight in this regard. Even when SSU footprints over start codons are compared only between the highly efficiently initiated mRNAs (as can be measured by the high ratio of the start codon SSU plie-ups *vs.* pile-ups in the 5'UTSs)[51, 266], different mRNAs demonstrate distinctively different footprint patterns (Fig. 7). Accounting for the attribution of the different start codon recognition stages to the different footprint 3'-end extensions over the start codons (as explained in Fig. 9 and the Rearrangement of the Scanning Complexes section), it can be suggested that the proportions of the SSU dwell time in each state vary across mRNAs. For example, YDL014W mRNA displays many +6 nt 3' extensions (19 nt footprint) and almost no +29 nt 3' extensions (37 nt footprint) (Fig. 7). In contrast, YLR208W demonstrates the exact opposite (almost no 19 nt but many 37 nt footprints), and YJR045C and YAL005C exhibit interim of the tendency with +16 nt 3' extensions (29 nt footprint) well-represented (Fig. 7). Thus, start codon recognition may be fine-tuned deeper than previously thought, and its control may involve not only pausing over the start sites, but also signals in mRNA that affect the dynamics of each of the stages, urging for further investigations of the underlying mechanisms.

Conclusion

Recent times have seen outstanding progress in deciphering the molecular mechanism of eukaryotic translation initiation by cap-dependent ribosome recruitment and 5' UTR scanning. Many of the original findings obtained through hundreds of painstaking biochemical and genetic studies have been substantiated by insight derived from high resolution crystallographic and cryo-EM structures of the small ribosomal subunit in complex with different complements of translation initiation factors. Thus, we now can relate much of the structural information to our models of the various sub-steps of initiation and approach a reasonable reconstruction of the dynamics of the entire process. Nevertheless, some challenges remain for the near-future. First, we still do not fully understand the mechanism of SSU locomotion during scanning, and the structural organisation of the scanning 'motor'. Second, there is no comprehensive understanding about the usage of different initiation factors across transcriptomes, in different organismal and cellular contexts. Given recent progress in cryo-EM and high-throughput sequencing technologies, both problems can now be directly approached, and we can expect some major developments in the coming years. Advances of single-molecule approaches[162, 424-427] and their merger with high-throughput sequencing techniques[428, 429] can be anticipated to result in the deeper insights there.

Another important limitation that needs to be acknowledged is that such a patchwork of insights gleaned from disparate data sources may only approximate the sequence of events for a generic or 'average' mRNA. From cumulative evidence over many years we can anticipate a pronounced and context-dependent variability across mRNAs even within the canonical initiation paradigm. For example, initiation may play out differently depending on the stage of the mRNA lifecycle. Clearly, the first round of translation initiation on nascent mRNA will have unique features, especially in regard to the initial steps of cap attachment and scanning[221]. The importance and extent of the cap-to-poly(A) closed-loop may vary between mRNAs[38], even between mRNAs derived from the same genes, as differential promoter usage and alternative 3' end cleavage and polyadenylation frequently generate isoforms with varying 5' and 3' UTRs[29, 430,431]. Aspects of the initiation mechanism may also be executed differently depending on subcellular localisation. For example, compared to 'free' cytosolic polysomes ER-attached ribosomes must contend with additional constraints for the formation of closed-loop interactions and transfer of the components during re-initiation. High-throughput sequencing-based methods such as ribosome profiling and TCP-seq will likely provide the transcriptome-wide data to illustrate and dissect these events[51, 266].

Acknowledgments

The work was supported by the Australian Research Council grant DP130101928 and Cancer Council ACT grant GNT1120469 to Thomas Preiss. We are very grateful to Susan Wagner and all members of Preiss laboratory for comments and suggestions during manuscript preparation. Authors declare no conflicts of interest.

References

1. Steitz TA, Moore PB. Perspectives on the ribosome. *Philos Trans R Soc Lond B Biol Sci* 2017, 372.
2. Wilson DN, Doudna Cate JH. The structure and function of the eukaryotic ribosome. *Cold Spring Harb Perspect Biol* 2012, 4.

3. Korostelev A, Noller HF. The ribosome in focus: new structures bring new insights. *Trends Biochem Sci* 2007, 32:434-441.
4. Steitz TA. On the structural basis of peptide-bond formation and antibiotic resistance from atomic structures of the large ribosomal subunit. *FEBS Lett* 2005, 579:955-958.
5. Spirin AS. The ribosome as a conveying thermal ratchet machine. *J Biol Chem* 2009, 284:21103-21119.
6. Frank J, Gonzalez RL, Jr. Structure and dynamics of a processive Brownian motor: the translating ribosome. *Annu Rev Biochem* 2010, 79:381-412.
7. Marintchev A, Wagner G. Translation initiation: structures, mechanisms and evolution. *Q Rev Biophys* 2004, 37:197-284.
8. Hinnebusch AG, Ivanov IP, Sonenberg N. Translational control by 5'-untranslated regions of eukaryotic mRNAs. *Science* 2016, 352:1413-1416.
9. Anderson WF, Bosch L, Gros F, Grunberg-Manago M, Ochoa S, Rich A, Staehelin T. Initiation of protein synthesis in prokaryotic and eukaryotic systems. Summary of EMBO Workshop. *FEBS Lett* 1974, 48:1-6.
10. Furuichi Y, Muthukrishnan S, Tomasz J, Shatkin AJ. Caps in eukaryotic mRNAs: mechanism of formation of reovirus mRNA 5'-terminal m7GpppGm-C. *Prog Nucleic Acid Res Mol Biol* 1976, 19:3-20.
11. Furuichi Y. Caps on Eukaryotic mRNAs. In: *eLS*: John Wiley & Sons, Ltd; 2014.
12. Decroly E, Canard B. Biochemical principles and inhibitors to interfere with viral capping pathways. *Curr Opin Virol* 2017, 24:87-96.
13. Shimotohno K, Kodama Y, Hashimoto J, Miura KI. Importance of 5'-terminal blocking structure to stabilize mRNA in eukaryotic protein synthesis. *Proc Natl Acad Sci U S A* 1977, 74:2734-2738.
14. Muthukrishnan S, Both GW, Furuichi Y, Shatkin AJ. 5'-Terminal 7-methylguanosine in eukaryotic mRNA is required for translation. *Nature* 1975, 255:33-37.
15. Shafritz DA, Weinstein JA, Safer B, Merrick WC, Weber LA, Hickey ED, Baglioni C. Evidence for role of m7G5'-phosphate group in recognition of eukaryotic mRNA by initiation factor IF-M3. *Nature* 1976, 261:291-294.
16. Arribas-Layton M, Wu D, Lykke-Andersen J, Song H. Structural and functional control of the eukaryotic mRNA decapping machinery. *Biochim Biophys Acta* 2013, 1829:580-589.
17. Labno A, Tomecki R, Dziembowski A. Cytoplasmic RNA decay pathways - Enzymes and mechanisms. *Biochim Biophys Acta* 2016, 1863:3125-3147.
18. Shine J, Dalgarno L. The 3'-terminal sequence of Escherichia coli 16S ribosomal RNA: complementarity to nonsense triplets and ribosome binding sites. *Proc Natl Acad Sci U S A* 1974, 71:1342-1346.
19. Shine J, Dalgarno L. Determinant of cistron specificity in bacterial ribosomes. *Nature* 1975, 254:34-38.
20. Yusupova GZ, Yusupov MM, Cate JH, Noller HF. The path of messenger RNA through the ribosome. *Cell* 2001, 106:233-241.
21. Kaminishi T, Wilson DN, Takemoto C, Harms JM, Kawazoe M, Schluenzen F, Hanawa-Suetsugu K, Shirouzu M, Fucini P, Yokoyama S. A snapshot of the 30S ribosomal subunit capturing mRNA via the Shine-Dalgarno interaction. *Structure* 2007, 15:289-297.
22. Baralle FE, Brownlee GG. AUG is the only recognisable signal sequence in the 5' non-coding regions of eukaryotic mRNA. *Nature* 1978, 274:84-87.
23. Heywood SM. Letter: Is there specificity in the initiation of protein synthesis in eukaryotic cells? *Dev Biol* 1973, 31:F1-2.
24. Shi Y, Manley JL. The end of the message: multiple protein-RNA interactions define the mRNA polyadenylation site. *Genes Dev* 2015, 29:889-897.

25. Viphakone N, Voisinet-Hakil F, Minvielle-Sebastia L. Molecular dissection of mRNA poly(A) tail length control in yeast. *Nucleic Acids Res* 2008, 36:2418-2433.
26. Richter JD. CPEB: a life in translation. *Trends Biochem Sci* 2007, 32:279-285.
27. Villalba A, Coll O, Gebauer F. Cytoplasmic polyadenylation and translational control. *Curr Opin Genet Dev* 2011, 21:452-457.
28. Beilharz TH, Preiss T. Widespread use of poly(A) tail length control to accentuate expression of the yeast transcriptome. *RNA* 2007, 13:982-997.
29. Turner RE, Pattison AD, Beilharz TH. Alternative polyadenylation in the regulation and dysregulation of gene expression. *Semin Cell Dev Biol* 2017.
30. Soetanto R, Hynes CJ, Patel HR, Humphreys DT, Evers M, Duan G, Parker BJ, Archer SK, Clancy JL, Graham RM, et al. Role of miRNAs and alternative mRNA 3'-end cleavage and polyadenylation of their mRNA targets in cardiomyocyte hypertrophy. *Biochim Biophys Acta* 2016, 1859:744-756.
31. Elkon R, Ugalde AP, Agami R. Alternative cleavage and polyadenylation: extent, regulation and function. *Nat Rev Genet* 2013, 14:496-506.
32. Charlesworth A, Meijer HA, de Moor CH. Specificity factors in cytoplasmic polyadenylation. *Wiley Interdiscip Rev RNA* 2013, 4:437-461.
33. Jalkanen AL, Coleman SJ, Wilusz J. Determinants and implications of mRNA poly(A) tail size--does this protein make my tail look big? *Semin Cell Dev Biol* 2014, 34:24-32.
34. D'Ambrogio A, Nagaoka K, Richter JD. Translational control of cell growth and malignancy by the CPEBs. *Nat Rev Cancer* 2013, 13:283-290.
35. Weill L, Belloc E, Bava FA, Mendez R. Translational control by changes in poly(A) tail length: recycling mRNAs. *Nat Struct Mol Biol* 2012, 19:577-585.
36. Tarun SZ, Jr., Sachs AB. Association of the yeast poly(A) tail binding protein with translation initiation factor eIF-4G. *Embo J* 1996, 15:7168-7177.
37. Preiss T, Hentze MW. From factors to mechanisms: translation and translational control in eukaryotes. *Curr Opin Genet Dev* 1999, 9:515-521.
38. Archer SK, Shirokikh NE, Hallwirth CV, Beilharz TH, Preiss T. Probing the closed-loop model of mRNA translation in living cells. *RNA Biol* 2015, 12:248-254.
39. Warner JR, Rich A, Hall CE. Electron Microscope Studies of Ribosomal Clusters Synthesizing Hemoglobin. *Science* 1962, 138:1399-1403.
40. Yazaki K, Yoshida T, Wakiyama M, Miura K. Polysomes of eukaryotic cells observed by electron microscopy. *J Electron Microsc (Tokyo)* 2000, 49:663-668.
41. Afonina ZA, Myasnikov AG, Shirokov VA, Klaholz BP, Spirin AS. Formation of circular polyribosomes on eukaryotic mRNA without cap-structure and poly(A)-tail: a cryo electron tomography study. *Nucleic Acids Res* 2014, 42:9461-9469.
42. Myasnikov AG, Afonina ZA, Menetret JF, Shirokov VA, Spirin AS, Klaholz BP. The molecular structure of the left-handed supra-molecular helix of eukaryotic polyribosomes. *Nat Commun* 2014, 5:5294.
43. Palade G. Intracellular aspects of the process of protein synthesis. *Science* 1975, 189:867.
44. Christensen AK, Bourne CM. Shape of large bound polysomes in cultured fibroblasts and thyroid epithelial cells. *Anat Rec* 1999, 255:116-129.
45. Ban N, Nissen P, Hansen J, Moore PB, Steitz TA. The complete atomic structure of the large ribosomal subunit at 2.4 A resolution. *Science* 2000, 289:905-920.
46. Tocilj A, Schlunzen F, Janell D, Gluhmann M, Hansen HA, Harms J, Bashan A, Bartels H, Agmon I, Franceschi F, et al. The small ribosomal subunit from Thermus thermophilus at 4.5 A resolution: pattern fittings and the identification of a functional site. *Proc Natl Acad Sci U S A* 1999, 96:14252-14257.
47. Clemons WM, Jr., May JL, Wimberly BT, McCutcheon JP, Capel MS, Ramakrishnan V. Structure of a bacterial 30S ribosomal subunit at 5.5 A resolution. *Nature* 1999, 400:833-840.

48. Cate JH, Yusupov MM, Yusupova GZ, Earnest TN, Noller HF. X-ray crystal structures of 70S ribosome functional complexes. *Science* 1999, 285:2095-2104.
49. Frank J. The mechanism of translation. *F1000Res* 2017, 6:198.
50. Ingolia NT, Ghaemmaghami S, Newman JR, Weissman JS. Genome-wide analysis in vivo of translation with nucleotide resolution using ribosome profiling. *Science* 2009, 324:218-223.
51. Archer SK, Shirokikh NE, Beilharz TH, Preiss T. Dynamics of ribosome scanning and recycling revealed by translation complex profiling. *Nature* 2016, 535:570-574.
52. McGlincy NJ, Ingolia NT. Transcriptome-wide measurement of translation by ribosome profiling. *Methods* 2017, 126:112-129.
53. Bogorad AM, Lin KY, Marintchev A. Novel mechanisms of eIF2B action and regulation by eIF2alpha phosphorylation. *Nucleic Acids Res* 2017, 45:11962-11979.
54. Wortham NC, Proud CG. eIF2B: recent structural and functional insights into a key regulator of translation. *Biochem Soc Trans* 2015, 43:1234-1240.
55. Jennings MD, Pavitt GD. A new function and complexity for protein translation initiation factor eIF2B. *Cell Cycle* 2014, 13:2660-2665.
56. Browning KS, Bailey-Serres J. Mechanism of cytoplasmic mRNA translation. *Arabidopsis Book* 2015, 13:e0176.
57. Monzingo AF, Dhaliwal S, Dutt-Chaudhuri A, Lyon A, Sadow JH, Hoffman DW, Robertus JD, Browning KS. The structure of eukaryotic translation initiation factor-4E from wheat reveals a novel disulfide bond. *Plant Physiol* 2007, 143:1504-1518.
58. Kropiwnicka A, Kuchta K, Lukaszewicz M, Kowalska J, Jemielity J, Ginalski K, Darzynkiewicz E, Zuberek J. Five eIF4E isoforms from Arabidopsis thaliana are characterized by distinct features of cap analogs binding. *Biochem Biophys Res Commun* 2015, 456:47-52.
59. Martinez-Silva AV, Aguirre-Martinez C, Flores-Tinoco CE, Alejandri-Ramirez ND, Dinkova TD. Translation initiation factor AteIF(iso)4E is involved in selective mRNA translation in Arabidopsis thaliana seedlings. *PLoS One* 2012, 7:e31606.
60. Freire ER, Sturm NR, Campbell DA, de Melo Neto OP. The Role of Cytoplasmic mRNA Cap-Binding Protein Complexes in Trypanosoma brucei and Other Trypanosomatids. *Pathogens* 2017, 6.
61. Klein C, Terrao M, Inchaustegui Gil D, Clayton C. Polysomes of Trypanosoma brucei: Association with Initiation Factors and RNA-Binding Proteins. *PLoS One* 2015, 10:e0135973.
62. Clayton CE. Gene expression in Kinetoplastids. *Curr Opin Microbiol* 2016, 32:46-51.
63. Smircich P, Eastman G, Bispo S, Duhagon MA, Guerra-Slompo EP, Garat B, Goldenberg S, Munroe DJ, Dallagiovanna B, Holetz F, et al. Ribosome profiling reveals translation control as a key mechanism generating differential gene expression in Trypanosoma cruzi. *BMC Genomics* 2015, 16:443.
64. Obayashi E, Luna RE, Nagata T, Martin-Marcos P, Hiraishi H, Singh CR, Erzberger JP, Zhang F, Arthanari H, Morris J, et al. Molecular Landscape of the Ribosome Pre-initiation Complex during mRNA Scanning: Structural Role for eIF3c and Its Control by eIF5. *Cell Rep* 2017, 18:2651-2663.
65. Fijalkowska D, Verbruggen S, Ndah E, Jonckheere V, Menschaert G, Van Damme P. eIF1 modulates the recognition of suboptimal translation initiation sites and steers gene expression via uORFs. *Nucleic Acids Res* 2017, 45:7997-8013.
66. Lomakin IB, Steitz TA. The initiation of mammalian protein synthesis and mRNA scanning mechanism. *Nature* 2013, 500:307-311.
67. Asano K. Why is start codon selection so precise in eukaryotes? *Translation* 2014, 2:e28387.
68. Jackson RJ, Hellen CU, Pestova TV. The mechanism of eukaryotic translation initiation and principles of its regulation. *Nat Rev Mol Cell Biol* 2010, 11:113-127.
69. Hinnebusch AG. Structural Insights into the Mechanism of Scanning and Start Codon Recognition in Eukaryotic Translation Initiation. *Trends Biochem Sci* 2017, 42:589-611.

70. Nag N, Lin KY, Edmonds KA, Yu J, Nadkarni D, Marintcheva B, Marintchev A. eIF1A/eIF5B interaction network and its functions in translation initiation complex assembly and remodeling. *Nucleic Acids Res* 2016, 44:7441-7456.
71. Lind C, Aqvist J. Principles of start codon recognition in eukaryotic translation initiation. *Nucleic Acids Res* 2016, 44:8425-8432.
72. Sokabe M, Fraser CS. Human eukaryotic initiation factor 2 (eIF2)-GTP-Met-tRNAi ternary complex and eIF3 stabilize the 43 S preinitiation complex. *J Biol Chem* 2014, 289:31827-31836.
73. Visweswaraiah J, Hinnebusch AG. Interface between 40S exit channel protein uS7/Rps5 and eIF2alpha modulates start codon recognition in vivo. *Elife* 2017, 6.
74. Jennings MD, Kershaw CJ, Adomavicius T, Pavitt GD. Fail-safe control of translation initiation by dissociation of eIF2alpha phosphorylated ternary complexes. *Elife* 2017, 6.
75. Jennings MD, Kershaw CJ, White C, Hoyle D, Richardson JP, Costello JL, Donaldson IJ, Zhou Y, Pavitt GD. eIF2beta is critical for eIF5-mediated GDP-dissociation inhibitor activity and translational control. *Nucleic Acids Res* 2016, 44:9698-9709.
76. Alone PV, Dever TE. Direct binding of translation initiation factor eIF2gamma-G domain to its GTPase-activating and GDP-GTP exchange factors eIF5 and eIF2B epsilon. *J Biol Chem* 2006, 281:12636-12644.
77. Kearse MG, Wilusz JE. Non-AUG translation: a new start for protein synthesis in eukaryotes. *Genes Dev* 2017, 31:1717-1731.
78. Sendoel A, Dunn JG, Rodriguez EH, Naik S, Gomez NC, Hurwitz B, Levorse J, Dill BD, Schramek D, Molina H, et al. Translation from unconventional 5' start sites drives tumour initiation. *Nature* 2017, 541:494-499.
79. Dmitriev SE, Terenin IM, Andreev DE, Ivanov PA, Dunaevsky JE, Merrick WC, Shatsky IN. GTP-independent tRNA delivery to the ribosomal P-site by a novel eukaryotic translation factor. *J Biol Chem* 2010, 285:26779-26787.
80. Vaidya AT, Lomakin IB, Joseph NN, Dmitriev SE, Steitz TA. Crystal Structure of the C-terminal Domain of Human eIF2D and Its Implications on Eukaryotic Translation Initiation. *J Mol Biol* 2017, 429:2765-2771.
81. Cate JH. Human eIF3: from 'blobology' to biological insight. *Philos Trans R Soc Lond B Biol Sci* 2017, 372.
82. Valasek LS, Zeman J, Wagner S, Beznoskova P, Pavlikova Z, Mohammad MP, Hronova V, Herrmannova A, Hashem Y, Gunisova S. Embraced by eIF3: structural and functional insights into the roles of eIF3 across the translation cycle. *Nucleic Acids Res* 2017.
83. Erzberger JP, Stengel F, Pellarin R, Zhang S, Schaefer T, Aylett CH, Cimermancic P, Boehringer D, Sali A, Aebersold R, et al. Molecular architecture of the 40SeIF1eIF3 translation initiation complex. *Cell* 2014, 158:1123-1135.
84. Merrick WC. eIF4F: a retrospective. *J Biol Chem* 2015, 290:24091-24099.
85. Pelletier J, Graff J, Ruggero D, Sonenberg N. Targeting the eIF4F translation initiation complex: a critical nexus for cancer development. *Cancer Res* 2015, 75:250-263.
86. Garcia-Garcia C, Frieda KL, Feoktistova K, Fraser CS, Block SM. RNA BIOCHEMISTRY. Factor-dependent processivity in human eIF4A DEAD-box helicase. *Science* 2015, 348:1486-1488.
87. Sun Y, Atas E, Lindqvist LM, Sonenberg N, Pelletier J, Meller A. Single-molecule kinetics of the eukaryotic initiation factor 4AI upon RNA unwinding. *Structure* 2014, 22:941-948.
88. Ozes AR, Feoktistova K, Avanzino BC, Fraser CS. Duplex unwinding and ATPase activities of the DEAD-box helicase eIF4A are coupled by eIF4G and eIF4B. *J Mol Biol* 2011, 412:674-687.
89. Papadopoulos E, Jenni S, Kabha E, Takrouri KJ, Yi T, Salvi N, Luna RE, Gavathiotis E, Mahalingam P, Arthanari H, et al. Structure of the eukaryotic translation initiation factor eIF4E in complex with 4EGI-1 reveals an allosteric mechanism for dissociating eIF4G. *Proc Natl Acad Sci U S A* 2014, 111:E3187-3195.

90. O'Leary SE, Petrov A, Chen J, Puglisi JD. Dynamic recognition of the mRNA cap by Saccharomyces cerevisiae eIF4E. *Structure* 2013, 21:2197-2207.
91. Villa N, Do A, Hershey JW, Fraser CS. Human eukaryotic initiation factor 4G (eIF4G) protein binds to eIF3c, -d, and -e to promote mRNA recruitment to the ribosome. *J Biol Chem* 2013, 288:32932-32940.
92. Zhao P, Liu Q, Miller WA, Goss DJ. Eukaryotic translation initiation factor 4G (eIF4G) coordinates interactions with eIF4A, eIF4B, and eIF4E in binding and translation of the barley yellow dwarf virus 3' cap-independent translation element (BTE). *J Biol Chem* 2017, 292:5921-5931.
93. Kumar P, Hellen CU, Pestova TV. Toward the mechanism of eIF4F-mediated ribosomal attachment to mammalian capped mRNAs. *Genes Dev* 2016, 30:1573-1588.
94. Andreou AZ, Harms U, Klostermeier D. eIF4B stimulates eIF4A ATPase and unwinding activities by direct interaction through its 7-repeats region. *RNA Biol* 2017, 14:113-123.
95. Sen ND, Zhou F, Harris MS, Ingolia NT, Hinnebusch AG. eIF4B stimulates translation of long mRNAs with structured 5' UTRs and low closed-loop potential but weak dependence on eIF4G. *Proc Natl Acad Sci U S A* 2016, 113:10464-10472.
96. Sun Y, Atas E, Lindqvist L, Sonenberg N, Pelletier J, Meller A. The eukaryotic initiation factor eIF4H facilitates loop-binding, repetitive RNA unwinding by the eIF4A DEAD-box helicase. *Nucleic Acids Res* 2012, 40:6199-6207.
97. Tang L, Morris J, Wan J, Moore C, Fujita Y, Gillaspie S, Aube E, Nanda J, Marques M, Jangal M, et al. Competition between translation initiation factor eIF5 and its mimic protein 5MP determines non-AUG initiation rate genome-wide. *Nucleic Acids Res* 2017.
98. Schuller AP, Wu CC, Dever TE, Buskirk AR, Green R. eIF5A Functions Globally in Translation Elongation and Termination. *Mol Cell* 2017, 66:194-205 e195.
99. Rossi D, Kuroshu R, Zanelli CF, Valentini SR. eIF5A and EF-P: two unique translation factors are now traveling the same road. *Wiley Interdiscip Rev RNA* 2014, 5:209-222.
100. Pisareva VP, Pisarev AV. eIF5 and eIF5B together stimulate 48S initiation complex formation during ribosomal scanning. *Nucleic Acids Res* 2014, 42:12052-12069.
101. Brina D, Miluzio A, Ricciardi S, Biffo S. eIF6 anti-association activity is required for ribosome biogenesis, translational control and tumor progression. *Biochim Biophys Acta* 2015, 1849:830-835.
102. Martineau Y, Derry MC, Wang X, Yanagiya A, Berlanga JJ, Shyu AB, Imataka H, Gehring K, Sonenberg N. Poly(A)-binding protein-interacting protein 1 binds to eukaryotic translation initiation factor 3 to stimulate translation. *Mol Cell Biol* 2008, 28:6658-6667.
103. Kahvejian A, Svitkin YV, Sukarieh R, M'Boutchou MN, Sonenberg N. Mammalian poly(A)-binding protein is a eukaryotic translation initiation factor, which acts via multiple mechanisms. *Genes Dev* 2005, 19:104-113.
104. Liberman N, Gandin V, Svitkin YV, David M, Virgili G, Jaramillo M, Holcik M, Nagar B, Kimchi A, Sonenberg N. DAP5 associates with eIF2beta and eIF4AI to promote Internal Ribosome Entry Site driven translation. *Nucleic Acids Res* 2015, 43:3764-3775.
105. Weisser M, Schafer T, Leibundgut M, Bohringer D, Aylett CHS, Ban N. Structural and Functional Insights into Human Re-initiation Complexes. *Mol Cell* 2017, 67:447-456 e447.
106. Pisareva VP, Pisarev AV. DHX29 reduces leaky scanning through an upstream AUG codon regardless of its nucleotide context. *Nucleic Acids Res* 2016, 44:4252-4265.
107. des Georges A, Dhote V, Kuhn L, Hellen CU, Pestova TV, Frank J, Hashem Y. Structure of mammalian eIF3 in the context of the 43S preinitiation complex. *Nature* 2015, 525:491-495.
108. Aylett CH, Ban N. Eukaryotic aspects of translation initiation brought into focus. *Philos Trans R Soc Lond B Biol Sci* 2017, 372.
109. Bitterman PB, Polunovsky VA. Translational control of cell fate: from integration of environmental signals to breaching anticancer defense. *Cell Cycle* 2012, 11:1097-1107.

110. Chu J, Cargnello M, Topisirovic I, Pelletier J. Translation Initiation Factors: Reprogramming Protein Synthesis in Cancer. *Trends Cell Biol* 2016, 26:918-933.
111. Jansen RP, Niessing D, Baumann S, Feldbrugge M. mRNA transport meets membrane traffic. *Trends Genet* 2014, 30:408-417.
112. Besse F, Ephrussi A. Translational control of localized mRNAs: restricting protein synthesis in space and time. *Nat Rev Mol Cell Biol* 2008, 9:971-980.
113. Bhat M, Robichaud N, Hulea L, Sonenberg N, Pelletier J, Topisirovic I. Targeting the translation machinery in cancer. *Nat Rev Drug Discov* 2015, 14:261-278.
114. Hershey JW. Regulation of protein synthesis and the role of eIF3 in cancer. *Braz J Med Biol Res* 2010, 43:920-930.
115. Hershey JW, Sonenberg N, Mathews MB. Principles of translational control: an overview. *Cold Spring Harb Perspect Biol* 2012, 4.
116. Topisirovic I, Svitkin YV, Sonenberg N, Shatkin AJ. Cap and cap-binding proteins in the control of gene expression. *Wiley Interdiscip Rev RNA* 2011, 2:277-298.
117. Sonenberg N, Hinnebusch AG. Regulation of translation initiation in eukaryotes: mechanisms and biological targets. *Cell* 2009, 136:731-745.
118. Proud CG. Mnks, eIF4E phosphorylation and cancer. *Biochim Biophys Acta* 2015, 1849:766-773.
119. Proud CG. mTOR Signalling in Health and Disease. *Biochem Soc Trans* 2011, 39:431-436.
120. Andaya A, Villa N, Jia W, Fraser CS, Leary JA. Phosphorylation stoichiometries of human eukaryotic initiation factors. *Int J Mol Sci* 2014, 15:11523-11538.
121. Meyuhas O. Ribosomal Protein S6 Phosphorylation: Four Decades of Research. *Int Rev Cell Mol Biol* 2015, 320:41-73.
122. Wittenberg AD, Azar S, Klochendler A, Stolovich-Rain M, Avraham S, Birnbaum L, Binder Gallimidi A, Katz M, Dor Y, Meyuhas O. Phosphorylated Ribosomal Protein S6 Is Required for Akt-Driven Hyperplasia and Malignant Transformation, but Not for Hypertrophy, Aneuploidy and Hyperfunction of Pancreatic beta-Cells. *PLoS One* 2016, 11:e0149995.
123. Slavov N, Semrau S, Airoldi E, Budnik B, van Oudenaarden A. Differential Stoichiometry among Core Ribosomal Proteins. *Cell Rep* 2015, 13:865-873.
124. Preiss T. All Ribosomes Are Created Equal. Really? *Trends Biochem Sci* 2016, 41:121-123.
125. Xue S, Tian S, Fujii K, Kladwang W, Das R, Barna M. RNA regulons in Hox 5' UTRs confer ribosome specificity to gene regulation. *Nature* 2015, 517:33-38.
126. Frydryskova K, Masek T, Borcin K, Mrvova S, Venturi V, Pospisek M. Distinct recruitment of human eIF4E isoforms to processing bodies and stress granules. *BMC Mol Biol* 2016, 17:21.
127. Coldwell MJ, Sack U, Cowan JL, Barrett RM, Vlasak M, Sivakumaran K, Morley SJ. Multiple isoforms of the translation initiation factor eIF4GII are generated via use of alternative promoters, splice sites and a non-canonical initiation codon. *Biochem J* 2012, 448:1-11.
128. Ghosh S, Lasko P. Loss-of-function analysis reveals distinct requirements of the translation initiation factors eIF4E, eIF4E-3, eIF4G and eIF4G2 in Drosophila spermatogenesis. *PLoS One* 2015, 10:e0122519.
129. Svitkin YV, Gradi A, Imataka H, Morino S, Sonenberg N. Eukaryotic initiation factor 4GII (eIF4GII), but not eIF4GI, cleavage correlates with inhibition of host cell protein synthesis after human rhinovirus infection. *J Virol* 1999, 73:3467-3472.
130. Lewis SM, Cerquozzi S, Graber TE, Ungureanu NH, Andrews M, Holcik M. The eIF4G homolog DAP5/p97 supports the translation of select mRNAs during endoplasmic reticulum stress. *Nucleic Acids Res* 2008, 36:168-178.
131. Sugiyama H, Takahashi K, Yamamoto T, Iwasaki M, Narita M, Nakamura M, Rand TA, Nakagawa M, Watanabe A, Yamanaka S. Nat1 promotes translation of specific proteins that induce differentiation of mouse embryonic stem cells. *Proc Natl Acad Sci U S A* 2017, 114:340-345.

132. Lu WT, Wilczynska A, Smith E, Bushell M. The diverse roles of the eIF4A family: you are the company you keep. *Biochem Soc Trans* 2014, 42:166-172.
133. Shahbazian D, Parsyan A, Petroulakis E, Hershey J, Sonenberg N. eIF4B controls survival and proliferation and is regulated by proto-oncogenic signaling pathways. *Cell Cycle* 2010, 9:4106-4109.
134. Kamenska A, Simpson C, Standart N. eIF4E-binding proteins: new factors, new locations, new roles. *Biochem Soc Trans* 2014, 42:1238-1245.
135. Han SJ, Vaccari S, Nedachi T, Andersen CB, Kovacina KS, Roth RA, Conti M. Protein kinase B/Akt phosphorylation of PDE3A and its role in mammalian oocyte maturation. *EMBO J* 2006, 25:5716-5725.
136. Castagnetti S, Hentze MW, Ephrussi A, Gebauer F. Control of oskar mRNA translation by Bruno in a novel cell-free system from Drosophila ovaries. *Development* 2000, 127:1063-1068.
137. Yarunin A, Harris RE, Ashe MP, Ashe HL. Patterning of the Drosophila oocyte by a sequential translation repression program involving the d4EHP and Belle translational repressors. *RNA Biol* 2011, 8:904-912.
138. Minshall N, Reiter MH, Weil D, Standart N. CPEB interacts with an ovary-specific eIF4E and 4E-T in early Xenopus oocytes. *J Biol Chem* 2007, 282:37389-37401.
139. Saletta F, Suryo Rahmanto Y, Richardson DR. The translational regulator eIF3a: the tricky eIF3 subunit! *Biochim Biophys Acta* 2010, 1806:275-286.
140. Sanchez AM, Csibi A, Raibon A, Docquier A, Lagirand-Cantaloube J, Leibovitch MP, Leibovitch SA, Bernardi H. eIF3f: a central regulator of the antagonism atrophy/hypertrophy in skeletal muscle. *Int J Biochem Cell Biol* 2013, 45:2158-2162.
141. Choudhuri A, Maitra U, Evans T. Translation initiation factor eIF3h targets specific transcripts to polysomes during embryogenesis. *Proc Natl Acad Sci U S A* 2013, 110:9818-9823.
142. Richter JD, Lasko P. Translational control in oocyte development. *Cold Spring Harb Perspect Biol* 2011, 3:a002758.
143. Kang MK, Han SJ. Post-transcriptional and post-translational regulation during mouse oocyte maturation. *BMB Rep* 2011, 44:147-157.
144. Abdelhaleem M. RNA helicases: regulators of differentiation. *Clin Biochem* 2005, 38:499-503.
145. Standart N, Minshall N. Translational control in early development: CPEB, P-bodies and germinal granules. *Biochem Soc Trans* 2008, 36:671-676.
146. Scheper GC, van der Knaap MS, Proud CG. Translation matters: protein synthesis defects in inherited disease. *Nat Rev Genet* 2007, 8:711-723.
147. Mitchell SF, Parker R. Principles and properties of eukaryotic mRNPs. *Mol Cell* 2014, 54:547-558.
148. Skabkin MA, Kiselyova OI, Chernov KG, Sorokin AV, Dubrovin EV, Yaminsky IV, Vasiliev VD, Ovchinnikov LP. Structural organization of mRNA complexes with major core mRNP protein YB-1. *Nucleic Acids Res* 2004, 32:5621-5635.
149. Castello A, Fischer B, Eichelbaum K, Horos R, Beckmann BM, Strein C, Davey NE, Humphreys DT, Preiss T, Steinmetz LM, et al. Insights into RNA biology from an atlas of mammalian mRNA-binding proteins. *Cell* 2012, 149:1393-1406.
150. Schwanhausser B, Busse D, Li N, Dittmar G, Schuchhardt J, Wolf J, Chen W, Selbach M. Global quantification of mammalian gene expression control. *Nature* 2011, 473:337-342.
151. Hinnebusch AG, Asano K, Olsen DS, Phan L, Nielsen KH, Valasek L. Study of translational control of eukaryotic gene expression using yeast. *Ann N Y Acad Sci* 2004, 1038:60-74.
152. Harding HP, Novoa I, Zhang Y, Zeng H, Wek R, Schapira M, Ron D. Regulated translation initiation controls stress-induced gene expression in mammalian cells. *Mol Cell* 2000, 6:1099-1108.

153. Gebauer F, Hentze MW. Molecular mechanisms of translational control. *Nat Rev Mol Cell Biol* 2004, 5:827-835.
154. Andreev DE, O'Connor PB, Loughran G, Dmitriev SE, Baranov PV, Shatsky IN. Insights into the mechanisms of eukaryotic translation gained with ribosome profiling. *Nucleic Acids Res* 2017, 45:513-526.
155. Gebauer F, Preiss T, Hentze MW. From cis-regulatory elements to complex RNPs and back. *Cold Spring Harb Perspect Biol* 2012, 4:a012245.
156. Fabian MR, Sonenberg N, Filipowicz W. Regulation of mRNA translation and stability by microRNAs. *Annu Rev Biochem* 2010, 79:351-379.
157. Humphreys DT, Westman BJ, Martin DI, Preiss T. MicroRNAs control translation initiation by inhibiting eukaryotic initiation factor 4E/cap and poly(A) tail function. *Proc Natl Acad Sci U S A* 2005, 102:16961-16966.
158. Shatsky IN, Dmitriev SE, Terenin IM, Andreev DE. Cap- and IRES-independent scanning mechanism of translation initiation as an alternative to the concept of cellular IRESs. *Mol Cells* 2010, 30:285-293.
159. Pisarev AV, Shirokikh NE, Hellen CU. Translation initiation by factor-independent binding of eukaryotic ribosomes to internal ribosomal entry sites. *C R Biol* 2005, 328:589-605.
160. Terenin IM, Smirnova VV, Andreev DE, Dmitriev SE, Shatsky IN. A researcher's guide to the galaxy of IRESs. *Cell Mol Life Sci* 2017, 74:1431-1455.
161. Yamamoto H, Unbehaun A, Spahn CMT. Ribosomal Chamber Music: Toward an Understanding of IRES Mechanisms. *Trends Biochem Sci* 2017, 42:655-668.
162. Johnson AG, Grosely R, Petrov AN, Puglisi JD. Dynamics of IRES-mediated translation. *Philos Trans R Soc Lond B Biol Sci* 2017, 372.
163. Chen CY, Sarnow P. Initiation of protein synthesis by the eukaryotic translational apparatus on circular RNAs. *Science* 1995, 268:415-417.
164. Legnini I, Di Timoteo G, Rossi F, Morlando M, Briganti F, Sthandier O, Fatica A, Santini T, Andronache A, Wade M, et al. Circ-ZNF609 Is a Circular RNA that Can Be Translated and Functions in Myogenesis. *Mol Cell* 2017, 66:22-37 e29.
165. Pamudurti NR, Bartok O, Jens M, Ashwal-Fluss R, Stottmeister C, Ruhe L, Hanan M, Wyler E, Perez-Hernandez D, Ramberger E, et al. Translation of CircRNAs. *Mol Cell* 2017, 66:9-21 e27.
166. Walters B, Thompson SR. Cap-Independent Translational Control of Carcinogenesis. *Front Oncol* 2016, 6:128.
167. Faye MD, Holcik M. The role of IRES trans-acting factors in carcinogenesis. *Biochim Biophys Acta* 2015, 1849:887-897.
168. Jackson RJ. The current status of vertebrate cellular mRNA IRESs. *Cold Spring Harb Perspect Biol* 2013, 5.
169. Thakor N, Smith MD, Roberts L, Faye MD, Patel H, Wieden HJ, Cate JHD, Holcik M. Cellular mRNA recruits the ribosome via eIF3-PABP bridge to initiate internal translation. *RNA Biol* 2017, 14:553-567.
170. Thakor N, Holcik M. IRES-mediated translation of cellular messenger RNA operates in eIF2alpha- independent manner during stress. *Nucleic Acids Res* 2012, 40:541-552.
171. Thoreen CC, Chantranupong L, Keys HR, Wang T, Gray NS, Sabatini DM. A unifying model for mTORC1-mediated regulation of mRNA translation. *Nature* 2012, 485:109-113.
172. Gandin V, Masvidal L, Hulea L, Gravel SP, Cargnello M, McLaughlan S, Cai Y, Balanathan P, Morita M, Rajakumar A, et al. nanoCAGE reveals 5' UTR features that define specific modes of translation of functionally related MTOR-sensitive mRNAs. *Genome Res* 2016, 26:636-648.
173. Bhattacharyya D, Diamond P, Basu S. An Independently folding RNA G-quadruplex domain directly recruits the 40S ribosomal subunit. *Biochemistry* 2015, 54:1879-1885.

174. Wolfe AL, Singh K, Zhong Y, Drewe P, Rajasekhar VK, Sanghvi VR, Mavrakis KJ, Jiang M, Roderick JE, Van der Meulen J, et al. RNA G-quadruplexes cause eIF4A-dependent oncogene translation in cancer. *Nature* 2014, 513:65-70.
175. Liang H, He S, Yang J, Jia X, Wang P, Chen X, Zhang Z, Zou X, McNutt MA, Shen WH, et al. PTENalpha, a PTEN isoform translated through alternative initiation, regulates mitochondrial function and energy metabolism. *Cell Metab* 2014, 19:836-848.
176. Krieger E, Vriend G. YASARA View - molecular graphics for all devices - from smartphones to workstations. *Bioinformatics* 2014, 30:2981-2982.
177. Llacer JL, Hussain T, Marler L, Aitken CE, Thakur A, Lorsch JR, Hinnebusch AG, Ramakrishnan V. Conformational Differences between Open and Closed States of the Eukaryotic Translation Initiation Complex. *Mol Cell* 2015, 59:399-412.
178. Konagurthu AS, Whisstock JC, Stuckey PJ, Lesk AM. MUSTANG: a multiple structural alignment algorithm. *Proteins* 2006, 64:559-574.
179. Simonetti A, Brito Querido J, Myasnikov AG, Mancera-Martinez E, Renaud A, Kuhn L, Hashem Y. eIF3 Peripheral Subunits Rearrangement after mRNA Binding and Start-Codon Recognition. *Mol Cell* 2016, 63:206-217.
180. Yamamoto H, Unbehaun A, Loerke J, Behrmann E, Collier M, Burger J, Mielke T, Spahn CM. Structure of the mammalian 80S initiation complex with initiation factor 5B on HCV-IRES RNA. *Nat Struct Mol Biol* 2014, 21:721-727.
181. Meyer KD, Patil DP, Zhou J, Zinoviev A, Skabkin MA, Elemento O, Pestova TV, Qian SB, Jaffrey SR. 5' UTR m(6)A Promotes Cap-Independent Translation. *Cell* 2015, 163:999-1010.
182. Lin S, Choe J, Du P, Triboulet R, Gregory RI. The m(6)A Methyltransferase METTL3 Promotes Translation in Human Cancer Cells. *Mol Cell* 2016, 62:335-345.
183. Kozak M. Alternative ways to think about mRNA sequences and proteins that appear to promote internal initiation of translation. *Gene* 2003, 318:1-23.
184. Kozak M. New ways of initiating translation in eukaryotes? *Mol Cell Biol* 2001, 21:1899-1907.
185. Lacerda R, Menezes J, Romao L. More than just scanning: the importance of cap-independent mRNA translation initiation for cellular stress response and cancer. *Cell Mol Life Sci* 2017, 74:1659-1680.
186. Schneider R, Agol VI, Andino R, Bayard F, Cavener DR, Chappell SA, Chen JJ, Darlix JL, Dasgupta A, Donze O, et al. New ways of initiating translation in eukaryotes. *Mol Cell Biol* 2001, 21:8238-8246.
187. Sweeney TR, Abaeva IS, Pestova TV, Hellen CU. The mechanism of translation initiation on Type 1 picornavirus IRESs. *EMBO J* 2014, 33:76-92.
188. Pestova TV, de Breyne S, Pisarev AV, Abaeva IS, Hellen CU. eIF2-dependent and eIF2-independent modes of initiation on the CSFV IRES: a common role of domain II. *Embo J* 2008, 27:1060-1072.
189. Skabkin MA, Skabkina OV, Dhote V, Komar AA, Hellen CU, Pestova TV. Activities of Ligatin and MCT-1/DENR in eukaryotic translation initiation and ribosomal recycling. *Genes Dev* 2010, 24:1787-1801.
190. Starck SR, Tsai JC, Chen K, Shodiya M, Wang L, Yahiro K, Martins-Green M, Shastri N, Walter P. Translation from the 5' untranslated region shapes the integrated stress response. *Science* 2016, 351:aad3867.
191. Akulich KA, Andreev DE, Terenin IM, Smirnova VV, Anisimova AS, Makeeva DS, Arkhipova VI, Stolboushkina EA, Garber MB, Prokofjeva MM, et al. Four translation initiation pathways employed by the leaderless mRNA in eukaryotes. *Sci Rep* 2016, 6:37905.
192. Jang SK, Paek KY. Cap-dependent translation is mediated by 'RNA looping' rather than 'ribosome scanning'. *RNA Biol* 2016, 13:1-5.
193. Caruthers JM, Johnson ER, McKay DB. Crystal structure of yeast initiation factor 4A, a DEAD-box RNA helicase. *Proc Natl Acad Sci U S A* 2000, 97:13080-13085.

194. Buchwald G, Ebert J, Basquin C, Sauliere J, Jayachandran U, Bono F, Le Hir H, Conti E. Insights into the recruitment of the NMD machinery from the crystal structure of a core EJC-UPF3b complex. *Proc Natl Acad Sci U S A* 2010, 107:10050-10055.
195. Fleming K, Ghuman J, Yuan X, Simpson P, Szendroi A, Matthews S, Curry S. Solution structure and RNA interactions of the RNA recognition motif from eukaryotic translation initiation factor 4B. *Biochemistry* 2003, 42:8966-8975.
196. Walker SE, Zhou F, Mitchell SF, Larson VS, Valasek L, Hinnebusch AG, Lorsch JR. Yeast eIF4B binds to the head of the 40S ribosomal subunit and promotes mRNA recruitment through its N-terminal and internal repeat domains. *RNA* 2013, 19:191-207.
197. Nielsen KH, Behrens MA, He Y, Oliveira CL, Jensen LS, Hoffmann SV, Pedersen JS, Andersen GR. Synergistic activation of eIF4A by eIF4B and eIF4G. *Nucleic Acids Res* 2011, 39:2678-2689.
198. Fan S, Jia MZ, Gong W. Crystal structure of the C-terminal region of human p97/DAP5. *Proteins* 2010, 78:2385-2390.
199. Schutz P, Bumann M, Oberholzer AE, Bieniossek C, Trachsel H, Altmann M, Baumann U. Crystal structure of the yeast eIF4A-eIF4G complex: an RNA-helicase controlled by protein-protein interactions. *Proc Natl Acad Sci U S A* 2008, 105:9564-9569.
200. Gruner S, Peter D, Weber R, Wohlbold L, Chung MY, Weichenrieder O, Valkov E, Igreja C, Izaurralde E. The Structures of eIF4E-eIF4G Complexes Reveal an Extended Interface to Regulate Translation Initiation. *Mol Cell* 2016, 64:467-479.
201. Safaee N, Kozlov G, Noronha AM, Xie J, Wilds CJ, Gehring K. Interdomain allostery promotes assembly of the poly(A) mRNA complex with PABP and eIF4G. *Mol Cell* 2012, 48:375-386.
202. Kozlov G, Menade M, Rosenauer A, Nguyen L, Gehring K. Molecular determinants of PAM2 recognition by the MLLE domain of poly(A)-binding protein. *J Mol Biol* 2010, 397:397-407.
203. Conte MR, Kelly G, Babon J, Sanfelice D, Youell J, Smerdon SJ, Proud CG. Structure of the eukaryotic initiation factor (eIF) 5 reveals a fold common to several translation factors. *Biochemistry* 2006, 45:4550-4558.
204. Bieniossek C, Schutz P, Bumann M, Limacher A, Uson I, Baumann U. The crystal structure of the carboxy-terminal domain of human translation initiation factor eIF5. *J Mol Biol* 2006, 360:457-465.
205. Hussain T, Llacer JL, Fernandez IS, Munoz A, Martin-Marcos P, Savva CG, Lorsch JR, Hinnebusch AG, Ramakrishnan V. Structural changes enable start codon recognition by the eukaryotic translation initiation complex. *Cell* 2014, 159:597-607.
206. Weber LA, Hickey ED, Baglioni C. Influence of potassium salt concentration and temperature on inhibition of mRNA translation by 7-methylguanosine5'-monophosphate. *J Biol Chem* 1978, 253:178-183.
207. He H, von der Haar T, Singh CR, Ii M, Li B, Hinnebusch AG, McCarthy JE, Asano K. The yeast eukaryotic initiation factor 4G (eIF4G) HEAT domain interacts with eIF1 and eIF5 and is involved in stringent AUG selection. *Mol Cell Biol* 2003, 23:5431-5445.
208. Asano K, Shalev A, Phan L, Nielsen K, Clayton J, Valasek L, Donahue TF, Hinnebusch AG. Multiple roles for the C-terminal domain of eIF5 in translation initiation complex assembly and GTPase activation. *Embo J* 2001, 20:2326-2337.
209. Hinnebusch AG. The scanning mechanism of eukaryotic translation initiation. *Annu Rev Biochem* 2014, 83:779-812.
210. Berset C, Zurbriggen A, Djafarzadeh S, Altmann M, Trachsel H. RNA-binding activity of translation initiation factor eIF4G1 from Saccharomyces cerevisiae. *RNA* 2003, 9:871-880.
211. von der Haar T, Gross JD, Wagner G, McCarthy JE. The mRNA cap-binding protein eIF4E in post-transcriptional gene expression. *Nat Struct Mol Biol* 2004, 11:503-511.
212. Avdulov S, Herrera J, Smith K, Peterson M, Gomez-Garcia JR, Beadnell TC, Schwertfeger KL, Benyumov AO, Manivel JC, Li S, et al. eIF4E threshold levels differ in governing normal and

neoplastic expansion of mammary stem and luminal progenitor cells. *Cancer Res* 2015, 75:687-697.
213. Gross JD, Moerke NJ, von der Haar T, Lugovskoy AA, Sachs AB, McCarthy JE, Wagner G. Ribosome loading onto the mRNA cap is driven by conformational coupling between eIF4G and eIF4E. *Cell* 2003, 115:739-750.
214. Ptushkina M, von der Haar T, Vasilescu S, Frank R, Birkenhager R, McCarthy JE. Cooperative modulation by eIF4G of eIF4E-binding to the mRNA 5' cap in yeast involves a site partially shared by p20. *EMBO J* 1998, 17:4798-4808.
215. Yanagiya A, Svitkin YV, Shibata S, Mikami S, Imataka H, Sonenberg N. Requirement of RNA binding of mammalian eukaryotic translation initiation factor 4GI (eIF4GI) for efficient interaction of eIF4E with the mRNA cap. *Mol Cell Biol* 2009, 29:1661-1669.
216. Borman AM, Michel YM, Kean KM. Biochemical characterisation of cap-poly(A) synergy in rabbit reticulocyte lysates: the eIF4G-PABP interaction increases the functional affinity of eIF4E for the capped mRNA 5'-end. *Nucleic Acids Res* 2000, 28:4068-4075.
217. Wei CC, Balasta ML, Ren J, Goss DJ. Wheat germ poly(A) binding protein enhances the binding affinity of eukaryotic initiation factor 4F and (iso)4F for cap analogues. *Biochemistry* 1998, 37:1910-1916.
218. Ptushkina M, von der Haar T, Karim MM, Hughes JM, McCarthy JE. Repressor binding to a dorsal regulatory site traps human eIF4E in a high cap-affinity state. *Embo J* 1999, 18:4068-4075.
219. Duncan R, Milburn SC, Hershey JW. Regulated phosphorylation and low abundance of HeLa cell initiation factor eIF-4F suggest a role in translational control. Heat shock effects on eIF-4F. *J Biol Chem* 1987, 262:380-388.
220. Hershey JW, Yanov J, Fakunding JL. Purification of protein synthesis initiation factors IF-1, IF-2, and IF-3 from Escherichia coli. *Methods Enzymol* 1979, 60:3-11.
221. Maquat LE, Tarn WY, Isken O. The pioneer round of translation: features and functions. *Cell* 2010, 142:368-374.
222. Baron-Benhamou J, Fortes P, Inada T, Preiss T, Hentze MW. The interaction of the cap-binding complex (CBC) with eIF4G is dispensable for translation in yeast. *Rna* 2003, 9:654-662.
223. Lejeune F, Ranganathan AC, Maquat LE. eIF4G is required for the pioneer round of translation in mammalian cells. *Nat Struct Mol Biol* 2004, 11:992-1000.
224. Altmann M, Sonenberg N, Trachsel H. Translation in Saccharomyces cerevisiae: initiation factor 4E-dependent cell-free system. *Mol Cell Biol* 1989, 9:4467-4472.
225. Paz I, Choder M. Eukaryotic translation initiation factor 4E-dependent translation is not essential for survival of starved yeast cells. *J Bacteriol* 2001, 183:4477-4483.
226. Zuberek J, Kubacka D, Jablonowska A, Jemielity J, Stepinski J, Sonenberg N, Darzynkiewicz E. Weak binding affinity of human 4EHP for mRNA cap analogs. *Rna* 2007, 13:691-697.
227. Kubacka D, Kamenska A, Broomhead H, Minshall N, Darzynkiewicz E, Standart N. Investigating the consequences of eIF4E2 (4EHP) interaction with 4E-transporter on its cellular distribution in HeLa cells. *PLoS One* 2013, 8:e72761.
228. Morita M, Ler LW, Fabian MR, Siddiqui N, Mullin M, Henderson VC, Alain T, Fonseca BD, Karashchuk G, Bennett CF, et al. A novel 4EHP-GIGYF2 translational repressor complex is essential for mammalian development. *Mol Cell Biol* 2012, 32:3585-3593.
229. Peter D, Weber R, Sandmeir F, Wohlbold L, Helms S, Bawankar P, Valkov E, Igreja C, Izaurralde E. GIGYF1/2 proteins use auxiliary sequences to selectively bind to 4EHP and repress target mRNA expression. *Genes Dev* 2017, 31:1147-1161.
230. Chapat C, Jafarnejad SM, Matta-Camacho E, Hesketh GG, Gelbart IA, Attig J, Gkogkas CG, Alain T, Stern-Ginossar N, Fabian MR, et al. Cap-binding protein 4EHP effects translation silencing by microRNAs. *Proc Natl Acad Sci U S A* 2017, 114:5425-5430.

231. van der Weyden L, White JK, Adams DJ, Logan DW. The mouse genetics toolkit: revealing function and mechanism. *Genome Biol* 2011, 12:224.
232. Osborne MJ, Volpon L, Kornblatt JA, Culjkovic-Kraljacic B, Baguet A, Borden KL. eIF4E3 acts as a tumor suppressor by utilizing an atypical mode of methyl-7-guanosine cap recognition. *Proc Natl Acad Sci U S A* 2013, 110:3877-3882.
233. Lee AS, Kranzusch PJ, Doudna JA, Cate JH. eIF3d is an mRNA cap-binding protein that is required for specialized translation initiation. *Nature* 2016, 536:96-99.
234. Lomakin IB, Stolboushkina EA, Vaidya AT, Zhao C, Garber MB, Dmitriev SE, Steitz TA. Crystal Structure of the Human Ribosome in Complex with DENR-MCT-1. *Cell Rep* 2017, 20:521-528.
235. Hashem Y, des Georges A, Dhote V, Langlois R, Liao HY, Grassucci RA, Hellen CU, Pestova TV, Frank J. Structure of the mammalian ribosomal 43S preinitiation complex bound to the scanning factor DHX29. *Cell* 2013, 153:1108-1119.
236. Valasek L, Nielsen KH, Hinnebusch AG. Direct eIF2-eIF3 contact in the multifactor complex is important for translation initiation in vivo. *EMBO J* 2002, 21:5886-5898.
237. Jivotovskaya AV, Valasek L, Hinnebusch AG, Nielsen KH. Eukaryotic translation initiation factor 3 (eIF3) and eIF2 can promote mRNA binding to 40S subunits independently of eIF4G in yeast. *Mol Cell Biol* 2006, 26:1355-1372.
238. Sokabe M, Fraser CS, Hershey JW. The human translation initiation multi-factor complex promotes methionyl-tRNAi binding to the 40S ribosomal subunit. *Nucleic Acids Res* 2012, 40:905-913.
239. Gilbert RJ, Gordiyenko Y, von der Haar T, Sonnen AF, Hofmann G, Nardelli M, Stuart DI, McCarthy JE. Reconfiguration of yeast 40S ribosomal subunit domains by the translation initiation multifactor complex. *Proc Natl Acad Sci U S A* 2007, 104:5788-5793.
240. Passmore LA, Schmeing TM, Maag D, Applefield DJ, Acker MG, Algire MA, Lorsch JR, Ramakrishnan V. The eukaryotic translation initiation factors eIF1 and eIF1A induce an open conformation of the 40S ribosome. *Mol Cell* 2007, 26:41-50.
241. Hinnebusch AG. Translational regulation of GCN4 and the general amino acid control of yeast. *Annu Rev Microbiol* 2005, 59:407-450.
242. Gunisova S, Beznoskova P, Mohammad MP, Vlckova V, Valasek LS. In-depth analysis of cis-determinants that either promote or inhibit reinitiation on GCN4 mRNA after translation of its four short uORFs. *RNA* 2016, 22:542-558.
243. Gunisova S, Valasek LS. Fail-safe mechanism of GCN4 translational control--uORF2 promotes reinitiation by analogous mechanism to uORF1 and thus secures its key role in GCN4 expression. *Nucleic Acids Res* 2014, 42:5880-5893.
244. Pestova TV, Lomakin IB, Lee JH, Choi SK, Dever TE, Hellen CU. The joining of ribosomal subunits in eukaryotes requires eIF5B. *Nature* 2000, 403:332-335.
245. Unbehaun A, Borukhov SI, Hellen CU, Pestova TV. Release of initiation factors from 48S complexes during ribosomal subunit joining and the link between establishment of codon-anticodon base-pairing and hydrolysis of eIF2-bound GTP. *Genes Dev* 2004, 18:3078-3093.
246. Gualerzi C, Risuleo G, Pon CL. Initial rate kinetic analysis of the mechanism of initiation complex formation and the role of initiation factor IF-3. *Biochemistry* 1977, 16:1684-1689.
247. Kozak M. Inability of circular mRNA to attach to eukaryotic ribosomes. *Nature* 1979, 280:82-85.
248. Kozak M. Regulation of translation in eukaryotic systems. *Annu Rev Cell Biol* 1992, 8:197-225.
249. Hashem Y, des Georges A, Dhote V, Langlois R, Liao HY, Grassucci RA, Pestova TV, Hellen CU, Frank J. Hepatitis-C-virus-like internal ribosome entry sites displace eIF3 to gain access to the 40S subunit. *Nature* 2013, 503:539-543.
250. Siridechadilok B, Fraser CS, Hall RJ, Doudna JA, Nogales E. Structural roles for human translation factor eIF3 in initiation of protein synthesis. *Science* 2005, 310:1513-1515.

251. Pisarev AV, Kolupaeva VG, Yusupov MM, Hellen CU, Pestova TV. Ribosomal position and contacts of mRNA in eukaryotic translation initiation complexes. *Embo J* 2008, 27:1609-1621.
252. LeFebvre AK, Korneeva NL, Trutschl M, Cvek U, Duzan RD, Bradley CA, Hershey JW, Rhoads RE. Translation initiation factor eIF4G-1 binds to eIF3 through the eIF3e subunit. *J Biol Chem* 2006, 281:22917-22932.
253. Zhou M, Sandercock AM, Fraser CS, Ridlova G, Stephens E, Schenauer MR, Yokoi-Fong T, Barsky D, Leary JA, Hershey JW, et al. Mass spectrometry reveals modularity and a complete subunit interaction map of the eukaryotic translation factor eIF3. *Proc Natl Acad Sci U S A* 2008, 105:18139-18144.
254. Sokabe M, Fraser CS. A helicase-independent activity of eIF4A in promoting mRNA recruitment to the human ribosome. *Proc Natl Acad Sci U S A* 2017, 114:6304-6309.
255. Berthelot K, Muldoon M, Rajkowitsch L, Hughes J, McCarthy JE. Dynamics and processivity of 40S ribosome scanning on mRNA in yeast. *Mol Microbiol* 2004, 51:987-1001.
256. Kozak M, Shatkin AJ. Migration of 40 S ribosomal subunits on messenger RNA in the presence of edeine. *J Biol Chem* 1978, 253:6568-6577.
257. Steitz JA. Polypeptide chain initiation: nucleotide sequences of the three ribosomal binding sites in bacteriophage R17 RNA. *Nature* 1969, 224:957-964.
258. Barondes SH, Nirenberg MW. Fate of a Synthetic Polynucleotide Directing Cell-Free Protein Synthesis II. Association with Ribosomes. *Science* 1962, 138:813-817.
259. Jackson R, Standart N. The awesome power of ribosome profiling. *RNA* 2015, 21:652-654.
260. Wolin SL, Walter P. Ribosome pausing and stacking during translation of a eukaryotic mRNA. *EMBO J* 1988, 7:3559-3569.
261. Both GW, Furuichi Y, Muthukrishnan S, Shatkin AJ. Ribosome binding to reovirus mRNA in protein synthesis requires 5' terminal 7-methylguanosine. *Cell* 1975, 6:185-195.
262. Kozak M, Shatkin AJ. Characterization of ribosome-protected fragments from reovirus messenger RNA. *J Biol Chem* 1976, 251:4259-4266.
263. Kozak M, Shatkin AJ. Sequences and properties of two ribosome binding sites from the small size class of reovirus messenger RNA. *J Biol Chem* 1977, 252:6895-6908.
264. Kolupaeva VG, Pestova TV, Hellen CU. An enzymatic footprinting analysis of the interaction of 40S ribosomal subunits with the internal ribosomal entry site of hepatitis C virus. *J Virol* 2000, 74:6242-6250.
265. Baranov PV, Michel AM. Illuminating translation with ribosome profiling spectra. *Nat Methods* 2016, 13:123-124.
266. Shirokikh NE, Archer SK, Beilharz TH, Powell D, Preiss T. Translation complex profile sequencing to study the in vivo dynamics of mRNA-ribosome interactions during translation initiation, elongation and termination. *Nat Protoc* 2017, 12:697-731.
267. Uemura S, Dorywalska M, Lee TH, Kim HD, Puglisi JD, Chu S. Peptide bond formation destabilizes Shine-Dalgarno interaction on the ribosome. *Nature* 2007, 446:454-457.
268. Petrov A, Grosely R, Chen J, O'Leary SE, Puglisi JD. Multiple Parallel Pathways of Translation Initiation on the CrPV IRES. *Mol Cell* 2016, 62:92-103.
269. Fuchs G, Petrov AN, Marceau CD, Popov LM, Chen J, O'Leary SE, Wang R, Carette JE, Sarnow P, Puglisi JD. Kinetic pathway of 40S ribosomal subunit recruitment to hepatitis C virus internal ribosome entry site. *Proc Natl Acad Sci U S A* 2015, 112:319-325.
270. Kozak M. How do eucaryotic ribosomes select initiation regions in messenger RNA? *Cell* 1978, 15:1109-1123.
271. Vassilenko KS, Alekhina OM, Dmitriev SE, Shatsky IN, Spirin AS. Unidirectional constant rate motion of the ribosomal scanning particle during eukaryotic translation initiation. *Nucleic Acids Res* 2011, 39:5555-5567.

272. Sierra JM, Meier D, Ochoa S. Effect of development on the translation of messenger RNA in Artemia salina embryos. *Proc Natl Acad Sci U S A* 1974, 71:2693-2697.
273. Pestova TV, Kolupaeva VG. The roles of individual eukaryotic translation initiation factors in ribosomal scanning and initiation codon selection. *Genes Dev* 2002, 16:2906-2922.
274. Maag D, Fekete CA, Gryczynski Z, Lorsch JR. A conformational change in the eukaryotic translation preinitiation complex and release of eIF1 signal recognition of the start codon. *Mol Cell* 2005, 17:265-275.
275. Shirokikh NE, Spirin AS. Poly(A) leader of eukaryotic mRNA bypasses the dependence of translation on initiation factors. *Proc Natl Acad Sci U S A* 2008, 105:10738-10743.
276. Skabkin MA, Skabkina OV, Hellen CU, Pestova TV. Reinitiation and other unconventional posttermination events during eukaryotic translation. *Mol Cell* 2013, 51:249-264.
277. Abaeva IS, Pestova TV, Hellen CU. Attachment of ribosomal complexes and retrograde scanning during initiation on the Halastavi arva virus IRES. *Nucleic Acids Res* 2016, 44:2362-2377.
278. Abaeva IS, Marintchev A, Pisareva VP, Hellen CUT, Pestova TV. Bypassing of stems versus linear base-by-base inspection of mammalian mRNAs during ribosomal scanning. *The EMBO journal* 2010, 30:115-129.
279. Dhote V, Sweeney TR, Kim N, Hellen CU, Pestova TV. Roles of individual domains in the function of DHX29, an essential factor required for translation of structured mammalian mRNAs. *Proc Natl Acad Sci U S A* 2012, 109:E3150-3159.
280. Pisareva VP, Pisarev AV, Komar AA, Hellen CU, Pestova TV. Translation initiation on mammalian mRNAs with structured 5'UTRs requires DExH-box protein DHX29. *Cell* 2008, 135:1237-1250.
281. Parsyan A, Svitkin Y, Shahbazian D, Gkogkas C, Lasko P, Merrick WC, Sonenberg N. mRNA helicases: the tacticians of translational control. *Nat Rev Mol Cell Biol* 2011, 12:235-245.
282. Abaeva IS, Marintchev A, Pisareva VP, Hellen CU, Pestova TV. Bypassing of stems versus linear base-by-base inspection of mammalian mRNAs during ribosomal scanning. *EMBO J* 2011, 30:115-129.
283. Sen ND, Zhou F, Ingolia NT, Hinnebusch AG. Genome-wide analysis of translational efficiency reveals distinct but overlapping functions of yeast DEAD-box RNA helicases Ded1 and eIF4A. *Genome Res* 2015, 25:1196-1205.
284. Soto-Rifo R, Rubilar PS, Limousin T, de Breyne S, Decimo D, Ohlmann T. DEAD-box protein DDX3 associates with eIF4F to promote translation of selected mRNAs. *EMBO J* 2012, 31:3745-3756.
285. Ranji A, Shkriabai N, Kvaratskhelia M, Musier-Forsyth K, Boris-Lawrie K. Features of double-stranded RNA-binding domains of RNA helicase A are necessary for selective recognition and translation of complex mRNAs. *J Biol Chem* 2011, 286:5328-5337.
286. Zhang Y, You J, Wang X, Weber J. The DHX33 RNA Helicase Promotes mRNA Translation Initiation. *Mol Cell Biol* 2015, 35:2918-2931.
287. Kozak M. Influence of mRNA secondary structure on binding and migration of 40S ribosomal subunits. *Cell* 1980, 19:79-90.
288. Kozak M. Leader length and secondary structure modulate mRNA function under conditions of stress. *Mol Cell Biol* 1988, 8:2737-2744.
289. Liu F, Putnam A, Jankowsky E. ATP hydrolysis is required for DEAD-box protein recycling but not for duplex unwinding. *Proc Natl Acad Sci U S A* 2008, 105:20209-20214.
290. Aitken CE, Lorsch JR. A mechanistic overview of translation initiation in eukaryotes. *Nat Struct Mol Biol* 2012, 19:568-576.
291. Voigts-Hoffmann F, Klinge S, Ban N. Structural insights into eukaryotic ribosomes and the initiation of translation. *Curr Opin Struct Biol* 2012, 22:768-777.

292. Rabl J, Leibundgut M, Ataide SF, Haag A, Ban N. Crystal structure of the eukaryotic 40S ribosomal subunit in complex with initiation factor 1. *Science* 2011, 331:730-736.
293. Weisser M, Voigts-Hoffmann F, Rabl J, Leibundgut M, Ban N. The crystal structure of the eukaryotic 40S ribosomal subunit in complex with eIF1 and eIF1A. *Nat Struct Mol Biol* 2013, 20:1015-1017.
294. Maag D, Lorsch JR. Communication between eukaryotic translation initiation factors 1 and 1A on the yeast small ribosomal subunit. *J Mol Biol* 2003, 330:917-924.
295. Emanuilov I, Sabatini DD, Lake JA, Freienstein C. Localization of eukaryotic initiation factor 3 on native small ribosomal subunits. *Proc Natl Acad Sci U S A* 1978, 75:1389-1393.
296. Srivastava S, Verschoor A, Frank J. Eukaryotic initiation factor 3 does not prevent association through physical blockage of the ribosomal subunit-subunit interface. *J Mol Biol* 1992, 226:301-304.
297. Aylett CH, Boehringer D, Erzberger JP, Schaefer T, Ban N. Structure of a yeast 40S-eIF1-eIF1A-eIF3-eIF3j initiation complex. *Nat Struct Mol Biol* 2015, 22:269-271.
298. Lomakin IB, Kolupaeva VG, Marintchev A, Wagner G, Pestova TV. Position of eukaryotic initiation factor eIF1 on the 40S ribosomal subunit determined by directed hydroxyl radical probing. *Genes Dev* 2003, 17:2786-2797.
299. Yu Y, Marintchev A, Kolupaeva VG, Unbehaun A, Veryasova T, Lai SC, Hong P, Wagner G, Hellen CU, Pestova TV. Position of eukaryotic translation initiation factor eIF1A on the 40S ribosomal subunit mapped by directed hydroxyl radical probing. *Nucleic Acids Res* 2009, 37:5167-5182.
300. Pestova TV, Borukhov SI, Hellen CU. Eukaryotic ribosomes require initiation factors 1 and 1A to locate initiation codons. *Nature* 1998, 394:854-859.
301. Lomakin IB, Shirokikh NE, Yusupov MM, Hellen CU, Pestova TV. The fidelity of translation initiation: reciprocal activities of eIF1, IF3 and YciH. *Embo J* 2006, 25:196-210.
302. Nanda JS, Saini AK, Munoz AM, Hinnebusch AG, Lorsch JR. Coordinated movements of eukaryotic translation initiation factors eIF1, eIF1A, and eIF5 trigger phosphate release from eIF2 in response to start codon recognition by the ribosomal preinitiation complex. *J Biol Chem* 2013, 288:5316-5329.
303. Martin-Marcos P, Nanda JS, Luna RE, Zhang F, Saini AK, Cherkasova VA, Wagner G, Lorsch JR, Hinnebusch AG. Enhanced eIF1 binding to the 40S ribosome impedes conformational rearrangements of the preinitiation complex and elevates initiation accuracy. *RNA* 2014, 20:150-167.
304. Zhang F, Saini AK, Shin BS, Nanda J, Hinnebusch AG. Conformational changes in the P site and mRNA entry channel evoked by AUG recognition in yeast translation preinitiation complexes. *Nucleic Acids Res* 2015, 43:2293-2312.
305. Saini AK, Nanda JS, Lorsch JR, Hinnebusch AG. Regulatory elements in eIF1A control the fidelity of start codon selection by modulating tRNA(i)(Met) binding to the ribosome. *Genes Dev* 2010, 24:97-110.
306. Fekete CA, Mitchell SF, Cherkasova VA, Applefield D, Algire MA, Maag D, Saini AK, Lorsch JR, Hinnebusch AG. N- and C-terminal residues of eIF1A have opposing effects on the fidelity of start codon selection. *Embo J* 2007, 26:1602-1614.
307. Cheung YN, Maag D, Mitchell SF, Fekete CA, Algire MA, Takacs JE, Shirokikh N, Pestova T, Lorsch JR, Hinnebusch AG. Dissociation of eIF1 from the 40S ribosomal subunit is a key step in start codon selection in vivo. *Genes Dev* 2007, 21:1217-1230.
308. Asano K, Clayton J, Shalev A, Hinnebusch AG. A multifactor complex of eukaryotic initiation factors, eIF1, eIF2, eIF3, eIF5, and initiator tRNA(Met) is an important translation initiation intermediate in vivo. *Genes Dev* 2000, 14:2534-2546.

309. Phan L, Zhang X, Asano K, Anderson J, Vornlocher HP, Greenberg JR, Qin J, Hinnebusch AG. Identification of a translation initiation factor 3 (eIF3) core complex, conserved in yeast and mammals, that interacts with eIF5. *Mol Cell Biol* 1998, 18:4935-4946.
310. Valasek L, Nielsen KH, Zhang F, Fekete CA, Hinnebusch AG. Interactions of eukaryotic translation initiation factor 3 (eIF3) subunit NIP1/c with eIF1 and eIF5 promote preinitiation complex assembly and regulate start codon selection. *Mol Cell Biol* 2004, 24:9437-9455.
311. Fletcher CM, Pestova TV, Hellen CU, Wagner G. Structure and interactions of the translation initiation factor eIF1. *Embo J* 1999, 18:2631-2637.
312. Luna RE, Arthanari H, Hiraishi H, Nanda J, Martin-Marcos P, Markus MA, Akabayov B, Milbradt AG, Luna LE, Seo HC, et al. The C-terminal domain of eukaryotic initiation factor 5 promotes start codon recognition by its dynamic interplay with eIF1 and eIF2beta. *Cell Rep* 2012, 1:689-702.
313. Karaskova M, Gunisova S, Herrmannova A, Wagner S, Munzarova V, Valasek L. Functional characterization of the role of the N-terminal domain of the c/Nip1 subunit of eukaryotic initiation factor 3 (eIF3) in AUG recognition. *J Biol Chem* 2012, 287:28420-28434.
314. Marintchev A. Roles of helicases in translation initiation: a mechanistic view. *Biochim Biophys Acta* 2013, 1829:799-809.
315. Marintchev A, Edmonds KA, Marintcheva B, Hendrickson E, Oberer M, Suzuki C, Herdy B, Sonenberg N, Wagner G. Topology and regulation of the human eIF4A/4G/4H helicase complex in translation initiation. *Cell* 2009, 136:447-460.
316. Zinoviev A, Hellen CU, Pestova TV. Multiple mechanisms of reinitiation on bicistronic calicivirus mRNAs. *Mol Cell* 2015, 57:1059-1073.
317. Fraser CS. Quantitative studies of mRNA recruitment to the eukaryotic ribosome. *Biochimie* 2015, 114:58-71.
318. Rice S, Lin AW, Safer D, Hart CL, Naber N, Carragher BO, Cain SM, Pechatnikova E, Wilson-Kubalek EM, Whittaker M, et al. A structural change in the kinesin motor protein that drives motility. *Nature* 1999, 402:778-784.
319. Kull FJ, Endow SA. Force generation by kinesin and myosin cytoskeletal motor proteins. *J Cell Sci* 2013, 126:9-19.
320. Chen H, Meisburger SP, Pabit SA, Sutton JL, Webb WW, Pollack L. Ionic strength-dependent persistence lengths of single-stranded RNA and DNA. *Proc Natl Acad Sci U S A* 2012, 109:799-804.
321. Chi Q, Wang G, Jiang J. The persistence length and length per base of single-stranded DNA obtained from fluorescence correlation spectroscopy measurements using mean field theory. *Physica A: Statistical Mechanics and its Applications* 2013, 392:1072-1079.
322. Spirin AS. How does a scanning ribosomal particle move along the 5'-untranslated region of eukaryotic mRNA? Brownian Ratchet model. *Biochemistry* 2009, 48:10688-10692.
323. Takyar S, Hickerson RP, Noller HF. mRNA helicase activity of the ribosome. *Cell* 2005, 120:49-58.
324. Qu X, Wen JD, Lancaster L, Noller HF, Bustamante C, Tinoco I, Jr. The ribosome uses two active mechanisms to unwind messenger RNA during translation. *Nature* 2011, 475:118-121.
325. Kuriyan J, O'Donnell M. Sliding clamps of DNA polymerases. *J Mol Biol* 1993, 234:915-925.
326. Pick E, Hofmann K, Glickman MH. PCI complexes: Beyond the proteasome, CSN, and eIF3 Troika. *Mol Cell* 2009, 35:260-264.
327. Matyskiela ME, Lander GC, Martin A. Conformational switching of the 26S proteasome enables substrate degradation. *Nat Struct Mol Biol* 2013, 20:781-788.
328. Gingras AC, Raught B, Sonenberg N. eIF4 initiation factors: effectors of mRNA recruitment to ribosomes and regulators of translation. *Annu Rev Biochem* 1999, 68:913-963.
329. Yoder-Hill J, Pause A, Sonenberg N, Merrick WC. The p46 subunit of eukaryotic initiation factor (eIF)-4F exchanges with eIF-4A. *J Biol Chem* 1993, 268:5566-5573.

330. Pause A, Methot N, Svitkin Y, Merrick WC, Sonenberg N. Dominant negative mutants of mammalian translation initiation factor eIF-4A define a critical role for eIF-4F in cap-dependent and cap-independent initiation of translation. *EMBO J* 1994, 13:1205-1215.
331. Delagoutte E, von Hippel PH. Molecular mechanisms of the functional coupling of the helicase (gp41) and polymerase (gp43) of bacteriophage T4 within the DNA replication fork. *Biochemistry* 2001, 40:4459-4477.
332. von Hippel PH, Delagoutte E. A general model for nucleic acid helicases and their "coupling" within macromolecular machines. *Cell* 2001, 104:177-190.
333. Phelps C, Lee W, Jose D, von Hippel PH, Marcus AH. Single-molecule FRET and linear dichroism studies of DNA breathing and helicase binding at replication fork junctions. *Proc Natl Acad Sci U S A* 2013, 110:17320-17325.
334. Tuller T, Ruppin E, Kupiec M. Properties of untranslated regions of the S. cerevisiae genome. *BMC Genomics* 2009, 10:391.
335. Cheng S, Sultana S, Goss DJ, Gallie DR. Translation initiation factor 4B homodimerization, RNA binding, and interaction with Poly(A)-binding protein are enhanced by zinc. *J Biol Chem* 2008, 283:36140-36153.
336. Kanitz A, Gypas F, Gruber AJ, Gruber AR, Martin G, Zavolan M. Comparative assessment of methods for the computational inference of transcript isoform abundance from RNA-seq data. *Genome Biol* 2015, 16:150.
337. Wang H, McManus J, Kingsford C. Isoform-level ribosome occupancy estimation guided by transcript abundance with Ribomap. *Bioinformatics* 2016, 32:1880-1882.
338. Martinez-Nunez RT, Sanford JR. Studying Isoform-Specific mRNA Recruitment to Polyribosomes with Frac-seq. *Methods Mol Biol* 2016, 1358:99-108.
339. Haimov O, Sinvani H, Dikstein R. Cap-dependent, scanning-free translation initiation mechanisms. *Biochim Biophys Acta* 2015, 1849:1313-1318.
340. Futterer J, Kiss-Laszlo Z, Hohn T. Nonlinear ribosome migration on cauliflower mosaic virus 35S RNA. *Cell* 1993, 73:789-802.
341. Yueh A, Schneider RJ. Selective translation initiation by ribosome jumping in adenovirus-infected and heat-shocked cells. *Genes Dev* 1996, 10:1557-1567.
342. Hemmings-Mieszczak M, Hohn T. A stable hairpin preceded by a short open reading frame promotes nonlinear ribosome migration on a synthetic mRNA leader. *RNA* 1999, 5:1149-1157.
343. Pooggin MM, Ryabova LA, He X, Futterer J, Hohn T. Mechanism of ribosome shunting in Rice tungro bacilliform pararetrovirus. *RNA* 2006, 12:841-850.
344. de Breyne S, Simonet V, Pelet T, Curran J. Identification of a cis-acting element required for shunt-mediated translational initiation of the Sendai virus Y proteins. *Nucleic Acids Res* 2003, 31:608-618.
345. Sherrill KW, Lloyd RE. Translation of cIAP2 mRNA is mediated exclusively by a stress-modulated ribosome shunt. *Mol Cell Biol* 2008, 28:2011-2022.
346. Yueh A, Schneider RJ. Translation by ribosome shunting on adenovirus and hsp70 mRNAs facilitated by complementarity to 18S rRNA. *Genes Dev* 2000, 14:414-421.
347. Koh DC, Edelman GM, Mauro VP. Physical evidence supporting a ribosomal shunting mechanism of translation initiation for BACE1 mRNA. *Translation (Austin)* 2013, 1:e24400.
348. Rogers GW, Jr., Edelman GM, Mauro VP. Differential utilization of upstream AUGs in the beta-secretase mRNA suggests that a shunting mechanism regulates translation. *Proc Natl Acad Sci U S A* 2004, 101:2794-2799.
349. Mihailovich M, Thermann R, Grohovaz F, Hentze MW, Zacchetti D. Complex translational regulation of BACE1 involves upstream AUGs and stimulatory elements within the 5' untranslated region. *Nucleic Acids Res* 2007, 35:2975-2985.

350. Lammich S, Schobel S, Zimmer AK, Lichtenthaler SF, Haass C. Expression of the Alzheimer protease BACE1 is suppressed via its 5'-untranslated region. *EMBO Rep* 2004, 5:620-625.
351. Dominguez DI, Ryabova LA, Pooggin MM, Schmidt-Puchta W, Futterer J, Hohn T. Ribosome shunting in cauliflower mosaic virus. Identification of an essential and sufficient structural element. *J Biol Chem* 1998, 273:3669-3678.
352. Pooggin MM, Hohn T, Futterer J. Role of a short open reading frame in ribosome shunt on the cauliflower mosaic virus RNA leader. *J Biol Chem* 2000, 275:17288-17296.
353. Pooggin MM, Futterer J, Hohn T. Cross-species functionality of pararetroviral elements driving ribosome shunting. *PLoS One* 2008, 3:e1650.
354. Vattem KM, Wek RC. Reinitiation involving upstream ORFs regulates ATF4 mRNA translation in mammalian cells. *Proc Natl Acad Sci U S A* 2004, 101:11269-11274.
355. Zhang F, Hinnebusch AG. An upstream ORF with non-AUG start codon is translated in vivo but dispensable for translational control of GCN4 mRNA. *Nucleic Acids Res* 2011, 39:3128-3140.
356. Hinnebusch AG. Translational regulation of GCN4 and the general amino acid control of yeast. *Annual review of microbiology* 2005, 59:407-450.
357. Luttermann C, Meyers G. Two alternative ways of start site selection in human norovirus reinitiation of translation. *J Biol Chem* 2014, 289:11739-11754.
358. Luttermann C, Meyers G. A bipartite sequence motif induces translation reinitiation in feline calicivirus RNA. *J Biol Chem* 2007, 282:7056-7065.
359. Meyers G. Translation of the minor capsid protein of a calicivirus is initiated by a novel termination-dependent reinitiation mechanism. *J Biol Chem* 2003, 278:34051-34060.
360. Somers J, Poyry T, Willis AE. A perspective on mammalian upstream open reading frame function. *Int J Biochem Cell Biol* 2013, 45:1690-1700.
361. Poyry TA, Jackson RJ. Mechanisms governing the selection of translation initiation sites on foot-and-mouth disease virus RNA. *J Virol* 2011, 85:10178-10188.
362. Powell ML, Leigh KE, Poyry TA, Jackson RJ, Brown TD, Brierley I. Further characterisation of the translational termination-reinitiation signal of the influenza B virus segment 7 RNA. *PLoS One* 2011, 6:e16822.
363. Poyry TA, Kaminski A, Connell EJ, Fraser CS, Jackson RJ. The mechanism of an exceptional case of reinitiation after translation of a long ORF reveals why such events do not generally occur in mammalian mRNA translation. *Genes Dev* 2007, 21:3149-3162.
364. Poyry TA, Kaminski A, Jackson RJ. What determines whether mammalian ribosomes resume scanning after translation of a short upstream open reading frame? *Genes Dev* 2004, 18:62-75.
365. McCormick CJ, Salim O, Lambden PR, Clarke IN. Translation termination reinitiation between open reading frame 1 (ORF1) and ORF2 enables capsid expression in a bovine norovirus without the need for production of viral subgenomic RNA. *J Virol* 2008, 82:8917-8921.
366. Napthine S, Lever RA, Powell ML, Jackson RJ, Brown TD, Brierley I. Expression of the VP2 protein of murine norovirus by a translation termination-reinitiation strategy. *PLoS One* 2009, 4:e8390.
367. Hemmings-Mieszczak M, Hohn T, Preiss T. Termination and peptide release at the upstream open reading frame are required for downstream translation on synthetic shunt-competent mRNA leaders. *Mol Cell Biol* 2000, 20:6212-6223.
368. Jackson RJ, Hellen CU, Pestova TV. Termination and post-termination events in eukaryotic translation. *Adv Protein Chem Struct Biol* 2012, 86:45-93.
369. Prosniak M, Dierov J, Okami K, Tilton B, Jameson B, Sawaya BE, Gartenhaus RB. A novel candidate oncogene, MCT-1, is involved in cell cycle progression. *Cancer Res* 1998, 58:4233-4237.

370. Schleich S, Strassburger K, Janiesch PC, Koledachkina T, Miller KK, Haneke K, Cheng YS, Kuchler K, Stoecklin G, Duncan KE, et al. DENR-MCT-1 promotes translation re-initiation downstream of uORFs to control tissue growth. *Nature* 2014, 512:208-212.
371. Tseng HY, Chen YA, Jen J, Shen PC, Chen LM, Lin TD, Wang YC, Hsu HL. Oncogenic MCT-1 activation promotes YY1-EGFR-MnSOD signaling and tumor progression. *Oncogenesis* 2017, 6:e313.
372. Kasiappan R, Shih HJ, Chu KL, Chen WT, Liu HP, Huang SF, Choy CO, Shu CL, Din R, Chu JS, et al. Loss of p53 and MCT-1 overexpression synergistically promote chromosome instability and tumorigenicity. *Mol Cancer Res* 2009, 7:536-548.
373. Hsu HL, Shi B, Gartenhaus RB. The MCT-1 oncogene product impairs cell cycle checkpoint control and transforms human mammary epithelial cells. *Oncogene* 2005, 24:4956-4964.
374. Matsuda D, Mauro VP. Base pairing between hepatitis C virus RNA and 18S rRNA is required for IRES-dependent translation initiation in vivo. *Proc Natl Acad Sci U S A* 2014, 111:15385-15389.
375. Mauro VP, Matsuda D. Translation regulation by ribosomes: Increased complexity and expanded scope. *RNA Biol* 2016, 13:748-755.
376. Chappell SA, Edelman GM, Mauro VP. Ribosomal tethering and clustering as mechanisms for translation initiation. *Proc Natl Acad Sci U S A* 2006, 103:18077-18082.
377. Dresios J, Chappell SA, Zhou W, Mauro VP. An mRNA-rRNA base-pairing mechanism for translation initiation in eukaryotes. *Nat Struct Mol Biol* 2006, 13:30-34.
378. Hu MC, Tranque P, Edelman GM, Mauro VP. rRNA-complementarity in the 5' untranslated region of mRNA specifying the Gtx homeodomain protein: evidence that base- pairing to 18S rRNA affects translational efficiency. *Proc Natl Acad Sci U S A* 1999, 96:1339-1344.
379. Tranque P, Hu MC, Edelman GM, Mauro VP. rRNA complementarity within mRNAs: a possible basis for mRNA-ribosome interactions and translational control. *Proc Natl Acad Sci U S A* 1998, 95:12238-12243.
380. Martin F, Menetret JF, Simonetti A, Myasnikov AG, Vicens Q, Prongidi-Fix L, Natchiar SK, Klaholz BP, Eriani G. Ribosomal 18S rRNA base pairs with mRNA during eukaryotic translation initiation. *Nat Commun* 2016, 7:12622.
381. Martin F, Barends S, Jaeger S, Schaeffer L, Prongidi-Fix L, Eriani G. Cap-assisted internal initiation of translation of histone H4. *Mol Cell* 2011, 41:197-209.
382. Smith E, Meyerrose TE, Kohler T, Namdar-Attar M, Bab N, Lahat O, Noh T, Li J, Karaman MW, Hacia JG, et al. Leaky ribosomal scanning in mammalian genomes: significance of histone H4 alternative translation in vivo. *Nucleic Acids Res* 2005, 33:1298-1308.
383. Luttermann C, Meyers G. The importance of inter- and intramolecular base pairing for translation reinitiation on a eukaryotic bicistronic mRNA. *Genes Dev* 2009, 23:331-344.
384. Meyers G. Characterization of the sequence element directing translation reinitiation in RNA of the calicivirus rabbit hemorrhagic disease virus. *J Virol* 2007, 81:9623-9632.
385. Paek KY, Hong KY, Ryu I, Park SM, Keum SJ, Kwon OS, Jang SK. Translation initiation mediated by RNA looping. *Proc Natl Acad Sci U S A* 2015, 112:1041-1046.
386. Schmitt E, Panvert M, Lazennec-Schurdevin C, Coureux PD, Perez J, Thompson A, Mechulam Y. Structure of the ternary initiation complex aIF2-GDPNP-methionylated initiator tRNA. *Nat Struct Mol Biol* 2012, 19:450-454.
387. Martin-Marcos P, Cheung YN, Hinnebusch AG. Functional elements in initiation factors 1, 1A, and 2beta discriminate against poor AUG context and non-AUG start codons. *Mol Cell Biol* 2011, 31:4814-4831.
388. Mitchell SF, Lorsch JR. Should I stay or should I go? Eukaryotic translation initiation factors 1 and 1A control start codon recognition. *J Biol Chem* 2008, 283:27345-27349.
389. Pisarev AV, Kolupaeva VG, Pisareva VP, Merrick WC, Hellen CU, Pestova TV. Specific functional interactions of nucleotides at key -3 and +4 positions flanking the initiation codon

with components of the mammalian 48S translation initiation complex. *Genes Dev* 2006, 20:624-636.
390. Algire MA, Maag D, Lorsch JR. Pi release from eIF2, not GTP hydrolysis, is the step controlled by start-site selection during eukaryotic translation initiation. *Mol Cell* 2005, 20:251-262.
391. Martin-Marcos P, Cheung YN, Hinnebusch AG. Functional elements in initiation factors 1, 1A and 2{beta} discriminate against poor AUG context and non-AUG start codons. *Mol Cell Biol* 2011.
392. Fraser CS, Lee JY, Mayeur GL, Bushell M, Doudna JA, Hershey JW. The j-subunit of human translation initiation factor eIF3 is required for the stable binding of eIF3 and its subcomplexes to 40 S ribosomal subunits in vitro. *J Biol Chem* 2004, 279:8946-8956.
393. Phan L, Schoenfeld LW, Valasek L, Nielsen KH, Hinnebusch AG. A subcomplex of three eIF3 subunits binds eIF1 and eIF5 and stimulates ribosome binding of mRNA and tRNA(i)Met. *EMBO J* 2001, 20:2954-2965.
394. Valasek LS. 'Ribozoomin'--translation initiation from the perspective of the ribosome-bound eukaryotic initiation factors (eIFs). *Curr Protein Pept Sci* 2012, 13:305-330.
395. Asano K, Phan L, Anderson J, Hinnebusch AG. Complex formation by all five homologues of mammalian translation initiation factor 3 subunits from yeast Saccharomyces cerevisiae. *J Biol Chem* 1998, 273:18573-18585.
396. Majumdar R, Maitra U. Regulation of GTP hydrolysis prior to ribosomal AUG selection during eukaryotic translation initiation. *EMBO J* 2005, 24:3737-3746.
397. Saini AK, Nanda JS, Martin-Marcos P, Dong J, Zhang F, Bhardwaj M, Lorsch JR, Hinnebusch AG. Eukaryotic translation initiation factor eIF5 promotes the accuracy of start codon recognition by regulating Pi release and conformational transitions of the preinitiation complex. *Nucleic Acids Res* 2015, 43:5673-5674.
398. Lorsch JR, Dever TE. Molecular view of 43 S complex formation and start site selection in eukaryotic translation initiation. *J Biol Chem* 2010, 285:21203-21207.
399. Kozak M. A short leader sequence impairs the fidelity of initiation by eukaryotic ribosomes. *Gene Expr* 1991, 1:111-115.
400. Terenin IM, Akulich KA, Andreev DE, Polyanskaya SA, Shatsky IN, Dmitriev SE. Sliding of a 43S ribosomal complex from the recognized AUG codon triggered by a delay in eIF2-bound GTP hydrolysis. *Nucleic Acids Res* 2016, 44:1882-1893.
401. Acker MG, Shin BS, Nanda JS, Saini AK, Dever TE, Lorsch JR. Kinetic analysis of late steps of eukaryotic translation initiation. *J Mol Biol* 2009, 385:491-506.
402. Fernandez IS, Bai XC, Hussain T, Kelley AC, Lorsch JR, Ramakrishnan V, Scheres SH. Molecular architecture of a eukaryotic translational initiation complex. *Science* 2013, 342:1240585.
403. Hussain T, Llacer JL, Wimberly BT, Kieft JS, Ramakrishnan V. Large-Scale Movements of IF3 and tRNA during Bacterial Translation Initiation. *Cell* 2016, 167:133-144 e113.
404. Choi SK, Lee JH, Zoll WL, Merrick WC, Dever TE. Promotion of met-tRNAiMet binding to ribosomes by yIF2, a bacterial IF2 homolog in yeast. *Science* 1998, 280:1757-1760.
405. Cuchalova L, Kouba T, Herrmannova A, Danyi I, Chiu WL, Valasek L. The RNA recognition motif of eukaryotic translation initiation factor 3g (eIF3g) is required for resumption of scanning of posttermination ribosomes for reinitiation on GCN4 and together with eIF3i stimulates linear scanning. *Mol Cell Biol* 2010, 30:4671-4686.
406. Mohammad MP, Munzarova Pondelickova V, Zeman J, Gunisova S, Valasek LS. In vivo evidence that eIF3 stays bound to ribosomes elongating and terminating on short upstream ORFs to promote reinitiation. *Nucleic Acids Res* 2017, 45:2658-2674.
407. Kolitz SE, Lorsch JR. Eukaryotic initiator tRNA: finely tuned and ready for action. *FEBS Lett* 2010, 584:396-404.

408. Dong J, Munoz A, Kolitz SE, Saini AK, Chiu WL, Rahman H, Lorsch JR, Hinnebusch AG. Conserved residues in yeast initiator tRNA calibrate initiation accuracy by regulating preinitiation complex stability at the start codon. *Genes Dev* 2014, 28:502-520.
409. Ingolia NT, Lareau LF, Weissman JS. Ribosome profiling of mouse embryonic stem cells reveals the complexity and dynamics of mammalian proteomes. *Cell* 2011, 147:789-802.
410. Hecht A, Glasgow J, Jaschke PR, Bawazer LA, Munson MS, Cochran JR, Endy D, Salit M. Measurements of translation initiation from all 64 codons in E. coli. *Nucleic Acids Res* 2017, 45:3615-3626.
411. Lind C, Esguerra M, Aqvist J. A close-up view of codon selection in eukaryotic initiation. *RNA Biol* 2017, 14:815-819.
412. Berthelot K, Muldoon M, Rajkowitsch L, Hughes J, McCarthy JEG. Dynamics and processivity of 40S ribosome scanning on mRNA in yeast. *Molecular microbiology* 2004, 51:987-1001.
413. Ivanov IP, Loughran G, Sachs MS, Atkins JF. Initiation context modulates autoregulation of eukaryotic translation initiation factor 1 (eIF1). *Proc Natl Acad Sci U S A* 2010, 107:18056-18060.
414. Kozak M. An analysis of 5'-noncoding sequences from 699 vertebrate messenger RNAs. *Nucleic Acids Res* 1987, 15:8125-8148.
415. Miyasaka H. The positive relationship between codon usage bias and translation initiation AUG context in Saccharomyces cerevisiae. *Yeast* 1999, 15:633-637.
416. Joshi CP, Zhou H, Huang X, Chiang VL. Context sequences of translation initiation codon in plants. *Plant Mol Biol* 1997, 35:993-1001.
417. Hellens RP, Brown CM, Chisnall MA, Waterhouse PM, Macknight RC. The Emerging World of Small ORFs. *Trends Plant Sci* 2016, 21:317-328.
418. Michel AM, Andreev DE, Baranov PV. Computational approach for calculating the probability of eukaryotic translation initiation from ribo-seq data that takes into account leaky scanning. *BMC Bioinformatics* 2014, 15:380.
419. Kozak M. Downstream secondary structure facilitates recognition of initiator codons by eukaryotic ribosomes. *Proc Natl Acad Sci U S A* 1990, 87:8301-8305.
420. Maicas E, Shago M, Friesen JD. Translation of the Saccharomyces cerevisiae tcm1 gene in the absence of a 5'-untranslated leader. *Nucleic Acids Res* 1990, 18:5823-5828.
421. Elfakess R, Dikstein R. A translation initiation element specific to mRNAs with very short 5'UTR that also regulates transcription. *PLoS One* 2008, 3:e3094.
422. Sinvani H, Haimov O, Svitkin Y, Sonenberg N, Tamarkin-Ben-Harush A, Viollet B, Dikstein R. Translational tolerance of mitochondrial genes to metabolic energy stress involves TISU and eIF1-eIF4GI cooperation in start codon selection. *Cell Metab* 2015, 21:479-492.
423. Elfakess R, Sinvani H, Haimov O, Svitkin Y, Sonenberg N, Dikstein R. Unique translation initiation of mRNAs-containing TISU element. *Nucleic Acids Res* 2011, 39:7598-7609.
424. Halstead JM, Lionnet T, Wilbertz JH, Wippich F, Ephrussi A, Singer RH, Chao JA. Translation. An RNA biosensor for imaging the first round of translation from single cells to living animals. *Science* 2015, 347:1367-1671.
425. Marchetti M, Malinowska A, Heller I, Wuite GJL. How to switch the motor on: RNA polymerase initiation steps at the single-molecule level. *Protein Sci* 2017, 26:1303-1313.
426. Wu B, Eliscovich C, Yoon YJ, Singer RH. Translation dynamics of single mRNAs in live cells and neurons. *Science* 2016, 352:1430-1435.
427. Morisaki T, Lyon K, DeLuca KF, DeLuca JG, English BP, Zhang Z, Lavis LD, Grimm JB, Viswanathan S, Looger LL, et al. Real-time quantification of single RNA translation dynamics in living cells. *Science* 2016, 352:1425-1429.
428. Manosas M, Camunas-Soler J, Croquette V, Ritort F. Single molecule high-throughput footprinting of small and large DNA ligands. *Nat Commun* 2017, 8:304.

429. Kim S, Streets AM, Lin RR, Quake SR, Weiss S, Majumdar DS. High-throughput single-molecule optofluidic analysis. *Nat Methods* 2011, 8:242-245.
430. Harrison PF, Powell DR, Clancy JL, Preiss T, Boag PR, Traven A, Seemann T, Beilharz TH. PAT-seq: a method to study the integration of 3'-UTR dynamics with gene expression in the eukaryotic transcriptome. *RNA* 2015, 21:1502-1510.
431. Clancy JL, Wei GH, Echner N, Humphreys DT, Beilharz TH, Preiss T. mRNA isoform diversity can obscure detection of miRNA-mediated control of translation. *RNA* 2011, 17:1025-1031.